Immune Surveillance by Effector and Memory CD8+ T Cells

Immune surveillance by effector and memory $CD8^+$ T cells

A dissertation presented

by

Scott McNabb Loughhead

to

The Division of Medical Sciences

in partial fulfillment of the requirements

for the degree of

Doctor of Philosophy

in the subject of

Immunology

Harvard University

Cambridge, Massachusetts

October 2015

Immune surveillance by effector and memory $CD8^+$ T cells

Abstract

During priming, $CD8^+$ T cells integrate a plethora of signals that affect their differentiation into subsets of $CD8^+$ T cells with distinct migratory properties and functions. Given that $CD8^+$ T cells exert their protective function via cell-cell contacts, the migratory patterns and spatial distribution of $CD8^+$ T cell subsets induced by primary challenge are of critical importance to the host. Dendritic cells (DCs), as the primary initiators of these responses, play a pivotal role in shaping the size and differentiation status of $CD8^+$ T cells that emerge. However, inadequate markers for $CD8^+$ T cell subsets have hindered study of their lineage relationships, as well as their migratory behaviors. Here, we use a novel marker for identification of $CD8^+$ T cell subsets to interrogate whether subsets of DCs skew $CD8^+$ T cell fate decisions, the differentiation pattern of $CD8^+$ T cell subsets, and the migratory behavior of these $CD8^+$ T cell subsets.

Within secondary lymphoid organs (SLOs), $CD8^+$ T cells encounter subsets of DCs that may differentially impact subsequent T cell fate decisions. While distinct DC subsets were found to influence $CD8^+$ T cell priming and subsequent differentiation *in vitro*, these differences were masked when priming occurred *in vivo*. This prompted us to delve deeper into how $CD8^+$ T cell subsets are defined *in vivo*. Classically, memory $CD8^+$ T cells are divided into two subsets: central memory T cells (T_{CM}) and effector memory T cells (T_{EM}). Based on the variable expression of the chemokine receptor, CX_3CR1, we define T_{CM} as CX_3CR1^- and T_{EM} as CX_3CR1^{high}. Additionally, a previously undefined subset of T cells was identified that express intermediate levels of CX_3CR1. Flow

cytometric analysis of the subsets migrating through murine peripheral tissues in the memory phase established CX_3CR1^{int} cells as the dominant subset, thus these cells have been termed peripheral memory T cells (T_{PM}). Lineage tracing of these three subsets established a uni-directional relationship where increasing levels of CX_3CR1 marked further terminal differentiation: T_{CM} (CX_3CR1^-) to T_{PM} (CX_3CR1^{int}) to T_{EM} (CX_3CR1^{hi}).

The finding that T_{PM}, and not T_{EM}, migrated through peripheral tissues was intriguing because it contradicted previous studies suggesting that T_{EM} had this migratory pattern. To resolve this contradiction, we visualized the migration of T_{EM} precursors, CX_3CR1^{hi} effector T cells (T_{Eff}), by intravital multi-photon microscopy (IV-MPM) in real-time. Surprisingly, CX_3CR1^{hi} T_{Eff} adhered to and patrolled along the dermal endothelium of mice. Specifically, migration was enriched along arteriolar endothelium and tended to be against blood flow. Patrolling occurred for both CX_3CR1^{hi} T_{Eff} and T_{EM} and was limited to CX_3CR1^{hi} $CD8^+$ T cells and CX_3CR1^{hi} monocytes, but was not dependent on functional CX_3CR1. Moreover, addition of cognate antigen (Ag) resulted in rapid stopping of Ag-specific T cells, suggesting that patrolling T cells scan arteriolar endothelium for cognate Ag. Together, these results challenge the paradigm that T_{EM} function by migration through peripheral tissues and establish a new migratory behavior by T_{EM} and their effector precursors that promotes intravascular scanning of arteriolar endothelium.

Table of Contents

Acknowledgments

I am indebted to many people who have helped to support and guide me along the meandering road towards a PhD. First, I would like to thank my thesis adviser, Uli von Andrian, who gave me the freedom to explore my scientific interests. He has never stopped questioning what I thought I knew and thinks outside of the box to address scientific problems. I can only hope that some of these traits have rubbed off on me. I would also like to thank my DAC members, Thorsten Mempel, Shannon Turley, Vijay Kuchroo, and Arlene Sharpe, as well as my dissertation defense examiners, Andy Lichtman, Mikael Pittet, and Darrell Irvine, who have generously taken the time to review and advise me on past and future experiments. I am also appreciative of the many members of the von Andrian lab, both past and present, who enriched my graduate experience and made the lab a fun place to be. To Carmen Gerlach, Mario Perro, David Alvarez, Ira Mazo, Aude Thiriot, Olga Barreiro, Rodrigo Gonzalez, and all the other foreigners that have come and gone, thank you for helpful research discussions and the constant reminder that there is a world outside of the United States. To Ashley Moseman, Jose Ordovas, and Jung Hwan Sung, thank you for creating such high expectations for what a graduate student can and should be.

I am also grateful to the mentors and programs that propelled me to graduate school. To Stephen Schoenberger, Ananda Goldrath, and Jayant Ghiara, who helped pique my interest in and supported my pursuit of a PhD in immunology. My appreciation goes to Harvard's Immunology Program and the Division of Medical Sciences for creating a welcoming, yet rigorous environment. I have made many friends within and

outside of Harvard, and I thank all of them for allowing my Boston experience to include camping and hiking adventures, river tubing, ski trips, happy hours, indoor soccer, and movie nights. To my former roommates Alex Kostic and Bryan McGuffie, thanks so much for all the good times.

Thank you to my east coast aunt and uncle, Beth and Jim, who provided a garage, a couch, or a respite from the city when I needed it. Three grandparents watched me start graduate school, but only one will see me finish. Even if they did not grasp exactly what I was doing, I am grateful for their tremendous enthusiasm towards my pursuits. I would also like to thank my brother, Eric Loughhead, who was always there for me when I needed a confidante or advice. To my parents, David Loughhead and Sandy McNabb, thank you so much for the support; financial, emotional, and otherwise that you have provided for me all these years. Also, thank you for always being there to remind me what the weather is like in California when a snowstorm is on its way towards Boston. Finally, I am deeply indebted to my girlfriend, Lauren Barclay, whose friendship, loyalty, and cooking nourishes me.

For my parents and brother

David, Sandy, and Eric

Chapter 1: Introduction

1.1 Immune surveillance

Mammals are rich in biological resources that include nucleotides, amino acids, and metabolites. As such, the body is under constant attack by bacteria, viruses, and tumor cells that seek to utilize an excessive share of resources at the expense of the host. The immune system acts as a filter that sifts through a tremendous amount of biomolecular information to limit resource utilization that is detrimental to the host. This feat requires a great deal of complexity as the immune system must accommodate proper function of organ systems while ruthlessly removing pathogenic microbes and cells. Additionally, the immune system must be efficient, so as to avoid incurring significant metabolic cost in its pursuit of pathogens. An elaborate division of labor between both hematopoietic and non-hematopoietic cells ensures that harm is recognized, contained, and that the appropriate effector cells are recruited to clear the noxious agent. Here, the focus will be placed on the role that dendritic cells (DCs) and $CD8^+$ T cells play in mediating effective protection of the host. Specifically, how distinct DC subsets acquire antigenic material and skew subsequent $CD8^+$ T cell responses towards particular fates, as well as how these induced $CD8^+$ T cell fates influence their surveillance behavior following pathogen clearance.

1.2 Dendritic cells: conductors of the adaptive orchestra

Naïve T cell responses are initiated in T cell zones of secondary lymphoid organs (SLOs) where DCs present antigens (Ags) that have been acquired peripherally or locally[1,2]. These naïve T cells will respond only to specific peptide-MHC (pMHC) complexes presented to them by resident or migratory DCs. Thus activated, naïve T cells

proliferate and differentiate according to pMHC and costimulatory molecule density, as well as cytokine milieu[3,4]. These activated T cells then egress from SLOs into the blood, now equipped with adhesive molecules to permit extravasation into peripheral tissues and licensed to kill. DCs therefore act as critical gatekeepers to the beneficial, as well as potentially deleterious effects of T cell responses.

DCs reside within peripheral tissues and SLOs and coordinately regulate antigen handling, migratory behavior, and stimulatory properties in order to maximize the likelihood that Ag-specific T cells will be effectively activated. Utilizing a plethora of receptors, DCs recognize pathogen-associated molecular patterns (PAMPs) that initiate a process called maturation. Maturation transiently increases the endocytic rate, which links internalized antigens to the inflammatory stimulus[5]. Additionally, DC endosomes are less acidic and contain fewer proteases than their macrophage counterparts, which minimizes Ag destruction and helps to preserve Ag for presentation to T cells[6]. DC activation by PAMPs also induces expression of the chemokine receptor, CCR7, which permits sensing of the chemotactic gradients that will guide peripheral DCs out of tissues and into draining lymph nodes (LNs)[1]. Once in the LN, DCs localize to the paracortex where CCR7-expressing T cells scan them for cognate Ag. Importantly, mice that lack CCR7 or its ligands fail to develop robust T cell responses due to the inefficiency with which T cells and DCs find each other[7,8]. Moreover, DC maturation induces upregulation of costimulatory surface molecules and cytokines that support T cell activation and priming, which will be discussed further in **1.6**.

The importance of DCs in eliciting T cell immunity was first appreciated using mixed lymphocyte reactions (MLR), where antigenic determinants are ill-defined[9].

Eventually, protein-pulsed DCs were shown to result in enhanced activation of T cells both *in vitro* and *in vivo*[10,11]. Punctual ablation of DCs using mice expressing diphtheria toxin receptor (DTR) under the control of the CD11c promoter demonstrated that CD11c-expressing cells are required for responses to listeria, malaria, HSV, and cell-associated Ag[12,13]. Interestingly, constitutive depletion of CD11c-expressing cells results in CD4 T cell-dependent auto-immunity, highlighting the alternative role for DCs in tolerance[14]. However, the results of these experiments are confounded by the fact that while CD11c is a marker of DCs, it is also expressed by a number of other cell populations, including macrophages. Using a more selective marker of conventional DCs, Zbtb46, to drive expression of DTR, investigators found that while T cell responses were impaired, this effect was muted compared to CD11c-DTR mice[15,16]. This suggests that the spared CD11c-expressing cells in this system have a non-redundant role in T cell immunity.

Conventional DCs (cDCs) can be divided into two distinct subsets based on phenotypic and functional attributes. The two subsets can be categorized as $CD8\alpha^+$ and $CD8\alpha^-$ DCs, so named for their phenotype within mouse spleen. Unfortunately, this poorly defines the two subsets because the CD8α DC subset does not express CD8α in peripheral tissues and is not present on the equivalent human DC subset[17,18]. Despite non-uniform expression of CD8α, these two subsets can generally be distinguished by expression of CD8α in lymphoid organs or CD103 in peripheral tissues for $CD8\alpha^+$ DC[18] whereas the $CD8\alpha^-$ subset can be distinguished by expression of either CD11b or CD4. While there may be distinctions within these subsets based on phenotype or tissue milieu, they will be referred to here as CD8 DCs and CD11b DCs.

Functionally, CD8 DCs appear to have a number of characteristics that aid in productive activation of $CD8^+$ T cells, while CD11b DCs support $CD4^+$ T cell activation. Strong evidence for this came from the identification that Ags targeted towards CD8 DCs primed $CD8^+$ T cell responses at the expense of $CD4^+$ T cell responses while Ags targeted towards CD11b DCs favored $CD4^+$ T cell responses[19]. Furthermore, CD8 DCs produce copious amounts of IL-12 compared to their CD11b counterparts. The importance of this is highlighted in *Toxoplasma gondii* infection where the absence of CD8 DCs leads to insufficient IL-12 production for effective $CD8^+$ T cell activation and consequent lethality[20]. CD8 DCs are also functionally distinct in their superior ability to cross-present Ags, as well as ingest apoptotic cells when compared to CD11b DCs. These features will be discussed in the next two sections.

1.3 Cross-presentation

$CD8^+$ T cells recognize peptides in the context of MHC-I. These MHC-I peptide complexes are derived from endogenous proteins, present in the cytosol, which are digested by the proteasome, and transported into the endoplasmic reticulum for MHC-I loading. Generally, this process serves to display to Ag-experienced $CD8^+$ T cells the intracellular contents of somatic cells. In this way, Ag-experienced $CD8^+$ T cells can scan the pMHC complexes on cells throughout the body and identify and kill any infected or transformed cells. However, priming of naïve $CD8^+$ T cells occurs in SLOs, where naïve T cells interact with DCs. Therefore, the classical MHC-I presentation pathway would require that DCs be directly infected or transformed in order for these peptides to be seen by naïve $CD8^+$ T cells. In 1976, it was identified that there is an exception to this

classical pathway, which has been termed cross-presentation[21]. Cross-presentation is the process by which exogenously derived peptide precursors are shunted towards the MHC-I pathway via endosomal escape into the cytosol or other mechanisms[22]. While the exact mechanism for this process remains elusive, the cues, context, and cellular players have become clearer.

Cross-presentation is most efficient among CD8 DCs[23]. When soluble antigen is given *in vitro* or *in vivo*, CD8 DCs drive greater proliferation of Ag-specific $CD8^+$ T cells on a per-cell basis compared to CD11b DCs[23,24]. While MHC-I presentation of soluble Ags is possible, it requires super-physiological concentrations of model Ags. Cross-presentation by CD8 DCs is most efficient for Ags present in apoptotic cells[25], which suggests that the manner in which Ags are recognized and internalized (i.e. soluble vs cell-associated) results in differential intracellular sorting of Ags for MHC-I or MHC-II presentation.

In less-contrived settings, where pathogens are used and Ag availability is not tightly controlled, CD8 DCs are still observed to be critical for priming $CD8^+$ T cell responses. Shortly after infection, when different DC populations are isolated from the draining LN for assessment of Ag presentation, pathogen-specific $CD8^+$ T cells proliferate in the presence of CD8 DCs, but not in the presence of CD11b DCs or pDCs[26]. This is true for infection with HSV [26,27], Vaccinia[28], Influenza [28], LCMV [29], and listeria[29]. Until recently, *in vivo* assessment of the functional role for CD8 DCs in CTL immunity has been hindered by lack of tools for depletion of this subset. However, the unexpected dependence of CD8 DCs on the transcription factor, BATF3, for development has permitted interrogation of the role for CD8 DCs in $CD8^+$ T cell responses[30]. These mice

have demonstrated a role for CD8 DCs in generating $CD8^+$ T cell responses to West Nile Virus[30], Influenza[31], and immunogenic tumors[30]. However, a compensatory role for BATF3 in C57BL/6 mice, in contrast to 129 SvEV mice, permits development of CD8 DCs[32] and limits a complete assessment of the role for CD8 DCs in the previously characterized systems, where immunodominant $CD8^+$ T cell epitopes are known[33].

1.4 Apoptotic cell acquisition by CD8 DCs: bring out your dead

Whereas CD8 DCs are proficient cross-presenters of soluble antigen both *in vitro* and *in vivo*[23,24], Ags from apoptotic cells are presented with greater efficiency. This is due to the unique ability of CD8 DCs to capture apoptotic cells compared to CD11b DCs[34,35]. During an infection, apoptotic cells will be enriched for relevant Ags, as their apoptosis is likely to be linked to the production of virions or other pathogenic material. In the steady state, apoptotic cells will also be generated and these Ags are presented in a tolerogenic context. Tolerogenic presentation of apoptotic cells will not be discussed further and the focus will be on productive priming of a $CD8^+$ T cell response in an inflammatory context.

Recognition and clearance of apoptotic cells is a critical aspect of homeostasis. Reflecting this importance, there are a number of receptors and bridge molecules that help to recognize apoptotic cells. Generally, apoptotic cells are recognized by phosphatidylserine (PS), which is normally retained on the inner leaflet of the plasma membrane, but is exposed during apoptosis. Since there are a multitude of PS receptors that could mediate capture by CD8 DCs, studies have generally focused on those receptors that are upregulated on CD8 DCs and absent on CD11b DCs.

The role for each of these receptors has been explored with different techniques and identified varying degrees of effect depending on the method of interrogation. There is, however, no consensus on which receptor(s) play(s) the dominant role in capture of apoptotic cells by CD8 DCs. DEC-205 is a C-type lectin that is over-expressed by CD8 DCs and plays a role in Ag uptake, but does not play a significant role in uptake of apoptotic cells[34]. CD36 is a scavenger receptor preferentially expressed by CD8 DCs, which was shown to play a role in capture of apoptotic cells by human monocyte-derived DCs (moDCs)[36], but subsequent studies in mice have not demonstrated a role for CD36 in apoptotic cell uptake by CD8 DCs [37,38]. The integrins $\alpha_V\beta_3$ and $\alpha_V\beta_5$ mediate uptake of apoptotic cells via the bridge molecule, milk fat globule-EGF factor 8 (MFG-E8), which has a PS binding domain. However, loss of these integrins does not significantly affect apoptotic cell uptake by CD8 DCs[38]. Scarf1 is another scavenger receptor that has been shown to mediate uptake utilizing the complement protein C1q as a bridge molecule. Studies *in vitro* and *in vivo* demonstrated that Scarf1 deficiency negatively affects apoptotic cell uptake by CD8 DCs, but was unable to show a defect in $CD8^+$ T cell priming[39]. A member of the Tyro-3, Axl, and Mer (TAM) family of receptor tyrosine kinases, Axl, reduces apoptotic cell uptake by bone marrow derived DCs (BMDCs) in combination with CD91[40]. Two members of the TIM (T-cell immunoglobulin domain and mucin domain) family of proteins have recently been identified as receptors for PS[41]. Blockade of TIM-3 partially blocks *in vitro* as well as *in vivo* uptake of apoptotic cells by DCs[42]. TIM-4, on the other hand, has been shown to be critically required for efferocytosis by peritoneal macrophages[43], but this requirement has not been assessed on CD8 DCs. The C-type lectin, Clec9a, is unusual in that it recognizes exposed F-actin

from necrotic cells[44], but is not necessary for apoptotic cell uptake. Instead, it is required for proper intracellular sorting of the necrotic cargo for subsequent cross-presentation[45]. Mice deficient in Clec9a have impaired CD8 T cell responses to HSV-1[46], vaccinia[47], and necrotic cell-associated antigen[46].

While CD8 DCs are required for cross-priming of CTLs in some models and this subset is known to engulf apoptotic cells efficiently, these two properties have not been mechanistically linked. **Chapter 2** will discuss whether the PS receptor, TIM-4, can link these two properties.

1.5 Three signal model of T cell activation

Naive $CD8^+$ T cells are primed within SLOs, where they interact with and search for their cognate Ag on DCs. Ag-laden DCs migrate from the periphery and convey a great deal of information for interpretation by T cells. This information is then integrated by T cells to determine whether to respond, and if so, what degree of response is required. These signals come in three forms: 1. TCR-pMHC engagement 2. Costimulatory/co-inhibitory surface interactions and 3. Soluble cytokines (**Figure 1.1**).

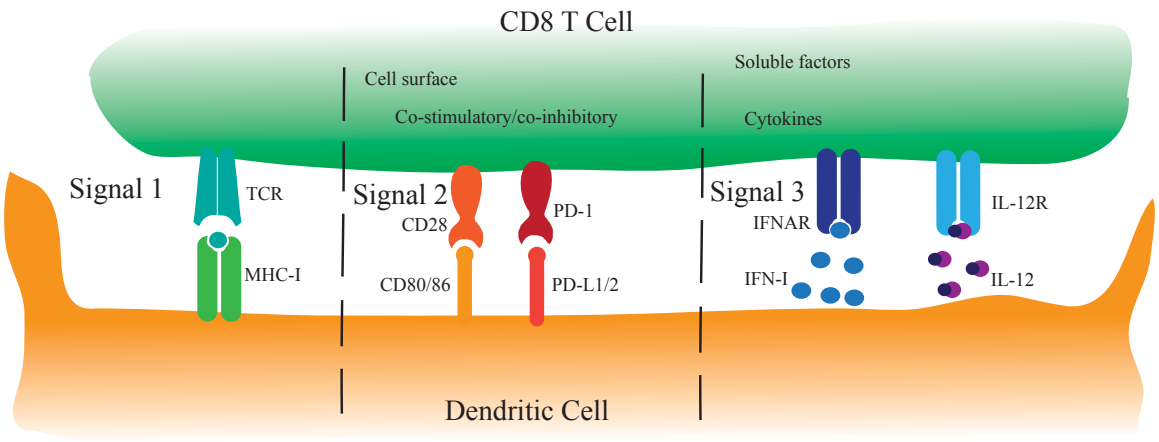

Figure 1.1: Three signals of T cell activation. Efficient T cell activation is comprised of three distinct signals. The receptive $CD8^+$ T cell (green) is shown interacting with a DC (orange).

Signal 1, TCR engagement, ensures specificity of the response and can be controlled at a number of different levels. The TCR repertoire contains a vast array of TCRs with varying affinities for particular Ags. High affinity interactions generate stronger TCR signaling and therefore greater expansion[48]. Signal strength can also be altered by the abundance of recognized pMHC complexes on the presenting cell. This acts to promote the production of $CD8^+$ T cells that effectively recognize the molecular constituents of the offending pathogen. Lastly, the duration that these pMHC complexes are present will influence the strength of signal 1. This can be altered by the stability of particular peptides within the peptide-binding groove of MHC-I, which will alter the half-life, and affect the duration of signaling[49]. Additionally, if pathogenic production of proteins continues, a steady source of Ag-loaded DCs will arrive from the periphery, providing a steady, durable source of pMHC complexes for TCR signaling.

Signals 2 and 3 provide inflammatory context, which help to amplify or dampen $CD8^+$ T cell responses. Signal 2 interactions occur via contact-dependent surface interactions with co-stimulatory or co-inhibitory molecules. CD28 and other co-stimulatory molecules amplify TCR signal strength, as well as alter cellular metabolism, cytokine production, and effector functions that promote T cell efficacy[50,51]. Co-inhibitory molecules like PD-1 serve as the counterpoint and dampen T cell responses[52]. The ligands for these receptors are expressed with variable distribution and timing, some being restricted to professional APCs, while others are expressed throughout the body. In general, their expression serves to communicate whether inflammation or tolerance is desired.

Signal 3 is a catch-all term for soluble signals that influence T cell responses. The inflammatory cytokines IFN-I and IL-12 can often have profound effects on the overall expansion and effector function of T cells during infection[53]. For example, T cells deficient in the receptor for IFN-I, IFNAR, fail to expand during LCMV infection[54], while T cells deficient in the IL-12R are impaired during vaccinia or listeria infection[55]. Aside from inflammatory cues, signal 3 may act to provide homing cues regarding the tissues affected. Through tissue metabolites, migratory DCs from the skin or peyer's patches induce distinct homing receptors on T cells that facilitate their efficient recruitment to target tissues[56,57].

These signals therefore act in concert to ensure a targeted, Ag-specific response is generated in a magnitude that is commensurate with the threat posed to the host[58]. While many of these signals have clear roles in determining T cell fates, whether or not subsets of DCs promote distinct fates during the long-term interaction that occurs during

priming[59] has not been explored. **Chapter 2** will address whether CD8 DCs or CD11b DCs promote distinct T cell fates during this initial encounter.

1.6 $CD8^+$ T cell subsets: division of labor

During an acute viral infection, pathogen-specific $CD8^+$ T cells expand vigorously until the pathogen is cleared. Following clearance, T cells undergo a massive contraction as Ag and inflammatory cytokines are withdrawn. A few weeks later, contraction is largely complete and a population of persisting memory T cells remains. These cells confer superior protection to the host upon secondary challenge due to greater precursor frequency, rapid proliferation, cytotoxic potential, and localization throughout the host. This expansion of T cells is, however, heterogeneous and groups of T cells can be binned into subsets based on phenotype, cytotoxicity, proliferative capacity, memory potential, and migratory behavior. In this way, T cell subsets serve to optimally protect the host.

Memory T cell survival

While there is a steep contraction phase following an acute T cell response, wherein 90-95% of effector T cells (T_{Eff}) die off, this levels off and a population of memory T cells (T_{Mem}) persists long-term. By comparing the phenotypic and transcriptional profile of T_{Eff} and T_{Mem}, a number of key factors have been identified as important for maintenance of T_{Mem}. During the effector phase, T_{Eff} express low levels of the anti-apoptotic factor, Bcl-2, and are susceptible to Bim-mediated apoptosis[60]. As contraction occurs, Bcl-2 expression among surviving T cells increases, suggestive of its

role in the survival of T_{Mem}[61]. The cytokines IL-7 and IL-15 also contribute to the persistence of T_{Mem}. IL-7 provides a survival signal for maintenance while IL-15 signaling results in a low level of basal proliferation[62]. Interestingly, TCR signaling, even at the level of low affinity, non-specific, MHC-I interactions does not appear to play a role in the maintenance of T_{Mem}[63]. Taken together, stable T_{Mem} populations are maintained through a balance between survival and proliferation.

Central vs effector memory

Among the circulating population of T_{Mem}, two subsets have been described based on the expression of the LN-homing molecules CCR7 and CD62L. Central memory T cells (T_{CM}) are defined as $CCR7^{+}CD62L^{+}$, while effector memory T cells (T_{EM}) are $CCR7^{-}CD62L^{-}$[64]. As such, T_{CM} circulate through SLOs while T_{EM} express inflammatory chemokine receptors that are believed to result in migration through peripheral tissues. T_{CM} proliferate and accumulate rapidly following re-challenge[65,66], but are slower to exert effector function compared to their T_{EM} counterparts[67]. This suggests a division of labor wherein T_{EM} circulate through peripheral tissues, ready to deploy immediate cytotoxicity while T_{CM} circulate through LNs, prepared to proliferate and provide a secondary influx of Ag-specific cells to combat the detected insult.

Defining lineage relationships

Naïve T cells (T_N) act as stem cells that can differentiate into the subsequent T_{Eff} and T_{Mem} populations. The precursor-product relationship between the subsets that can be identified in the effector and memory phase is one that has and continues to confound

immunologists. One of the inherent problems with defining these relationships is that many of the cardinal features of T_{Mem} cells are lost on T_{Eff}. This is true for both activated T_N and T_{Mem}, which lose CCR7 and CD62L in the effector phase. During contraction, CCR7 and CD62L are slowly reacquired by a subset of cells. The kinetics of this led to speculation that T_{EM} give rise to T_{CM} as the percentage of $CCR7^-CD62L^-$ (T_{EM}) population fell, while the $CCR7^+CD62L^+$ (T_{CM}) grew[65]. Additionally, infection following transfer of $CD62L^-$ T_{EM} generated both $CD62L^+$, as well as $CD62L^-$ T_{Mem}, while infection following transfer of $CD62L^+$ T_{CM} gave only $CD62L^+$ T_{Mem}. This suggested that T_{CM} was the more terminally differentiated cell type since it could give rise only to itself while T_{EM} appeared capable of generating both itself and T_{CM}[65]. However, these experiments were done using transfer of non-physiological numbers of TCR-tg T cells[68,69]. When $CD62L^-$ T_{Mem} were derived from endogenous Ag-specific T cells, transfer experiments showed that this was a stable phenotype that did not convert to $CD62L^{+}$[70] (**Figure 1.2**).

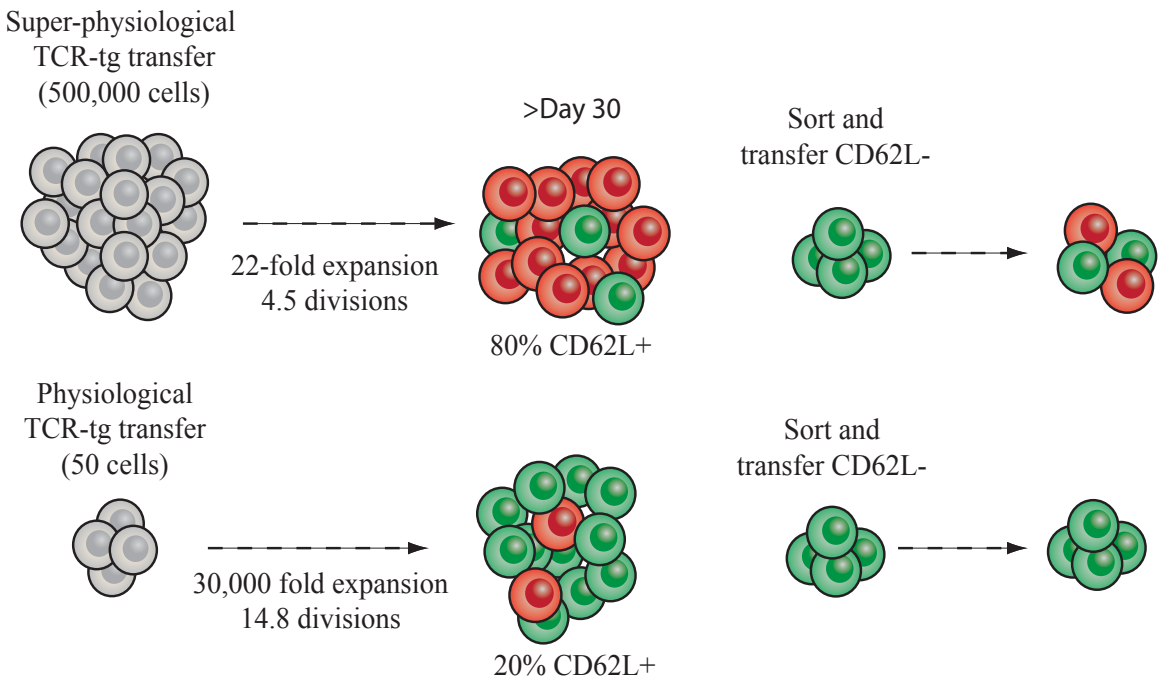

Figure 1.2: Establishing lineage relationships. Adoptive transfer of super-physiological numbers of naïve Ag-specific T cells (grey) and subsequent infection drives less expansion and greater numbers of $CD62L^+$ T cells (red) in the memory phase when compared to adoptive transfer of physiological numbers of Ag-specific T cells. Sorting and transfer of $CD62L^-$ T cells (green) from these settings gives rise to the indicated distribution of CD62L subsets in the ensuing memory phase[65,70].

Given that CCR7 and CD62L are lost in the effector phase, other markers have been used as surrogates to predict persistence and reacquisition of T_{Mem} markers. KLRG-1 and IL-7Rα together predict the persistence and cytokine profile of T_{Eff} in the memory phase[71,72]. Generally, KLRG-1^+IL-7Rα^- T_{Eff} are more susceptible to death during the contraction phase and produce less IL-2, consistent with a T_{EM} fate, while the persistence and cytokine profile of KLRG-1^-IL-7Rα^+ T_{Eff} is consistent with a T_{CM} fate. Ag and inflammatory duration drive greater proliferation, terminal differentiation, and favor T_{EM}

development[68,71,73]. This is consistent with a linear differentiation model, wherein an accumulation of TCR and inflammatory signaling promote differentiation towards T_{EM} with reduced pluripotency compared to T_{CM}.

An alternative hypothesis is that naïve T cell precursors are more susceptible to particular fates, given the same signaling context. While this predilection has not been formally ruled out, single naïve precursors are capable of producing a wide array of T cell fates[74]. Additionally, single precursors that have undergone extensive proliferation assume a terminally differentiated T_{EM} phenotype, while single precursors that have generated smaller "families" are more likely to express CD62L and CD27, markers of T_{CM}[75,76]. This is again consistent with the concept that greater proliferation drives further differentiation and suggests a linear differentiation model.

1.7 T cell migration: where do memories go?

Following priming in LNs, $CD8^+$ T cells egress via the efferent lymph and are carried back into the blood[77]. Guided by chemokine gradients and retained by antigen, T cells quickly extravasate into inflamed tissues and exert their effector functions.

T_{CM} populations are equipped with the LN-homing molecules CCR7 and CD62L, whereas T_{EM} are not. Given that T cells isolated from the afferent lymph, which drains peripheral tissues, were found to be ag-experienced[78], T_{EM} were ascribed to be the memory population that migrates through peripheral tissues and through the afferent lymph on its way back to the blood. This provided an elegant mechanism of surveillance, wherein T_{CM} surveyed tissue-draining antigens via LN interactions, providing reactive memory, while T_{EM} surveyed peripheral tissues directly, providing protective memory[79].

Evidence for this hypothesis accumulated as investigators expanded their tissues of interrogation and found T cells in peripheral tissues that were $CD62L^-$ and displayed an activated phenotype, even in the absence of apparent stimulation[80-82]. The relationship between these tissue-isolated cells and those cells isolated from the afferent lymph remained to be determined. The tissue-isolated T cells could be transient migrants, poised to enter afferent lymph; alternatively, they could be resident. Evidence for the latter emerged when tissue graft studies demonstrated that memory T cells from skin failed to emigrate from the tissue or join the circulating pool[83]. Parabiosis studies of immune and naïve mice further solidified the case that tissue-resident T cells fail to re-enter the circulating pool of memory T cells and are retained long-term within the tissue[84]. These cells are now termed tissue-resident memory T cells (T_{RM}) and form an integral part of T cell-mediated protection.

T_{RM} generation, maintenance, and function

The generation of T_{RM} is now appreciated as a common feature of the T cell response to infection. During the effector phase, T cells are recruited to tissues by inflammatory chemokines and a fraction of these will persist long-term in the absence of further antigenic stimulation[85]. Following infection, there is a transient window for seeding of peripheral tissues related to the Ag-induced plasticity of T cells, as well as the presence of inflammatory chemokines for recruitment[86]. Infection of tissues induces local chemokine production, which effectively recruits T_{Eff} cells and generates a T_{RM} population proportionate to the level of local inflammation[84]. Interestingly, KLRG-1^+ and KLRG-1^- T_{Eff} cells are recruited to the tissue, but KLRG-1^+ T_{Eff} cells are not capable of

generating T_{RM}[87]. It is not currently understood why KLRG-1$^+$ cells do not give rise to T_{RM}, but it may be related to a number of migratory requirements and tissue signals that are not effectively perceived by these KLRG-1$^+$ T cells.

Once in the tissue, the phenotype and transcriptional profile of T_{Eff} begins to change. These changes vary by tissue, are induced by signals within the tissue, and are necessary for survival and residence[87]. TGF-β signaling promotes upregulation of molecules involved in retaining cells within the tissue while IL-15 promotes survival[87]. T cells are retained by down-regulation of Klf2, which down-regulates S1PR1[88] and reduces egress from the tissue[89]. Upregulation of CD69 similarly promotes retention by metabolizing S1P ligands and preventing egress[87,89]. The integrin, CD103, binds to tissue-derived E-cadherin and its expression is correlated with T_{RM} and promotes tissue retention[87,90,91].

Once resident, T_{RM} provide local protection that is superior to that conferred by circulating T_{Mem}[83,84]. Protection presumably depends to some extent on direct killing of infected target cells, although this remains to be shown. However, TCR-triggering of T_{RM} results in the production of a number of effector cytokines that act on local cells to promote an environment that will effectively quench recurring infection. IFNγ production promotes inflammatory chemokine production that recruits circulating T_{Mem}[92] and the generation of an anti-viral state to limit productive infection of the local parenchyma[93]. Additionally, TNFα facilitates maturation and migration of DCs while IL-2 bolsters NK cell activity[94].

T_{CM}, T_{EM}, and T_{RM}: Putting it all together

As discussed above, much has been learned in the last few years about the generation, maintenance, and function of T_{RM}. However, the way that this newly discovered subset fits into the T_{CM}/T_{EM} paradigm needs to be re-visited. The original dogma for immune surveillance proposed that T_{CM} surveyed SLOs while T_{EM} migrated through peripheral tissues (**Figure 1.3**), which provided an elegant system for scanning the body for recurring insult. As the relative importance for T_{RM} in scanning peripheral tissues continues to grow[95], the more we must reconsider the conclusion that activated T cells in afferent lymph[78] are indeed T_{EM}. As part of this re-examination, we should be prepared to address the role for T_{EM} if they do not migrate through peripheral tissues. These are issues that will be dealt with and discussed in **Chapter 3** and **Chapter 4**.

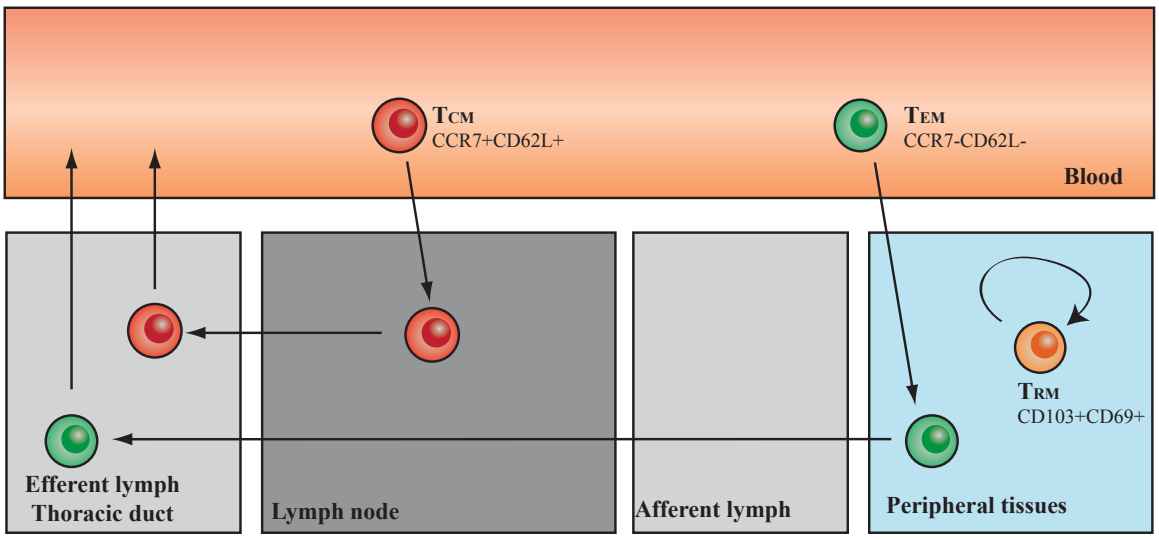

Figure 1.3: Migratory patterns of T_{CM}, T_{EM}, and T_{RM}. T_{CM} (red) are defined by expression of the LN-trafficking molecules CCR7 and CD62L and circulate through blood and LNs. T_{EM} (green) lack CCR7 and CD62L and are presumed to migrate through peripheral tissues, which they exit via the afferent lymph and re-enter the circulation. T_{RM} (orange) fail to circulate, are retained within peripheral tissues, and express CD103 and CD69.

1.8 References

1. Alvarez, D., Vollmann, E. H. & Andrian, von, U. H. Mechanisms and consequences of dendritic cell migration. *Immunity* **29,** 325–342 (2008).
2. Lanzavecchia, A. & Sallusto, F. Regulation of T cell immunity by dendritic cells. *Cell* **106,** 263–266 (2001).
3. Henrickson, S. E., Perro, M., Loughhead, S. M., Senman, B., Stutte, S., Quigley, M., Alexe, G., Iannacone, M., Flynn, M. P., Omid, S., Jesneck, J. L., Imam, S., Mempel, T. R., Mazo, I. B., Haining, W. N. & Andrian, von, U. H. Antigen

availability determines $CD8^+$ T cell-dendritic cell interaction kinetics and memory fate decisions. *Immunity* **39,** 496–507 (2013).

4. Andrian, von, U. H. & Mempel, T. R. Homing and cellular traffic in lymph nodes. *Nat Rev Immunol* **3,** 867–878 (2003).

5. West, M. A., Wallin, R. P. A., Matthews, S. P., Svensson, H. G., Zaru, R., Ljunggren, H.-G., Prescott, A. R. & Watts, C. Enhanced dendritic cell antigen capture via toll-like receptor-induced actin remodeling. *Science* **305,** 1153–1157 (2004).

6. Savina, A., Jancic, C., Hugues, S., Guermonprez, P., Vargas, P., Moura, I. C., Lennon-Duménil, A.-M., Seabra, M. C., Raposo, G. & Amigorena, S. NOX2 controls phagosomal pH to regulate antigen processing during crosspresentation by dendritic cells. *Cell* **126,** 205–218 (2006).

7. Förster, R., Schubel, A., Breitfeld, D., Kremmer, E., Renner-Müller, I., Wolf, E. & Lipp, M. CCR7 Coordinates the Primary Immune Response by Establishing Functional Microenvironments in Secondary Lymphoid Organs. *Cell* **99,** 23–33 (1999).

8. Gunn, M. D., Kyuwa, S., Tam, C., Kakiuchi, T., Matsuzawa, A., Williams, L. T. & Nakano, H. Mice lacking expression of secondary lymphoid organ chemokine have defects in lymphocyte homing and dendritic cell localization. *J Exp Med* **189,** 451–460 (1999).

9. Inaba, K., Young, J. W. & Steinman, R. M. Direct activation of CD8+ cytotoxic T lymphocytes by dendritic cells. *J Exp Med* **166,** 182–194 (1987).

10. Inaba, K., Metlay, J. P., Crowley, M. T. & Steinman, R. M. Dendritic cells pulsed

with protein antigens in vitro can prime antigen-specific, MHC-restricted T cells in situ. *J Exp Med* **172,** 631–640 (1990).

11. Crowley, M., Inaba, K. & Steinman, R. M. Dendritic cells are the principal cells in mouse spleen bearing immunogenic fragments of foreign proteins. *J Exp Med* **172,** 383–386 (1990).

12. Kassim, S. H., Rajasagi, N. K., Zhao, X., Chervenak, R. & Jennings, S. R. In vivo ablation of CD11c-positive dendritic cells increases susceptibility to herpes simplex virus type 1 infection and diminishes NK and T-cell responses. *J Virol* **80,** 3985–3993 (2006).

13. Jung, S., Unutmaz, D., Wong, P., Sano, G.-I., De los Santos, K., Sparwasser, T., Wu, S., Vuthoori, S., Ko, K., Zavala, F., Pamer, E. G., Littman, D. R. & Lang, R. A. In vivo depletion of CD11c+ dendritic cells abrogates priming of CD8+ T cells by exogenous cell-associated antigens. *Immunity* **17,** 211–220 (2002).

14. Ohnmacht, C., Pullner, A., King, S. B. S., Drexler, I., Meier, S., Brocker, T. & Voehringer, D. Constitutive ablation of dendritic cells breaks self-tolerance of CD4 T cells and results in spontaneous fatal autoimmunity. *Journal of Experimental Medicine* **206,** 549–559 (2009).

15. Meredith, M. M., Liu, K., Darrasse-Jeze, G., Kamphorst, A. O., Schreiber, H. A., Guermonprez, P., Idoyaga, J., Cheong, C., Yao, K. H., Niec, R. E. & Nussenzweig, M. C. Expression of the zinc finger transcription factor zDC (Zbtb46, Btbd4) defines the classical dendritic cell lineage. *Journal of Experimental Medicine* **209,** 1153–1165 (2012).

16. Satpathy, A. T., KC, W., Albring, J. C., Edelson, B. T., Kretzer, N. M.,

Bhattacharya, D., Murphy, T. L. & Murphy, K. M. Zbtb46 expression distinguishes classical dendritic cells and their committed progenitors from other immune lineages. *Journal of Experimental Medicine* **209,** 1135–1152 (2012).

17. Poulin, L. F., Salio, M., Griessinger, E., Anjos-Afonso, F., Craciun, L., Chen, J.-L., Keller, A. M., Joffre, O., Zelenay, S., Nye, E., Le Moine, A., Faure, F., Donckier, V., Sancho, D., Cerundolo, V., Bonnet, D. & Reis e Sousa, C. Characterization of human DNGR-1+ BDCA3+ leukocytes as putative equivalents of mouse CD8alpha+ dendritic cells. *Journal of Experimental Medicine* **207,** 1261–1271 (2010).
18. Edelson, B. T., KC, W., Juang, R., Kohyama, M., Benoit, L. A., Klekotka, P. A., Moon, C., Albring, J. C., Ise, W., Michael, D. G., Bhattacharya, D., Stappenbeck, T. S., Holtzman, M. J., Sung, S.-S. J., Murphy, T. L., Hildner, K. & Murphy, K. M. Peripheral CD103+ dendritic cells form a unified subset developmentally related to CD8alpha+ conventional dendritic cells. *Journal of Experimental Medicine* **207,** 823–836 (2010).
19. Dudziak, D., Kamphorst, A. O., Heidkamp, G. F., Buchholz, V. R., Trumpfheller, C., Yamazaki, S., Cheong, C., Liu, K., Lee, H.-W., Park, C. G., Steinman, R. M. & Nussenzweig, M. C. Differential antigen processing by dendritic cell subsets in vivo. *Science* **315,** 107–111 (2007).
20. Mashayekhi, M., Sandau, M. M., Dunay, I. R., Frickel, E. M., Khan, A., Goldszmid, R. S., Sher, A., Ploegh, H. L., Murphy, T. L., Sibley, L. D. & Murphy, K. M. CD8α(+) dendritic cells are the critical source of interleukin-12 that controls acute infection by Toxoplasma gondii tachyzoites. *Immunity* **35,** 249–259 (2011).

21. Bevan, M. J. Cross-priming for a secondary cytotoxic response to minor H antigens with H-2 congenic cells which do not cross-react in the cytotoxic assay. *J Exp Med* **143,** 1283–1288 (1976).

22. Vyas, J. M., Van Der Veen, A. G. & Ploegh, H. L. The known unknowns of antigen processing and presentation. *Nat Rev Immunol* **8,** 607–618 (2008).

23. Schnorrer, P., Behrens, G. M. N., Wilson, N. S., Pooley, J. L., Smith, C. M., El-Sukkari, D., Davey, G., Kupresanin, F., Li, M., Maraskovsky, E., Belz, G. T., Carbone, F. R., Shortman, K., Heath, W. R. & Villadangos, J. A. The dominant role of CD8+ dendritic cells in cross-presentation is not dictated by antigen capture. *Proc Natl Acad Sci USA* **103,** 10729–10734 (2006).

24. Pooley, J. L., Heath, W. R. & Shortman, K. Cutting edge: intravenous soluble antigen is presented to CD4 T cells by CD8- dendritic cells, but cross-presented to CD8 T cells by CD8+ dendritic cells. *The Journal of Immunology* **166,** 5327–5330 (2001).

25. Haan, den, J. M., Lehar, S. M. & Bevan, M. J. CD8(+) but not CD8(-) dendritic cells cross-prime cytotoxic T cells in vivo. *J Exp Med* **192,** 1685–1696 (2000).

26. Allan, R. S., Smith, C. M., Belz, G. T., van Lint, A. L., Wakim, L. M., Heath, W. R. & Carbone, F. R. Epidermal viral immunity induced by CD8alpha+ dendritic cells but not by Langerhans cells. *Science* **301,** 1925–1928 (2003).

27. Smith, C. M., Belz, G. T., Wilson, N. S., Villadangos, J. A., Shortman, K., Carbone, F. R. & Heath, W. R. Cutting edge: conventional CD8 alpha+ dendritic cells are preferentially involved in CTL priming after footpad infection with herpes simplex virus-1. *The Journal of Immunology* **170,** 4437–4440 (2003).

28. Belz, G. T., Smith, C. M., Eichner, D., Shortman, K., Karupiah, G., Carbone, F. R. & Heath, W. R. Cutting edge: conventional CD8 alpha+ dendritic cells are generally involved in priming CTL immunity to viruses. *The Journal of Immunology* **172,** 1996–2000 (2004).

29. Belz, G. T., Shortman, K., Bevan, M. J. & Heath, W. R. CD8alpha+ dendritic cells selectively present MHC class I-restricted noncytolytic viral and intracellular bacterial antigens in vivo. *The Journal of Immunology* **175,** 196–200 (2005).

30. Hildner, K., Edelson, B. T., Purtha, W. E., Diamond, M., Matsushita, H., Kohyama, M., Calderon, B., Schraml, B. U., Unanue, E. R., Diamond, M. S., Schreiber, R. D., Murphy, T. L. & Murphy, K. M. Batf3 deficiency reveals a critical role for CD8alpha+ dendritic cells in cytotoxic T cell immunity. *Science* **322,** 1097–1100 (2008).

31. Waithman, J., Zanker, D., Xiao, K., Oveissi, S., Wylie, B., Ng, R., Tögel, L. & Chen, W. Resident CD8(+) and migratory CD103(+) dendritic cells control CD8 T cell immunity during acute influenza infection. *PLoS ONE* **8,** e66136 (2013).

32. Tussiwand, R., Lee, W.-L., Murphy, T. L., Mashayekhi, M., Wumesh, K. C., Albring, J. C., Satpathy, A. T., Rotondo, J. A., Edelson, B. T., Kretzer, N. M., Wu, X., Weiss, L. A., Glasmacher, E., Li, P., Liao, W., Behnke, M., Lam, S. S. K., Aurthur, C. T., Leonard, W. J., Singh, H., Stallings, C. L., Sibley, L. D., Schreiber, R. D. & Murphy, K. M. Compensatory dendritic cell development mediated by BATF-IRF interactions. *Nature* **490,** 502–507 (2012).

33. Mott, K. R., Maazi, H., Allen, S. J., Zandian, M., Matundan, H., Ghiasi, Y. N., Sharifi, B. G., Underhill, D., Akbari, O. & Ghiasi, H. Batf3 deficiency is not

critical for the generation of CD8α$^+$ dendritic cells. *Immunobiology* **220,** 518–524 (2015).

34. Iyoda, T., Shimoyama, S., Liu, K., Omatsu, Y., Akiyama, Y., Maeda, Y., Takahara, K., Steinman, R. M. & Inaba, K. The CD8+ dendritic cell subset selectively endocytoses dying cells in culture and in vivo. *J Exp Med* **195,** 1289–1302 (2002).

35. Desch, A. N., Randolph, G. J., Murphy, K., Gautier, E. L., Kedl, R. M., Lahoud, M. H., Caminschi, I., Shortman, K., Henson, P. M. & Jakubzick, C. V. CD103+ pulmonary dendritic cells preferentially acquire and present apoptotic cell-associated antigen. *Journal of Experimental Medicine* **208,** 1789–1797 (2011).

36. Albert, M. L., Pearce, S. F., Francisco, L. M., Sauter, B., Roy, P., Silverstein, R. L. & Bhardwaj, N. Immature dendritic cells phagocytose apoptotic cells via alphavbeta5 and CD36, and cross-present antigens to cytotoxic T lymphocytes. *J Exp Med* **188,** 1359–1368 (1998).

37. Belz, G. T., Vremec, D., Febbraio, M., Corcoran, L., Shortman, K., Carbone, F. R. & Heath, W. R. CD36 is differentially expressed by CD8+ splenic dendritic cells but is not required for cross-presentation in vivo. *The Journal of Immunology* **168,** 6066–6070 (2002).

38. Schulz, O., Pennington, D. J., Hodivala-Dilke, K., Febbraio, M. & Sousa, C. R. E. CD36 or alphavbeta3 and alphavbeta5 integrins are not essential for MHC class I cross-presentation of cell-associated antigen by CD8 alpha+ murine dendritic cells. *J Immunol* **168,** 6057–6065 (2002).

39. Ramirez-Ortiz, Z. G., Pendergraft, W. F., Prasad, A., Byrne, M. H., Iram, T.,

Blanchette, C. J., Luster, A. D., Hacohen, N., Khoury, El, J. & Means, T. K. The scavenger receptor SCARF1 mediates the clearance of apoptotic cells and prevents autoimmunity. *Nat Immunol* **14,** 917–926 (2013).

40. Subramanian, M., Hayes, C. D., Thome, J. J., Thorp, E., Matsushima, G. K., Herz, J., Farber, D. L., Liu, K., Lakshmana, M. & Tabas, I. An AXL/LRP-1/RANBP9 complex mediates DC efferocytosis and antigen cross-presentation in vivo. *J. Clin. Invest.* **124,** 1296–1308 (2014).

41. Kuchroo, V. K., Dardalhon, V., Xiao, S. & Anderson, A. C. New roles for TIM family members in immune regulation. *Nat Rev Immunol* **8,** 577–580 (2008).

42. Nakayama, M., Akiba, H., Takeda, K., Kojima, Y., Hashiguchi, M., Azuma, M., Yagita, H. & Okumura, K. Tim-3 mediates phagocytosis of apoptotic cells and cross-presentation. *Blood* **113,** 3821–3830 (2009).

43. Miyanishi, M., Tada, K., Koike, M., Uchiyama, Y., Kitamura, T. & Nagata, S. Identification of Tim4 as a phosphatidylserine receptor. *Nature* **450,** 435–439 (2007).

44. Ahrens, S., Zelenay, S., Sancho, D., Hanč, P., Kjær, S., Feest, C., Fletcher, G., Durkin, C., Postigo, A., Skehel, M., Batista, F., Thompson, B., Way, M., Reis e Sousa, C. & Schulz, O. F-Actin Is an Evolutionarily Conserved Damage-Associated Molecular Pattern Recognized by DNGR-1, a Receptor for Dead Cells. *Immunity* **36,** 635–645 (2012).

45. Sancho, D., Joffre, O. P., Keller, A. M., Rogers, N. C., Martínez, D., Hernanz-Falcón, P., Rosewell, I. & Reis e Sousa, C. Identification of a dendritic cell receptor that couples sensing of necrosis to immunity. *Nature* **458,** 899–903

(2009).

46. Zelenay, S., Keller, A. M., Whitney, P. G., Schraml, B. U., Deddouche, S., Rogers, N. C., Schulz, O., Sancho, D. & Reis e Sousa, C. The dendritic cell receptor DNGR-1 controls endocytic handling of necrotic cell antigens to favor cross-priming of CTLs in virus-infected mice. *J. Clin. Invest.* **122,** 1615–1627 (2012).

47. Iborra, S., Izquierdo, H. M., Martínez-López, M., Blanco-Menéndez, N., Reis e Sousa, C. & Sancho, D. The DC receptor DNGR-1 mediates cross-priming of CTLs during vaccinia virus infection in mice. *J. Clin. Invest.* **122,** 1628–1643 (2012).

48. Zehn, D., Lee, S. Y. & Bevan, M. J. Complete but curtailed T-cell response to very low-affinity antigen. *Nature* **458,** 211–214 (2009).

49. Henrickson, S. E., Mempel, T. R., Mazo, I. B., Liu, B., Artyomov, M. N., Zheng, H., Peixoto, A., Flynn, M. P., Senman, B., Junt, T., Wong, H. C., Chakraborty, A. K. & Andrian, von, U. H. T cell sensing of antigen dose governs interactive behavior with dendritic cells and sets a threshold for T cell activation. *Nat Immunol* **9,** 282–291 (2008).

50. Greenwald, R. J., Freeman, G. J. & Sharpe, A. H. The B7 family revisited. *Annu. Rev. Immunol.* **23,** 515–548 (2005).

51. Watts, T. H. TNF/TNFR family members in costimulation of T cell responses. *Annu. Rev. Immunol.* **23,** 23–68 (2005).

52. Chen, L. & Flies, D. B. Molecular mechanisms of T cell co-stimulation and co-inhibition. *Nat Rev Immunol* **13,** 227–242 (2013).

53. Curtsinger, J. M. & Mescher, M. F. Inflammatory cytokines as a third signal for T

cell activation. *Curr Opin Immunol* 1–8 (2010). doi:10.1016/j.coi.2010.02.013

54. Kolumam, G. A., Thomas, S., Thompson, L. J., Sprent, J. & Murali-Krishna, K. Type I interferons act directly on CD8 T cells to allow clonal expansion and memory formation in response to viral infection. *J Exp Med* **202,** 637–650 (2005).

55. Xiao, Z., Casey, K. A., Jameson, S. C., Curtsinger, J. M. & Mescher, M. F. Programming for CD8 T cell memory development requires IL-12 or type I IFN. *J Immunol* **182,** 2786–2794 (2009).

56. Sigmundsdottir, H., Pan, J., Debes, G. F., Alt, C., Habtezion, A., Soler, D. & Butcher, E. C. DCs metabolize sunlight-induced vitamin D3 to 'program' T cell attraction to the epidermal chemokine CCL27. *Nat Immunol* **8,** 285–293 (2007).

57. Mora, J. R., Bono, M.-R., Manjunath, N., Weninger, W., Cavanagh, L. L., Rosemblatt, M. & Andrian, von, U. H. Selective imprinting of gut-homing T cells by Peyer's patch dendritic cells. *Nature* **424,** 88–93 (2003).

58. Marchingo, J. M., Kan, A., Sutherland, R. M., Duffy, K. R., Wellard, C. J., Belz, G. T., Lew, A. M., Dowling, M. R., Heinzel, S. & Hodgkin, P. D. T cell signaling. Antigen affinity, costimulation, and cytokine inputs sum linearly to amplify T cell expansion. *Science* **346,** 1123–1127 (2014).

59. Mempel, T. R., Henrickson, S. E. & Andrian, von, U. H. T-cell priming by dendritic cells in lymph nodes occurs in three distinct phases. *Nature* **427,** 154–159 (2004).

60. Hughes, P. D., Belz, G. T., Fortner, K. A., Budd, R. C., Strasser, A. & Bouillet, P. Apoptosis regulators Fas and Bim cooperate in shutdown of chronic immune responses and prevention of autoimmunity. *Immunity* **28,** 197–205 (2008).

61. Grayson, J. M., Zajac, A. J., Altman, J. D. & Ahmed, R. Cutting edge: increased expression of Bcl-2 in antigen-specific memory CD8+ T cells. *The Journal of Immunology* **164,** 3950–3954 (2000).

62. Goldrath, A. W., Sivakumar, P. V., Glaccum, M., Kennedy, M. K., Bevan, M. J., Benoist, C., Mathis, D. & Butz, E. A. Cytokine requirements for acute and Basal homeostatic proliferation of naive and memory CD8+ T cells. *J Exp Med* **195,** 1515–1522 (2002).

63. Murali-Krishna, K., Lau, L. L., Sambhara, S., Lemonnier, F., Altman, J. & Ahmed, R. Persistence of memory CD8 T cells in MHC class I-deficient mice. *Science* **286,** 1377–1381 (1999).

64. Sallusto, F., Lenig, D., Förster, R., Lipp, M. & Lanzavecchia, A. Two subsets of memory T lymphocytes with distinct homing potentials and effector functions. *Nature* **401,** 708–712 (1999).

65. Wherry, E. J., Teichgräber, V., Becker, T. C., Masopust, D., Kaech, S. M., Antia, R., Andrian, von, U. H. & Ahmed, R. Lineage relationship and protective immunity of memory CD8 T cell subsets. *Nat Immunol* **4,** 225–234 (2003).

66. Roberts, A. D., Ely, K. H. & Woodland, D. L. Differential contributions of central and effector memory T cells to recall responses. *J Exp Med* **202,** 123–133 (2005).

67. Wolint, P., Betts, M. R., Koup, R. A. & Oxenius, A. Immediate cytotoxicity but not degranulation distinguishes effector and memory subsets of CD8+ T cells. *J Exp Med* **199,** 925–936 (2004).

68. Badovinac, V. P., Haring, J. S. & Harty, J. T. Initial T cell receptor transgenic cell precursor frequency dictates critical aspects of the CD8(+) T cell response to

infection. *Immunity* **26,** 827–841 (2007).

69. Blattman, J. N., Antia, R., Sourdive, D. J. D., Wang, X., Kaech, S. M., Murali-Krishna, K., Altman, J. D. & Ahmed, R. Estimating the precursor frequency of naive antigen-specific CD8 T cells. *J Exp Med* **195,** 657–664 (2002).

70. Marzo, A. L., Klonowski, K. D., Le Bon, A., Borrow, P., Tough, D. F. & Lefrançois, L. Initial T cell frequency dictates memory CD8+ T cell lineage commitment. *Nat Immunol* **6,** 793–799 (2005).

71. Sarkar, S., Kalia, V., Haining, W. N., Konieczny, B. T., Subramaniam, S. & Ahmed, R. Functional and genomic profiling of effector CD8 T cell subsets with distinct memory fates. *Journal of Experimental Medicine* **205,** 625–640 (2008).

72. Kaech, S. M., Tan, J. T., Wherry, E. J., Konieczny, B. T., Surh, C. D. & Ahmed, R. Selective expression of the interleukin 7 receptor identifies effector CD8 T cells that give rise to long-lived memory cells. *Nat Immunol* **4,** 1191–1198 (2003).

73. Joshi, N. S., Cui, W., Chandele, A., Lee, H. K., Urso, D. R., Hagman, J., Gapin, L. & Kaech, S. M. Inflammation directs memory precursor and short-lived effector CD8(+) T cell fates via the graded expression of T-bet transcription factor. *Immunity* **27,** 281–295 (2007).

74. Stemberger, C., Huster, K. M., Koffler, M., Anderl, F., Schiemann, M., Wagner, H. & Busch, D. H. A single naive CD8+ T cell precursor can develop into diverse effector and memory subsets. *Immunity* **27,** 985–997 (2007).

75. Gerlach, C., Rohr, J. C., Perié, L., van Rooij, N., van Heijst, J. W. J., Velds, A., Urbanus, J., Naik, S. H., Jacobs, H., Beltman, J. B., de Boer, R. J. & Schumacher, T. N. M. Heterogeneous differentiation patterns of individual CD8+ T cells.

Science **340,** 635–639 (2013).

76. Buchholz, V. R., Flossdorf, M., Hensel, I., Kretschmer, L., Weissbrich, B., Gräf, P., Verschoor, A., Schiemann, M., Höfer, T. & Busch, D. H. Disparate individual fates compose robust CD8+ T cell immunity. *Science* **340,** 630–635 (2013).

77. Andrian, von, U. H. & Mackay, C. R. T-cell function and migration. Two sides of the same coin. *N Engl J Med* **343,** 1020–1034 (2000).

78. Mackay, C. R., Marston, W. L. & Dudler, L. Naive and memory T cells show distinct pathways of lymphocyte recirculation. *J Exp Med* **171,** 801–817 (1990).

79. Sallusto, F., Geginat, J. & Lanzavecchia, A. Central memory and effector memory T cell subsets: function, generation, and maintenance. *Annu. Rev. Immunol.* **22,** 745–763 (2004).

80. Hawke, S., Stevenson, P. G., Freeman, S. & Bangham, C. R. Long-term persistence of activated cytotoxic T lymphocytes after viral infection of the central nervous system. *J Exp Med* **187,** 1575–1582 (1998).

81. Hogan, R. J., Usherwood, E. J., Zhong, W., Roberts, A. A., Dutton, R. W., Harmsen, A. G. & Woodland, D. L. Activated antigen-specific CD8+ T cells persist in the lungs following recovery from respiratory virus infections. *The Journal of Immunology* **166,** 1813–1822 (2001).

82. Masopust, D., Vezys, V., Marzo, A. L. & Lefrançois, L. Preferential localization of effector memory cells in nonlymphoid tissue. *Science* **291,** 2413–2417 (2001).

83. Gebhardt, T., Wakim, L. M., Eidsmo, L., Reading, P. C., Heath, W. R. & Carbone, F. R. Memory T cells in nonlymphoid tissue that provide enhanced local immunity during infection with herpes simplex virus. *Nat Immunol* **10,** 524–530 (2009).

84. Jiang, X., Clark, R. A., Liu, L., Wagers, A. J., Fuhlbrigge, R. C. & Kupper, T. S. Skin infection generates non-migratory memory CD8+ TRM cells providing global skin immunity. *Nature* 1–6 (2012). doi:10.1038/nature10851

85. Shin, H. & Iwasaki, A. A vaccine strategy that protects against genital herpes by establishing local memory T cells. *Nature* **491,** 463–467 (2012).

86. Masopust, D., Choo, D., Vezys, V., Wherry, E. J., Duraiswamy, J., Akondy, R., Wang, J., Casey, K. A., Barber, D. L., Kawamura, K. S., Fraser, K. A., Webby, R. J., Brinkmann, V., Butcher, E. C., Newell, K. A. & Ahmed, R. Dynamic T cell migration program provides resident memory within intestinal epithelium. *Journal of Experimental Medicine* **207,** 553–564 (2010).

87. Mackay, L. K., Rahimpour, A., Ma, J. Z., Collins, N., Stock, A. T., Hafon, M.-L., Vega-Ramos, J., Lauzurica, P., Mueller, S. N., Stefanovic, T., Tscharke, D. C., Heath, W. R., Inouye, M., Carbone, F. R. & Gebhardt, T. The developmental pathway for CD103(+)CD8(+) tissue-resident memory T cells of skin. *Nat Immunol* **14,** 1294–1301 (2013).

88. Skon, C. N., Lee, J.-Y., Anderson, K. G., Masopust, D., Hogquist, K. A. & Jameson, S. C. Transcriptional downregulation of S1pr1 is required for the establishment of resident memory CD8(+) T cells. *Nat Immunol* **14,** 1285–1293 (2013).

89. Cyster, J. G. & Schwab, S. R. Sphingosine-1-phosphate and lymphocyte egress from lymphoid organs. *Annu. Rev. Immunol.* **30,** 69–94 (2012).

90. Gebhardt, T., Whitney, P. G., Zaid, A., Mackay, L. K., Brooks, A. G., Heath, W. R., Carbone, F. R. & Mueller, S. N. Different patterns of peripheral migration by

memory CD4+ and CD8+ T cells. *Nature* **477,** 216–219 (2011).

91. Ariotti, S., Beltman, J. B., Chodaczek, G., Hoekstra, M. E., van Beek, A. E., Gomez-Eerland, R., Ritsma, L., van Rheenen, J., Marée, A. F. M., Zal, T., de Boer, R. J., Haanen, J. B. A. G. & Schumacher, T. N. Tissue-resident memory CD8+ T cells continuously patrol skin epithelia to quickly recognize local antigen. *Proceedings of the National Academy of Sciences* **109,** 19739–19744 (2012).

92. Schenkel, J. M., Fraser, K. A., Vezys, V. & Masopust, D. Sensing and alarm function of resident memory CD8+ T cells. *Nat Immunol* **14,** 509–513 (2013).

93. Ariotti, S., Hogenbirk, M. A., Dijkgraaf, F. E., Visser, L. L., Hoekstra, M. E., Song, J.-Y., Jacobs, H., Haanen, J. B. & Schumacher, T. N. T cell memory. Skin-resident memory $CD8^+$ T cells trigger a state of tissue-wide pathogen alert. *Science* **346,** 101–105 (2014).

94. Schenkel, J. M., Fraser, K. A., Beura, L. K., Pauken, K. E., Vezys, V. & Masopust, D. T cell memory. Resident memory CD8 T cells trigger protective innate and adaptive immune responses. *Science* **346,** 98–101 (2014).

95. Steinert, E. M., Schenkel, J. M., Fraser, K. A., Beura, L. K., Manlove, L. S., Igyarto, B. Z., Southern, P. J. & Masopust, D. Quantifying Memory CD8 T Cells Reveals Regionalization of Immunosurveillance. *Cell* **161,** 737–749 (2015).

Chapter 2: CD8 DCs in effective priming of $CD8^+$ T cell responses

2.1 Abstract

Naïve $CD8^+$ T cells circulate through the blood, home to lymph nodes (LNs), in constant search of cognate Ag. Within the LN, T cells scan the surface of available DCs, including both CD11b DCs and CD8 DCs. If sufficient antigen (Ag) is recognized, T cells will engage in durable interactions with DCs that result in proliferation and generation of a heterogeneous population of T cells with differential homing properties, cytotoxicity, and ability to persist into the memory phase[1-3]. A number of model systems have shown that CD8 DCs are superior in their capacity to stimulate $CD8^+$ T cell responses[4,5], which is attributed in large part to their efficient cross-presentation of Ags acquired from apoptotic cells[6]. However, the relative contributions of cross-presentation and Ag acquisition have been difficult to separate as the receptor mediating efficient acquisition of apoptotic cells has not been defined. Here, we explore whether the phosphatidylserine receptor, T cell immunoglobulin domain and mucin domain-4 (TIM-4)[7], contributes to efficient Ag acquisition by CD8 DCs for subsequent cross-presentation to $CD8^+$ T cells. We identify that while TIM-4 deficiency significantly affects uptake *in vitro*, its role *in vivo* appears redundant. Additionally, we investigate whether signals beyond TCR-pMHC interactions may influence $CD8^+$ T cell fate during priming. Specifically, we use peptide-pulsed CD8 DCs and CD11b DCs to normalize differences in TCR-pMHC and uncover potential costimulatory or cytokine pathways that may impact T cell fate decisions. We establish that while CD8 DCs and CD11b DCs skew towards different T cell fates *in vitro*, the role for accessory cells during priming is highlighted *in vivo* as these differences are masked when priming occurs in the LN.

2.2 Attributions

The following individuals contributed to the work described in this chapter: Scott M. Loughhead (S.M.L.), Aude Thiriot (A.T.), Vijay K. Kuchroo (V.K.K.), and Ulrich H. von Andrian (U.H.v.A.).

S.M.L. designed, performed, analyzed experiments, and wrote the chapter. A.T. helped sort DC subsets and perform RT-PCR experiments. V.K.K. provided reagents and mice. U.H.v.A. aided with study design.

2.3 Introduction

In mice that lack CD8 DCs, $CD8^+$ T cell responses are significantly impaired[4,8]. Activation and expansion of $CD8^+$ T cells is controlled by integration of three signals: 1. TCR ligation by peptide-MHC complexes 2. Contact-dependent costimulatory/co-inhibitory interactions and 3. Soluble cytokines[9]. The diminished $CD8^+$ T cell responses in mice that lack CD8 DCs may therefore be the result of a significant reduction in any one of these three signals, or a combination thereof. TCR-pMHC engagement is of critical importance as signals 2 and 3 serve largely to amplify or dampen this initial stimulus. Therefore, significant emphasis has been placed on the role of efficient cross-presentation and acquisition of apoptotic cells by CD8 DCs for their role in initiating $CD8^+$ T cell responses. Dissecting the physiological importance of these two traits has been difficult, as no receptor has been identified that mediates this enhanced apoptotic cell uptake.

TIM-4 is a member of the T cell immunoglobulin domain and mucin domain (TIM) family of proteins and is a receptor for phosphatidylserine (PS), which mediates uptake of apoptotic cells by cells expressing TIM-4[10-12]. As the name suggests, TIM protein expression is largely restricted to T cells[7]. However, of the four identified TIM family members, TIM-4 does not appear to be expressed by T cells and is instead expressed by antigen presenting cells (APCs)[13]. In addition to mediating uptake of apoptotic cells, TIM-4 interacts with TIM-1, but the consequences of this interaction have opposing effects depending on the context[13-15]. Mice that lack TIM-4 eventually develop mild auto-immunity in the form of auto-antibodies without displaying overt symptoms[16]. TIM-4 is upregulated by maturation[15] and expression is enriched within the CD8 DC population[13]. However, the role for TIM-4 in apoptotic cell acquisition by CD8 DCs has not been investigated.

In addition to presentation pathways that result in greater MHC-I presentation, CD8 DCs may further promote robust $CD8^+$ T cell responses through other mechanisms. Specifically, differential costimulatory or cytokine signals conferred during priming may affect the overall outcome of the ensuing T cell response. CD8 DCs have been shown to produce substantially more of the signal 3 cytokines, IL-12 and IFN-α, than their CD11b counterparts[17-19]. *In vivo*, this prolific production of IL-12 by CD8 DCs has been linked to control of *Toxoplasma gondii* through effective promotion of $CD8^+$ T cell responses and their effector functions[20]. Additionally, activated CD11b DCs produce greater amounts of the inflammatory chemokines CCL3, CCL4, and CCL5, which may support interactions and activation of distinct T cell responses[21,22]. *In vitro*, priming of $CD8^+$ T cells by CD11b DCs results in prolonged proliferation due to enhanced production of IL-

2 compared to $CD8^+$ T cells primed by CD8 DCs[23]. The mechanism for this remains unclear, but appears to be contact-dependent as supernatant from opposing DC subsets is incapable of restoring IL-2 production[18]. During priming in LNs, $CD8^+$ T cells scan the surface of DCs bearing cognate Ag, which eventually results in a durable and prolonged contact with a single DC[2,3]. The intense exchange of information during this interaction may result in distinct T cell fates depending on the DC subset involved. We therefore sought to uncover whether and how DC subsets might govern the subsequent T cell fate.

2.4 Methods

Mice – C57BL/6, Balb/C, *BATF3*$^{-/-}$, *IL-12RB2*$^{-/-}$, OT-I, *CD45.1*$^{+/+}$, and β-Actin GFP mice were purchased from Jackson laboratories. P14 mice were from Taconic farms. *TIM4*$^{-/-}$ mice (on C57BL/6 background) were a kind gift from Dr. Vijay Kuchroo.

Cells – DCs were purified by positive immunomagnetic sorting (Miltenyi Biotec) from spleens of donor C57BL/6, *TIM4*$^{-/-}$, or *BATF3*$^{-/-}$ mice that had been implanted with a Flt3L secreting mouse melanoma cell line as described[24]. $CD11c^+$ MACS kit (130-052-001) was used for immunomagnetic sorting of DCs from C57BL/6, *TIM-4*$^{-/-}$, and *BATF3*$^{-/-}$ mice. CD8 DC MACS kit (130-091-169) was used for immunomagnetic sorting of CD8 DCs from *BATF3* littermates.

Viruses – Recombinant VSV expressing ovalbumin (VSV-OVA) was subcutaneously injected with 10^4 or 10^5 p.f.u in the hind footpads of isofluorane-anesthetized mice. Recombinant influenza strain PR/8 expressing gp33 (PR8-gp33) was a generous gift from

Dr. Arlene Sharpe. Mice were infected by intra-tracheal instillation of 20ul virus into avertin-anesthetized mice. LCMV-Armstrong expressing ovalbumin (LCMV-OVA) was a generous gift from Dr. Juan C. de la Torre. Mice were intravenously infected with 10^4 f.f.u. LCMV-OVA.

Apoptotic cell engulfment assay – Thymocytes were isolated from 6-week old C57BL/6 mice and labeled with 1uM CMFDA (Molecular Probes). Following labeling, cells were treated with 10uM dexamethasone (Sigma-Aldrich). EG7 cells were UV-irradiated for 2min, then labeled with 1uM CMFDA (Molecular Probes). For *in vivo* apoptotic B cell engulfment, B cells were enriched from the spleens of Balb/C mice using immunomagnetic CD43 MACS sorting (130-049-801). Cells were labeled with 1uM CMFDA (Molecular Probes) and 10^7 B cells were intravenously injected.

Antibodies – Antibodies for flow cytometry were purchased from Biolegend. TIM-4 (RMT4-54), IL-12/23p40 (C17.8), CD8α (53-6.7), CD11b (M1/70), CD80 (16-10A1), CD86 (GL-1), PD-L1 (10F.9G2), PD-L2 (TY25), CD45.1 (A20), CD45.2 (104), Ox40L (RM134L), ICOSL (HK5.3), Vα2 (B20.1), IFNγ (XMG1.2), IL-2 (JES6-5H4). TIM-4 antibodies (5G3 and 3H11) for blockade were provided by Dr. Vijay Kuchroo and used at 10ug/ml. Isotype control (HRPN) was from Bio X Cell and used at 10ug/ml. Cells acquired on FACS Canto (BD).

qPCR – RNA extracted using RNeasy mini plus kit (Qiagen). cDNA generated using iScript cDNA synthesis kit (BioRad). Primers: IL-12/23 (p40) – FWD: GACCATCAC-TGTCAAAGAGTTTCTAGAT, RVS: AGGAAAGTCTTGTTTTTGAAATTTTTTAA IL-27 (p28) - FWD: TCGATTGCCAGGAGTGAAC, RVS: GAAGTGTGGTAGCGAGGAAG, IL-35 (EBI3) - FWD: CAAGGAACAGAGCCACAGAG, RVS: GGGATACCGAGAAGCATGG, IL-6 - FWD: CAAAGCCAGAGTCCTTCAGAG, RVS: GTCCTTAGCCACTCCTTCTG, GAPDH - FWD: AATGGTGAAGGTCGGTGTG, RVS: ACAAGCTTCCCATTCTCGG. Samples amplified and analyzed using LightCycler II (Roche).

Proliferation assay – TCR-tg cells were isolated by immunomagnetic sorting using CD8α^+ T cell isolation kit (130-104-075). Cells were labeled with 1uM CFSE (Molecular Probes). Peptide-pulsing of DCs was at 37^{o}C for 1hr in the presence of 1ug/ml LPS (Sigma-Aldrich). KAVYNFATM and SIINFEKL peptides (Anaspec) were used at 1uM.

Intracellular cytokine secretion – Cells were stimulated 4-5hrs in the presence of 1ug/ml GolgiPlug. Cell membranes were permeabilized for intracellular staining using Cytofix/Cytoperm^{TM} (BD).

Competitive homing – Cells were labeled with 1uM CMFDA or 5uM CMTMR (Molecular probes). For confocal microscopy, LNs were fixed with 4% paraformaldehyde, then dehydrated using 20% sucrose in PBS. Tissues were then frozen

in OCT with 2-methylbutane. 20um sections were cut and stained on slides. Images were generated on Olympus FV1000 confocal microscope.

IL-2 ELISA – Supernatant from 48hr T cell co-cultures was analyzed for IL-2 expression using IL-2 ELISA MAX^{TM} (Biolegend) according to manufacturer's instructions.

2.5 Results

TIM-4 is preferentially expressed by CD8 DCs following maturation

Given the known interaction between TIM-4 and phosphatidylserine (PS)[10-12], we assayed splenic dendritic cell subsets for their expression of TIM-4 by flow cytometry. Freshly isolated DCs, regardless of subset, expressed low levels of TIM-4 when compared to controls (**Figure 2.1 A,B**). However, after four hours in culture, maturing CD8 DCs expressed high levels of TIM-4 while the expression of TIM-4 on CD11b DCs remained low (**Figure 2.1 C**). Although TIM-4 upregulation with maturation has been shown for bulk populations of DCs[15], the restrictive pattern on CD8 DCs has not been described. The confined expression of TIM-4 on CD8 DCs suggested that this receptor may be involved in the enhanced engulfment of apoptotic cells by this subset[25,26]. Notably, maturation was required for induction of TIM-4, which implied that it would play a role on CD8 DCs in an inflammatory context. Other PS receptors that have been analyzed on CD8 DCs do not vary with maturation[25,27-29], which makes an interpretation of how these receptors target certain antigens for tolerance and others for activation difficult. TIM-4 was therefore promising as a receptor on CD8 DCs that could mediate apoptotic cell uptake and target the associated antigens for cross-presentation and subsequent activation of $CD8^+$ T cells.

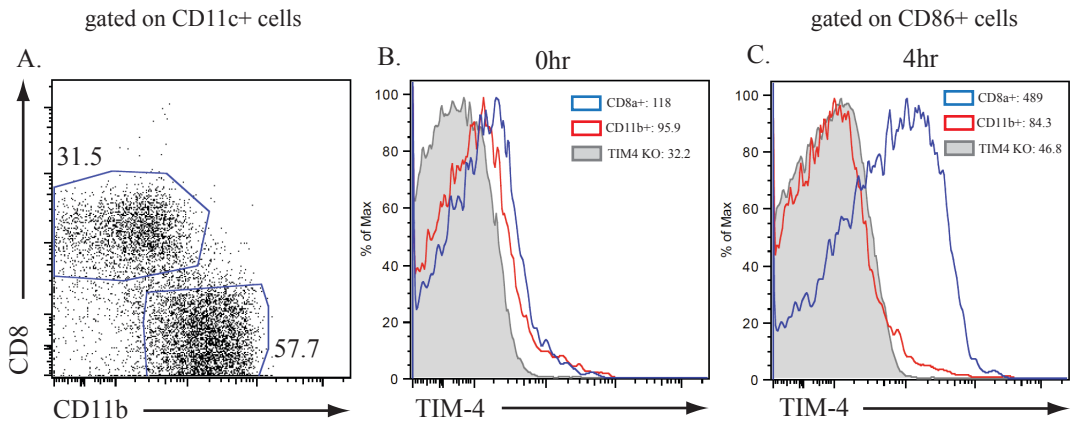

Figure 2.1: CD8 DCs preferentially express TIM-4 after maturation. DCs purified from the spleens of Flt3l-treated WT or TIM-4 KO mice by $CD11c^+$ MACS separation were analyzed for TIM-4 expression by flow cytometry (**A-C**). Representative gating strategy for distinguishing CD8 DCs and CD11b DCs (**A**). TIM-4 expression immediately after isolation among indicated subsets (**B**). TIM-4 expression among indicated subsets after 4 hours of culture in 1ug/ml LPS (**C**). Numbers indicate TIM-4 gMFI.

Apoptotic cell uptake by CD8 DCs is deficient in the absence of TIM-4

To test whether TIM-4 could facilitate uptake of apoptotic cells, mature splenic DCs from WT and TIM-4 KO mice were co-cultured with fluorescently labeled apoptotic thymocytes (**Figure 2.2 A**). As has been described[26], CD8 DCs from WT mice accumulated more apoptotic bodies in a temperature-dependent manner (**Figure 2.2 B**). However, splenic CD8 DCs from TIM-4 KO mice were significantly impaired in their ability to engulf apoptotic cells (**Figure 2.2 B,C**). This dependence on TIM-4 for engulfment of apoptotic bodies was surprising given the amount of redundancy for PS receptors.

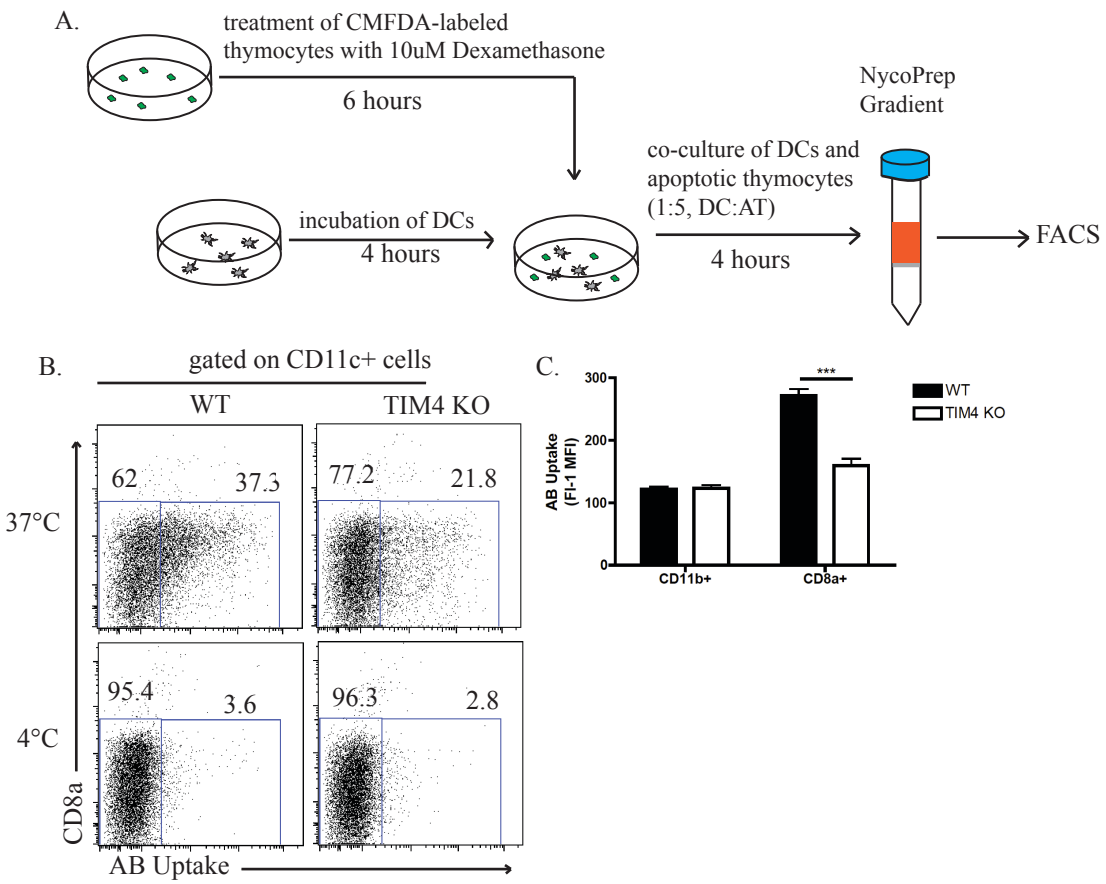

Figure 2.2: TIM-4 is required for optimal engulfment of apoptotic cells by CD8 DCs. DCs purified from Flt3l-treated WT or TIM4 KO mice by $CD11c^+$ MACS sorting were cultured for 4 hours prior to addition of CMFDA-labeled dexamethasone-treated thymocytes. After 4 hours of co-culture at 37^o C or 4^o C, apoptotic bodies (AB) were washed away by NycoDenz gradient and DCs were analyzed by flow cytometry (**A**). Representative plots for splenic DCs are shown in (**B**). Gates show percentage of DCs positive or negative for apoptotic cell uptake, irrespective of subset. Quantification of AB uptake for the indicated subsets of splenic DCs (**C**). Statistical analysis using paired t test (*** indicates $p<0.001$).

Blocking TIM-4 abrogates cross-presentation of apoptotic cell-associated antigens

The observation that TIM-4 played a significant role in the capture of apoptotic cells led us to assess whether antigens from these cells could be processed and presented on MHC-I. We therefore utilized the thymoma cell line, EG7, which constitutively expresses the model Ag, ovalbumin[30]. The activation and proliferation of transgenic OT-I T cells depends upon MHC-I presentation of the ovalbumin-derived peptide, SIINFEKL. If TIM-4 is required for uptake and subsequent cross-presentation of apoptotic cell-associated Ags, then blockade of TIM-4 should result in decreased proliferation of OT-I T cells. Indeed, when TIM-4 function was inhibited using blocking antibodies during co-culture of WT DCs with apoptotic EG7 cells (**Figure 2.3 A**), OT-I T cell proliferation was significantly reduced (**Figure 2.3 B,C**). Given the apparent costimulatory role of TIM-4 for CD4 T cells[13,15], OT-I T cell proliferation was assessed on SIINFEKL-pulsed DCs in the presence of TIM-4 blocking antibodies and no differences in proliferation could be found. This demonstrated that TIM-4 blockade affected OT-I proliferation independently of a costimulatory defect and was mediated through deficient capture of apoptotic cells.

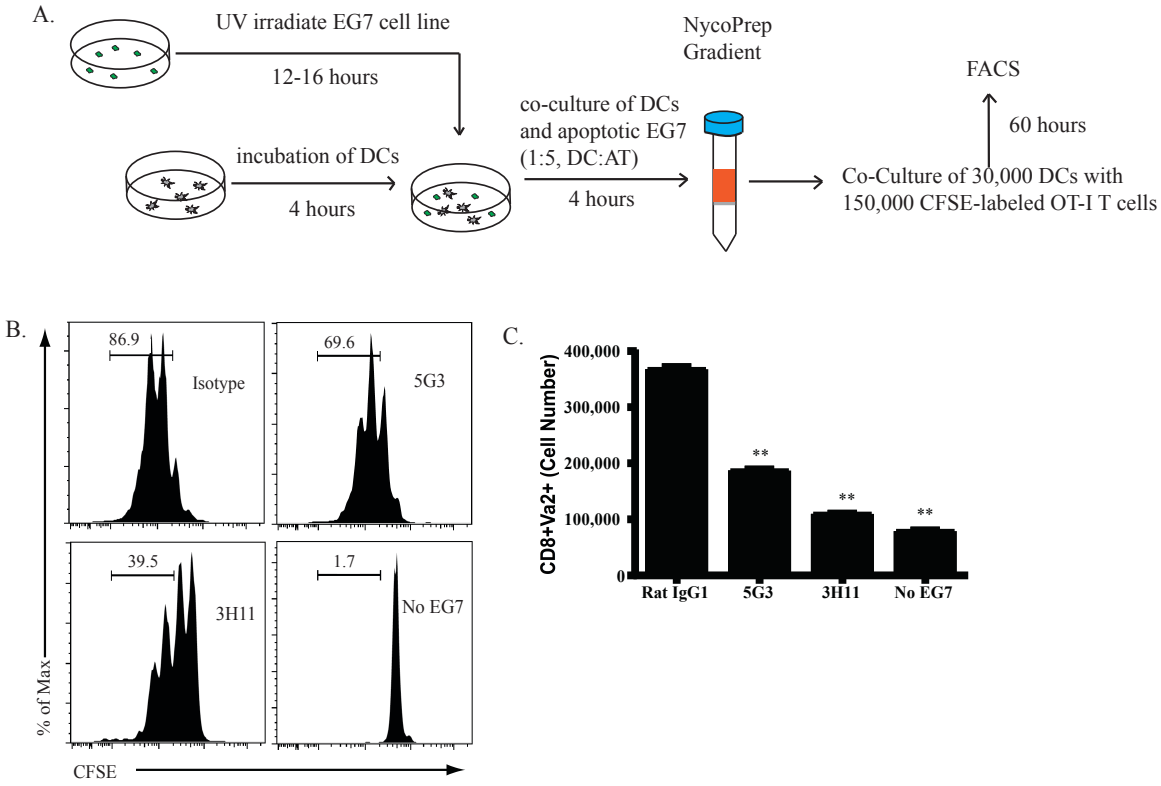

Figure 2.3: TIM-4 blockade decreases cross-presentation of apoptotic cell-associated antigens. DCs purified from Flt3l-treated WT mice were cultured for 4 hours. Prior to addition of UV-irradiated EG7 cells, 10ug/ml of either isotype control or TIM-4 blocking antibodies (5G3 and 3H11) were added to the culture (**A**). After 4 hours, apoptotic cells were washed away by NycoDenz gradient and DCs were cultured with CFSE-labeled OT-I T cells. CFSE dilution of OT-I cells and the percentage of cells with 2^+ divisions at 60 hours is shown (**B**). Total numbers of OT-I T cells at 60 hours (**C**). Statistical analysis compared to isotype using paired t test (** indicates $p<0.01$).

Assessing the physiological role for TIM-4 on CD8 DCs

To test whether TIM-4 played a role in apoptotic cell capture *in vivo*, WT and TIM-4 KO mice were intravenously injected with fluorescently labeled allogeneic B

cells. NK cells kill these B cells, which results in the generation of apoptotic bodies that are captured by CD8 DCs[25]. Both WT and TIM-4 KO mice efficiently captured apoptotic cells (**Figure 2.4 A,B**), which suggested that TIM-4 did not play a role in acquisition of apoptotic cells, at least in this context.

However, it was unclear whether this mildly inflammatory system was ideal for interrogating TIM-4 function *in vivo*. During many viral infections, infected cells become factories of viral proteins, until apoptosis or necrosis result. Therefore, in the context of an infection, targeting apoptotic cells for cross-presentation is an efficient way to generate $CD8^+$ T cell immunity, as these dying cells will be an enriched source of viral Ags. It has already been shown that in a number of viral infections, CD8 DCs efficiently capture viral Ag for presentation to $CD8^+$ T cells[31-33]. We therefore assayed whether TIM-4 affected $CD8^+$ T cell priming in a viral context. To this end, we subcutaneously infected WT and TIM-4 KO mice with VSV-OVA after adoptive transfer of OT-I cells. Regardless of the infectious dose, T cells accumulated with similar kinetics in the blood and LNs (**Figure 2.4 C**). This indicated that presentation of viral Ag during VSV infection likely did not depend upon TIM-4. In parallel, we performed experiments using a recombinant strain of influenza, PR8-gp33. Ag-specific responses were tracked using p14 T cells, which recognized the gp33 epitope. After intra-tracheal infection of WT and TIM-4 KO mice, weight was monitored daily and on day 9, tissues were harvested for analysis by flow cytometry. As shown, weight loss in WT and TIM4 KO mice was comparable (**Figure 2.4 D**) and the percentage of Ag-specific T cells in the blood, spleen, and lung at day 9 was also similar (**Figure 2.4 E**).

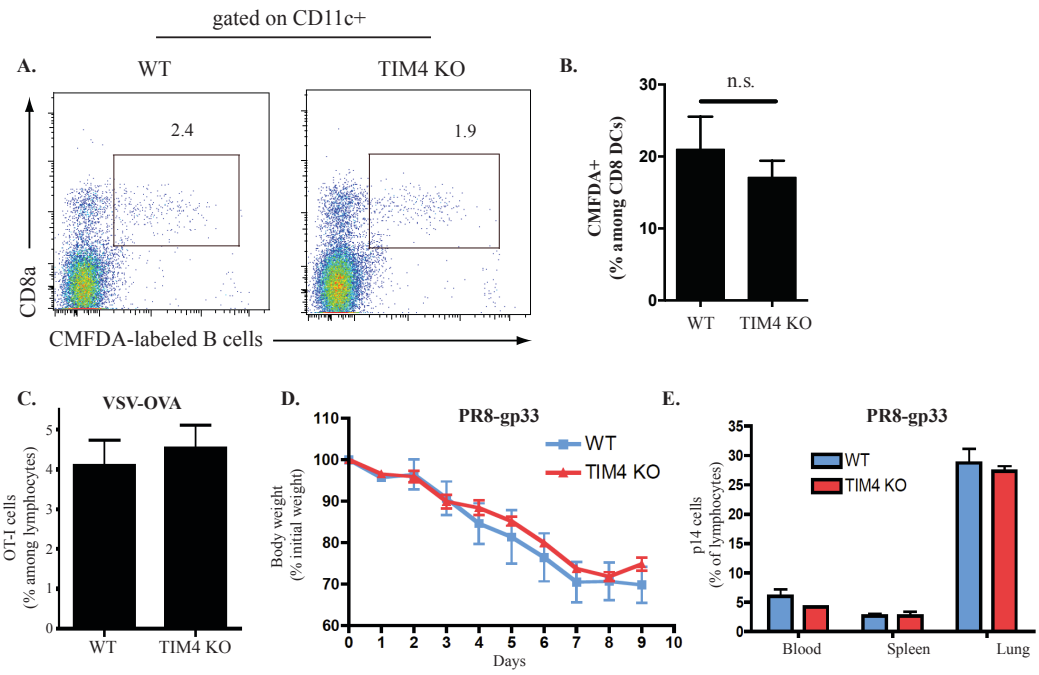

Figure 2.4: TIM-4 does not affect apoptotic cell uptake or CD8$^+$ T cell priming *in vivo*. 10^7 CMFDA labeled Balb/c B cells were i.v. injected into WT or TIM-4 KO mice (C57BL/6 background) and uptake in spleen was assessed 12hrs later. Representative plots of CD11c$^+$ cells from spleens of WT and TIM-4 KO are shown (**A**). Percentage of CD8 DCs positive for uptake of apoptotic B cells (**B**). Percentage of OT-I cells among total leukocytes in blood at day 6 following subcutaneous footpad infection with $4x10^5$ p.f.u. VSV-OVA (**C**). WT and TIM-4 KO mice were infected via the intra-tracheal route with a sub-lethal dose of PR8-gp33 after transfer of p14 CD45.1 cells. Weight loss was monitored daily (**D**) and accumulation of p14 TCR-tg cells within blood, spleen, and lung was assessed on day 9 post-infection (**E**).

Signals ancillary to MHC-I differ by DC subset

Given the apparently minimal role of TIM-4 for CD8$^+$ T cell priming *in vivo*, we sought to investigate whether the field's focus on signal 1 as the major driver of CD8$^+$ T

cell responses by CD8 DCs had masked other potential differences in Ag presentation by DC subsets. We therefore analyzed the expression of a number of different molecules on DC subsets that have been shown to play a role in $CD8^+$ T cell fate decisions [34-36]. Expression was analyzed on immature DCs as well as DCs that had been matured overnight. Mature CD11b DCs displayed no differences in MHC-II expression and modestly lower amounts of MHC-I (**Figure 2.5 A**). Costimulatory molecule expression was largely identical between CD8 DCs and CD11b DCs, except for PD-L2, which was strongly upregulated by maturation on CD8 DCs (**Figure 2.5 B**). Lastly, the expression of a number of cytokines highlighted dramatic differences in the cytokine milieu produced by DC subsets (**Figure 2.5 C**). While the role for some of these cytokines in influencing $CD8^+$ T cell fates is still poorly understood[37-39], it suggested that signals perceived by $CD8^+$ T cells in the presence of DC subsets may be significantly different.

Figure 2.5: DC subset expression of molecules influencing $CD8^+$ T cell activation and differentiation. Splenic DCs were isolated from Flt3l-treated mice and gated based on the expression of CD11b and CD8α. Shown are histograms of the expression of MHC-I, MHC-II, and various costimulatory molecules as measured by flow cytometry upon isolation (immature) and after overnight maturation (18 hrs) with 1ug/ml LPS (mature) (**A,B**). To measure the production of IL-12b by ICS, DCs were stimulated overnight (18hrs) at 4C (immature) or 37C (mature) and cytokine measured after 4hrs of GolgiPlug. For RT-PCR measurements, DC subsets were separated by cell sorting and RNA isolated immediately or after 4hrs of LPS stimulation. Measurements are shown relative to GAPDH. Fold change indicates fold induction over 0hr time point (**C**). CD8 DCs are shown in blue. CD11b DCs shown in black.

Figure 2.5 (Continued):

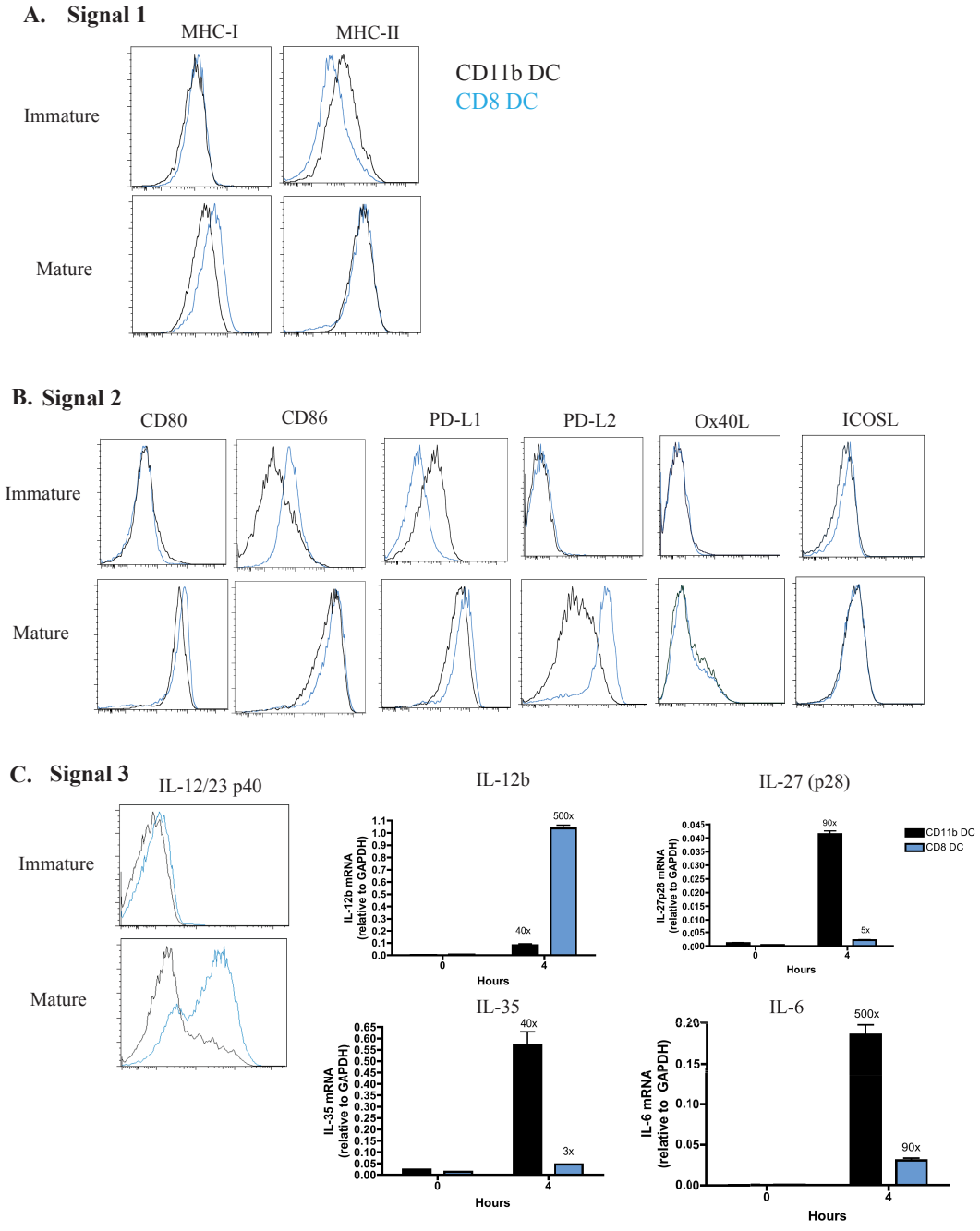

Peptide-pulsed CD8 DCs drive greater IFNγ production from CD8$^+$ T cells than CD11b DCs

To isolate DC subsets in sufficient quantities, DCs were expanded *in vivo* by treatment with a tumor expressing Flt3l[24]. CD8 DCs were purified from spleens of C57Bl/6 mice by magnetic separation tailored for CD8 DC isolation. CD11b DCs were purified by CD11c magnetic separation from BATF3 KO mice, which lack CD8 DCs[4]. This allowed simple isolation of DC subsets that were 80-90% pure (**Figure 2.6 A**). To uncover differences in CD8$^+$ T cell priming by these DC subsets irrespective of Ag processing, DC subsets were peptide-pulsed, then co-cultured with Ag-specific CFSE-labeled T cells. The kinetics of CFSE dilution, as well as phenotypic markers (CD44, CD69, and CD25) were similar among CD8$^+$ T cells primed with either DC subset. However, CD8$^+$ T cells primed with CD8 DCs (called T_{8DC}) showed significantly higher levels of IFNγ production at 48hr when compared to CD8$^+$ T cells primed with CD11b DCs (called T_{11bDC}) (**Figure 2.6 B**). Because CD8 DCs produce copious amounts of IL-12[17-19], we checked if this difference in IFNγ production was IL-12 dependent using IL-12R KO T cells. Indeed, when T_{8DC} cells could no longer sense IL-12, their IFNγ production was reduced to that of T_{11bDC} (**Figure 2.6 B,C**). IL-2 production also differed and was found to be produced in greater quantities by T_{11bDC}, as has been described[23] (**Figure 2.6 D**). Interestingly, decreased IL-2 production by T_{8DC} cells was not the result of IL-12 signaling as IL-2 production was unaffected by the absence of IL-12R signaling.

T_{8DC} accumulate more in blood than T_{11bDC} and appear more terminally differentiated

To examine the effector differentiation of T_{8DC} and T_{11bDC}, congenic T cells were primed *in vitro* for 48 hours, then co-transferred into naïve recipients. Accumulation in the blood was tracked over time and revealed that T_{8DC} accumulated to an average 8-fold greater extent than T_{11bDC} (**Figure 2.6 E**). Given the greater accumulation and known role for IL-12 in driving effector differentiation[40], we expected that T_{8DC} in the blood would be phenotypically more effector differentiated. Indeed, T_{8DC} were phenotypically enriched for short-lived effector cells (SLEC), as measured by KLRG-1 and CD62L (**Figure 2.6 F**). Conversely, T_{11bDC} appeared less terminally differentiated and were skewed towards memory precursor effector cells (MPEC). Even in the memory phase, 35 days after priming, T_{8DC} still were skewed towards IFNγ production alone while T_{11bDC} were skewed towards production of both IL-2 and IFNγ indicating that CD11b DCs may skew towards T_{CM} fates while CD8 DCs skew towards T_{EM} fates (**Figure 2.6 G**).

Figure 2.6: *In vitro* priming results in effector skewing after adoptive transfer. CD11b DCs were isolated from Flt3l-treated BATF3 KO mice using $CD11c^+$ MACS beads. CD8 DCs were isolated from Flt3l-treated BATF3 littermate controls using CD8 DC MACS kit. Plots show representative purity of DCs isolated in this manner (**A**). CD8 DCs and CD11b DCs were pulsed with 1uM KAVYNFATM peptide for 1hr at 37^o C in the presence of 1ug/ml LPS. After washing DC subsets were co-cultured with CFSE-labeled p14 TCR-tg cells. After 48hrs of co-culture, IFNγ production without restimulation was assessed by intracellular cytokine staining (**B,C**). Additionally, supernatant from 48hr cultures was tested for IL-2 abundance by ELISA (**D**). For *in vitro* prime and transfer, OT-I CD45.1 cells were cultured with SIINFEKL-pulsed CD8 DCs while OT-I CD45.1/.2 cells were cultured with SIINFEKL-pulsed CD11b DCs. After 48hrs, equal numbers of cells from each culture were intravenously injected into naïve mice. OT-I cells from each culture were identified by differential CD45.1/.2 expression in the blood and tracked over time (**E**). Differentially primed OT-I cells were phenotyped by CD62L and KLRG-1 expression (**F**). 35 days after transfer, spleens were isolated and cells were restimulated with SIINFEKL for intracellular cytokine staining of IFNγ and IL-2 (**G**). (** indicates $p<0.01$, *** indicates $p<0.001$, **** indicates $p<0.0001$)

Figure 2.6 (Continued):

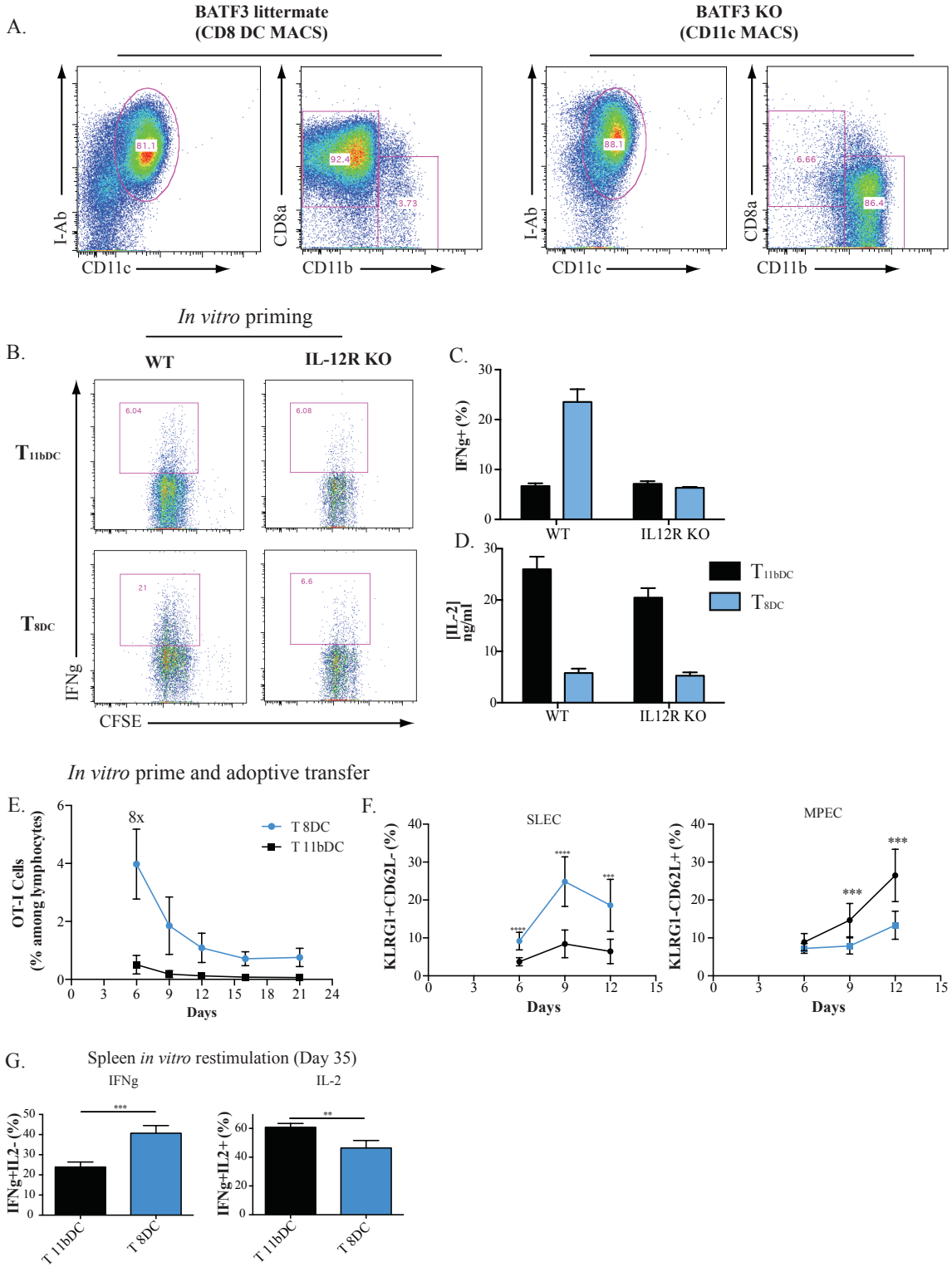

CD8 DCs migrate to draining LNs

While DC subsets were capable of imparting differential cytokine production by $CD8^+$ T cells *in vitro*, it was not clear whether this would be imparted during priming within the LN, where many other cellular players could dilute the signals of a given DC subset. To begin, successful migration to draining LNs by both DC subsets was assessed, as this has been controversial[3,41-43]. When injected subcutaneously, expression of CD11b and CD8α can distinguish DC subsets. However, staining DCs in draining LNs fails to reveal a discernible CD8 DC population[3] (**Figure 2.7 A**), which has led to the interpretation that CD8 DCs do not migrate to draining LNs when injected subcutaneously. To formally test this, differentially labeled CD8 DCs and CD11b DCs were co-injected sub-cutaneously (s.c.) into the footpad of mice. Twenty-four hours later, both CD11b DCs and CD8 DCs could be found in the draining LN. CD8 DCs within the draining LN retained their light scatter properties, indicating larger size and granularity (**Figure 2.7 B,C**). Interestingly, although CD8α staining could not resolve the two DC subsets in the draining LN and was reduced compared to the input, it was brighter on CD8 DCs than CD11b DCs in the draining LN. In contrast, CD11b staining was equivocal between the two subsets in the draining LN. Although this demonstrated that CD8 DCs were capable of migrating to LNs, their relative capacity to do so remained to be determined. Competitive migration experiments demonstrated that CD8 DCs were equally capable of migrating to draining LNs (**Figure 2.7 D**). Additionally, both subsets could be found in the paracortex of the LN (**Figure 2.7 E**). This resolved the issue of CD8 DC migration to LNs and could refute potentially disparate outcomes for *in vivo* immunizations that might be ascribed to differences in migration between DC subsets.

Figure 2.7: CD8 DCs migrate to draining LNs. DCs were purified from Flt3l-treated WT mice and input DCs were stained for expression of CD11b and CD8α prior to injection. DCs were subsequently labeled with CMFDA and injected subcutaneously into the footpad. 24hr after injection, the draining popLN was harvested and migrated DCs were stained for CD11b and CD8α expression (**A**). CD11b DCs and CD8 DCs were FACS sorted from Flt3l-treated β-actin GFP mice to 98% purity on the basis of CD11b and CD8α expression. CD8 DCs were subcutaneously injected into one footpad and CD11b DCs into the contralateral footpad. 24hr after injection, popLNs were harvested and the phenotype of DC subsets in the draining LNs was assessed (**B,C**). Additionally, sorted DC subsets from WT mice were labeled were differentially labeled with CMFDA or CMTMR. DC subsets were mixed 1:1 and injected into the footpads of CD45.1 mice. 24hr after injection, popLNs were harvested and the relative frequency of CD8 DCs and CD11b DCs within the draining LN was compared by flow cytometry, as well as localization by confocal microscopy (**D,E**).

Figure 2.7 (Continued):

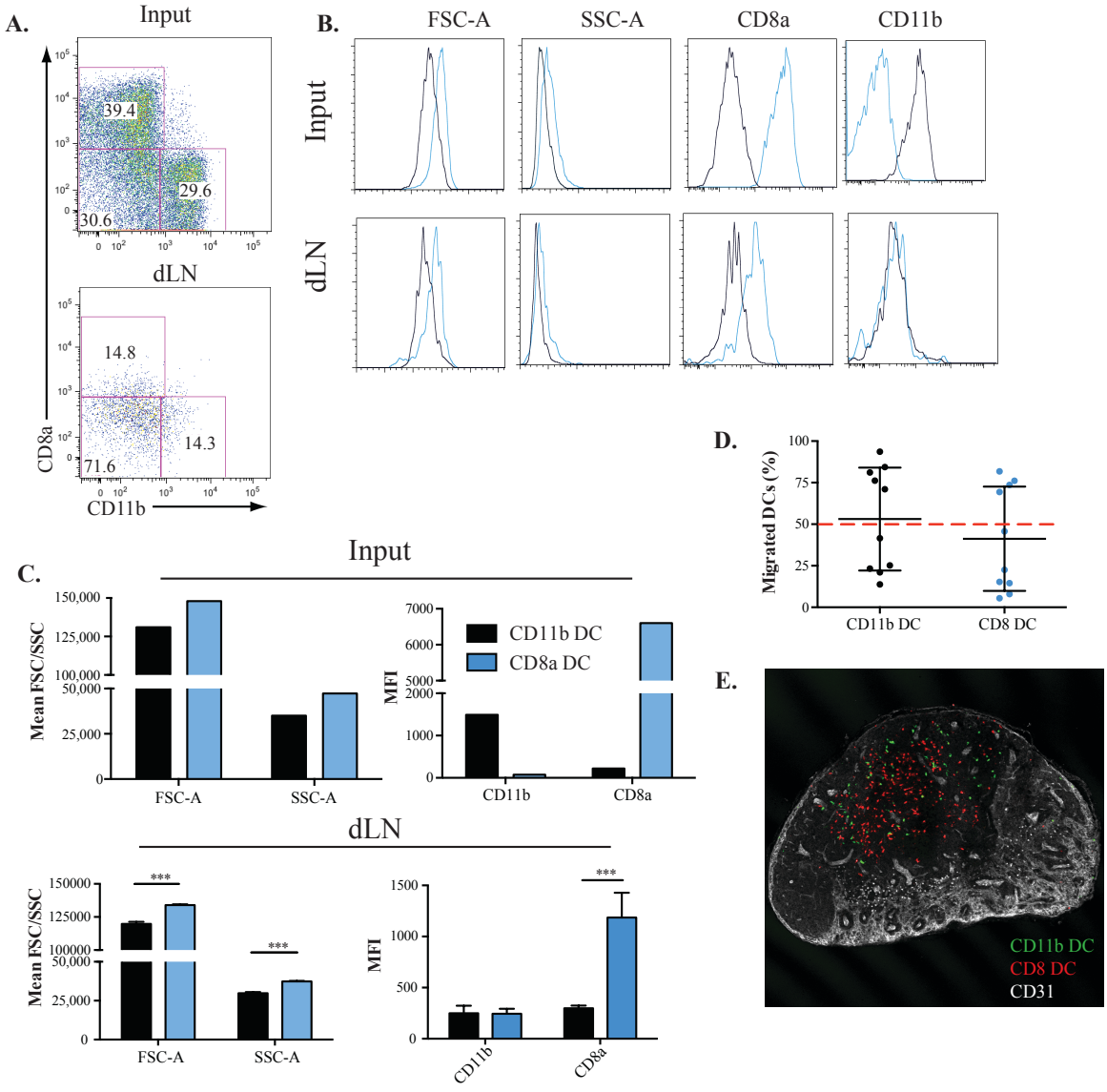

In vivo *immunization with peptide-pulsed CD8 DCs fails to drive greater effector differentiation of CD8$^+$ T cells than CD11b DCs*

To test *in vivo* skewing of T cell responses, mice were immunized with peptide-pulsed CD8 DCs or CD11b DCs and adoptively transferred TCR-tg responses were used to track the magnitude and phenotype of the ensuing response. Surprisingly, T cell

responses were similar in magnitude (**Figure 2.8 A**). Although statistically significant, these differences were subtle compared to those seen when T cells were primed *in vitro* prior to transfer. Additionally, differences in the phenotype and cytokine production in the effector and memory phase were no longer present (**Figure 2.7 B,C**). In parallel, peptide-pulsed CD8 DCs and CD11b DCs were used to prime endogenous $CD8^+$ T cell responses. In the memory phase, similar numbers of IFNγ-producing cells were present following restimulation (**Figure 2.8 D**). Given that IL-2 production is indicative of enhanced recall capacity[44,45], we investigated the secondary expansion of T cells primed by either subset using LCMV expressing OVA. Five days after infection, T cells from both immunized groups had generated T cell responses of similar magnitude and with similar cytokine production (**Figure 2.8 E**).

Figure 2.8: *In vivo* priming by DC subsets fails to skew T cell fates. DC subsets were purified from Flt3l-treated BATF3 KO or BATF3 littermate mice. Naïve C57BL/6 mice were immunized subcutaneously in the footpad with SIINFEKL-pulsed CD8 DCs or CD11b DCs on three consecutive days. 24hrs after the first DC immunization, OT-I CD45.1 cells were adoptively transferred. Accumulation and phenotype of OT-I cells in the blood was measured over time (**A,B**). 60 days after transfer, spleens were harvested and cytokine production was assessed after peptide restimulation (**C**). Endogenous memory responses were generated by a single footpad immunization with SIINFEKL-pulsed DC subsets. Spleens from one group of mice were restimulated with SIINFEKL on day 40 post-immunization (**D**). Another group of mice was challenged with intravenous LCMV-OVA and spleens restimulated with SIINFEKL five days after challenge (**E**).

Figure 2.8 (Continued):

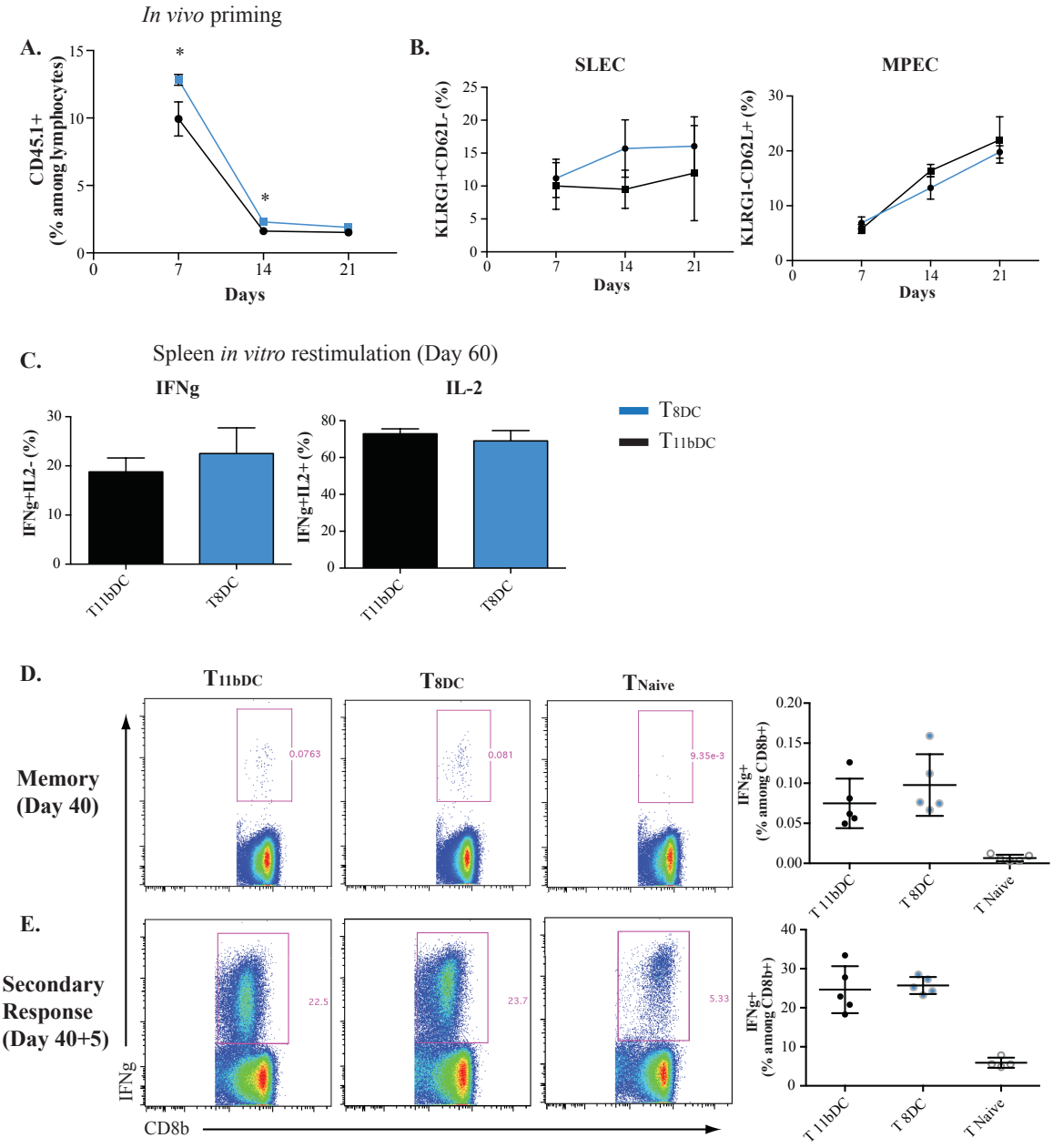

2.6 Discussion

DC subsets differentially contribute to $CD8^+$ T cell responses through distinct means of Ag capture[4,25] and accessory molecules that amplify or dampen T cell

responses[9,35,46]. Here, we have explored the role for the PS receptor, TIM-4, in mediating uptake of apoptotic cells by CD8 DCs. CD8 DCs selectively upregulated TIM-4 compared to CD11b DCs. *In vitro*, CD8 DCs were largely dependent on TIM-4 for ingestion of apoptotic cells and subsequent cross-presentation of associated Ags. However, in *in vivo* settings, these dependencies were no longer apparent as T cell responses were normal in TIM-4 KO during VSV-OVA and PR8-gp33 infection and apoptotic allogeneic B cells were efficiently captured by CD8 DCs in the spleen.

In systems independent of differential Ag capture, peptide-pulsed CD11b DCs and CD8 DCs were found to drive divergent $CD8^+$ T cell responses *in vitro*. IFNγ production was enhanced on T_{8DC} while IL-2 production was enhanced on T_{11bDC}. Increased IFNγ production was dependent on IL-12 production from CD8 DCs, but did not contribute to differences in IL-2 production. When *in vitro* primed T cells were adoptively transferred, T_{8DC} took on a terminally differentiated phenotype while T_{11bDC} were phenotypically more memory-like. However, when priming by distinct DC subsets occurred in draining LNs, these differences were masked.

These findings thus highlight the complex coordination that takes place to ensure appropriate $CD8^+$ T cell responses. While some systems can demonstrate dependence on a particular cell subset or molecule to significantly alter $CD8^+$ T cell responses[4,20,47], these are exceptions. In general, $CD8^+$ T cell responses are initiated by the coordinate involvement of multiple cell types and molecules[48,49], where depletion of any one may be concealed by compensation by others.

2.7 References

1. Henrickson, S. E., Perro, M., Loughhead, S. M., Senman, B., Stutte, S., Quigley, M., Alexe, G., Iannacone, M., Flynn, M. P., Omid, S., Jesneck, J. L., Imam, S., Mempel, T. R., Mazo, I. B., Haining, W. N. & Andrian, von, U. H. Antigen availability determines $CD8^+$ T cell-dendritic cell interaction kinetics and memory fate decisions. *Immunity* **39,** 496–507 (2013).
2. Henrickson, S. E., Mempel, T. R., Mazo, I. B., Liu, B., Artyomov, M. N., Zheng, H., Peixoto, A., Flynn, M. P., Senman, B., Junt, T., Wong, H. C., Chakraborty, A. K. & Andrian, von, U. H. T cell sensing of antigen dose governs interactive behavior with dendritic cells and sets a threshold for T cell activation. *Nat Immunol* **9,** 282–291 (2008).
3. Mempel, T. R., Henrickson, S. E. & Andrian, von, U. H. T-cell priming by dendritic cells in lymph nodes occurs in three distinct phases. *Nature* **427,** 154–159 (2004).
4. Hildner, K., Edelson, B. T., Purtha, W. E., Diamond, M., Matsushita, H., Kohyama, M., Calderon, B., Schraml, B. U., Unanue, E. R., Diamond, M. S., Schreiber, R. D., Murphy, T. L. & Murphy, K. M. Batf3 deficiency reveals a critical role for CD8alpha+ dendritic cells in cytotoxic T cell immunity. *Science* **322,** 1097–1100 (2008).
5. Torti, N., Walton, S. M., Murphy, K. M. & Oxenius, A. Batf3 transcription factor-dependent DC subsets in murine CMV infection: differential impact on T-cell priming and memory inflation. *European journal of immunology* **41,** 2612–2618 (2011).

6. Nierkens, S., Tel, J., Janssen, E. & Adema, G. J. Antigen cross-presentation by dendritic cell subsets: one general or all sergeants? *Trends Immunol* (2013). doi:10.1016/j.it.2013.02.007

7. Kuchroo, V. K., Dardalhon, V., Xiao, S. & Anderson, A. C. New roles for TIM family members in immune regulation. *Nat Rev Immunol* **8,** 577–580 (2008).

8. Waithman, J., Zanker, D., Xiao, K., Oveissi, S., Wylie, B., Ng, R., Tögel, L. & Chen, W. Resident CD8(+) and migratory CD103(+) dendritic cells control CD8 T cell immunity during acute influenza infection. *PLoS ONE* **8,** e66136 (2013).

9. Curtsinger, J. M. & Mescher, M. F. Inflammatory cytokines as a third signal for T cell activation. *Curr Opin Immunol* 1–8 (2010). doi:10.1016/j.coi.2010.02.013

10. Kobayashi, N., Karisola, P., Peña-Cruz, V., Dorfman, D. M., Jinushi, M., Umetsu, S. E., Butte, M. J., Nagumo, H., Chernova, I., Zhu, B., Sharpe, A. H., Ito, S., Dranoff, G., Kaplan, G. G., Casasnovas, J. M., Umetsu, D. T., DeKruyff, R. H. & Freeman, G. J. TIM-1 and TIM-4 glycoproteins bind phosphatidylserine and mediate uptake of apoptotic cells. *Immunity* **27,** 927–940 (2007).

11. Miyanishi, M., Tada, K., Koike, M., Uchiyama, Y., Kitamura, T. & Nagata, S. Identification of Tim4 as a phosphatidylserine receptor. *Nature* **450,** 435–439 (2007).

12. Santiago, C., Ballesteros, A., Martínez-Muñoz, L., Mellado, M., Kaplan, G. G., Freeman, G. J. & Casasnovas, J. M. Structures of T cell immunoglobulin mucin protein 4 show a metal-Ion-dependent ligand binding site where phosphatidylserine binds. *Immunity* **27,** 941–951 (2007).

13. Meyers, J. H., Chakravarti, S., Schlesinger, D., Illes, Z., Waldner, H., Umetsu, S.

E., Kenny, J., Zheng, X. X., Umetsu, D. T., DeKruyff, R. H., Strom, T. B. & Kuchroo, V. K. TIM-4 is the ligand for TIM-1, and the TIM-1-TIM-4 interaction regulates T cell proliferation. *Nat Immunol* **6,** 455–464 (2005).

14. Mizui, M., Shikina, T., Arase, H., Suzuki, K., Yasui, T., Rennert, P. D., Kumanogoh, A. & Kikutani, H. Bimodal regulation of T cell-mediated immune responses by TIM-4. *International Immunology* **20,** 695–708 (2008).
15. Rodriguez-Manzanet, R., Meyers, J. H., Balasubramanian, S., Slavik, J., Kassam, N., Dardalhon, V., Greenfield, E. A., Anderson, A. C., Sobel, R. A., Hafler, D. A., Strom, T. B. & Kuchroo, V. K. TIM-4 expressed on APCs induces T cell expansion and survival. *The Journal of Immunology* **180,** 4706–4713 (2008).
16. Rodriguez-Manzanet, R., Sanjuan, M. A., Wu, H. Y., Quintana, F. J., Xiao, S., Anderson, A. C., Weiner, H. L., Green, D. R. & Kuchroo, V. K. T and B cell hyperactivity and autoimmunity associated with niche-specific defects in apoptotic body clearance in TIM-4-deficient mice. *Proc Natl Acad Sci USA* **107,** 8706–8711 (2010).
17. Hochrein, H., Shortman, K., Vremec, D., Scott, B., Hertzog, P. & O'Keeffe, M. Differential production of IL-12, IFN-alpha, and IFN-gamma by mouse dendritic cell subsets. *The Journal of Immunology* **166,** 5448–5455 (2001).
18. Winkel, K. D., Kronin, V., Krummel, M. F. & Shortman, K. The nature of the signals regulating CD8 T cell proliferative responses to CD8alpha+ or CD8alpha- dendritic cells. *European journal of immunology* **27,** 3350–3359 (1997).
19. Naik, S. H., Proietto, A. I., Wilson, N. S., Dakic, A., Schnorrer, P., Fuchsberger, M., Lahoud, M. H., O'keeffe, M., Shao, Q.-X., Chen, W.-F., Villadangos, J. A.,

Shortman, K. & Wu, L. Cutting edge: generation of splenic CD8+ and CD8- dendritic cell equivalents in Fms-like tyrosine kinase 3 ligand bone marrow cultures. *The Journal of Immunology* **174,** 6592–6597 (2005).

20. Mashayekhi, M., Sandau, M. M., Dunay, I. R., Frickel, E. M., Khan, A., Goldszmid, R. S., Sher, A., Ploegh, H. L., Murphy, T. L., Sibley, L. D. & Murphy, K. M. CD8α(+) dendritic cells are the critical source of interleukin-12 that controls acute infection by Toxoplasma gondii tachyzoites. *Immunity* **35,** 249–259 (2011).
21. Proietto, A. I., O'keeffe, M., Gartlan, K., Wright, M. D., Shortman, K., Wu, L. & Lahoud, M. H. Differential production of inflammatory chemokines by murine dendritic cell subsets. *Immunobiology* **209,** 163–172 (2004).
22. Castellino, F., Huang, A. Y., Altan-Bonnet, G., Stoll, S., Scheinecker, C. & Germain, R. N. Chemokines enhance immunity by guiding naive CD8+ T cells to sites of CD4+ T cell-dendritic cell interaction. *Nature* **440,** 890–895 (2006).
23. Kronin, V., Winkel, K., Süss, G., Kelso, A., Heath, W., Kirberg, J., Boehmer, von, H. & Shortman, K. A subclass of dendritic cells regulates the response of naive CD8 T cells by limiting their IL-2 production. *The Journal of Immunology* **157,** 3819–3827 (1996).
24. Mach, N., Gillessen, S., Wilson, S. B., Sheehan, C., Mihm, M. & Dranoff, G. Differences in dendritic cells stimulated in vivo by tumors engineered to secrete granulocyte-macrophage colony-stimulating factor or Flt3-ligand. *Cancer Res* **60,** 3239–3246 (2000).
25. Iyoda, T., Shimoyama, S., Liu, K., Omatsu, Y., Akiyama, Y., Maeda, Y., Takahara, K., Steinman, R. M. & Inaba, K. The CD8+ dendritic cell subset

selectively endocytoses dying cells in culture and in vivo. *J Exp Med* **195,** 1289–1302 (2002).

26. Schnorrer, P., Behrens, G. M. N., Wilson, N. S., Pooley, J. L., Smith, C. M., El-Sukkari, D., Davey, G., Kupresanin, F., Li, M., Maraskovsky, E., Belz, G. T., Carbone, F. R., Shortman, K., Heath, W. R. & Villadangos, J. A. The dominant role of CD8+ dendritic cells in cross-presentation is not dictated by antigen capture. *Proc Natl Acad Sci USA* **103,** 10729–10734 (2006).

27. Ramirez-Ortiz, Z. G., Pendergraft, W. F., Prasad, A., Byrne, M. H., Iram, T., Blanchette, C. J., Luster, A. D., Hacohen, N., Khoury, El, J. & Means, T. K. The scavenger receptor SCARF1 mediates the clearance of apoptotic cells and prevents autoimmunity. *Nat Immunol* **14,** 917–926 (2013).

28. Nakayama, M., Akiba, H., Takeda, K., Kojima, Y., Hashiguchi, M., Azuma, M., Yagita, H. & Okumura, K. Tim-3 mediates phagocytosis of apoptotic cells and cross-presentation. *Blood* **113,** 3821–3830 (2009).

29. Belz, G. T., Vremec, D., Febbraio, M., Corcoran, L., Shortman, K., Carbone, F. R. & Heath, W. R. CD36 is differentially expressed by CD8+ splenic dendritic cells but is not required for cross-presentation in vivo. *The Journal of Immunology* **168,** 6066–6070 (2002).

30. Moore, M. W., Carbone, F. R. & Bevan, M. J. Introduction of soluble protein into the class I pathway of antigen processing and presentation. *Cell* **54,** 777–785 (1988).

31. Allan, R. S., Smith, C. M., Belz, G. T., van Lint, A. L., Wakim, L. M., Heath, W. R. & Carbone, F. R. Epidermal viral immunity induced by CD8alpha+ dendritic

cells but not by Langerhans cells. *Science* **301,** 1925–1928 (2003).

32. Smith, C. M., Belz, G. T., Wilson, N. S., Villadangos, J. A., Shortman, K., Carbone, F. R. & Heath, W. R. Cutting edge: conventional CD8 alpha+ dendritic cells are preferentially involved in CTL priming after footpad infection with herpes simplex virus-1. *The Journal of Immunology* **170,** 4437–4440 (2003).

33. Belz, G. T., Shortman, K., Bevan, M. J. & Heath, W. R. CD8alpha+ dendritic cells selectively present MHC class I-restricted noncytolytic viral and intracellular bacterial antigens in vivo. *The Journal of Immunology* **175,** 196–200 (2005).

34. Mousavi, S. F., Soroosh, P., Takahashi, T., Yoshikai, Y., Shen, H., Lefrançois, L., Borst, J., Sugamura, K. & Ishii, N. OX40 costimulatory signals potentiate the memory commitment of effector CD8+ T cells. *J Immunol* **181,** 5990–6001 (2008).

35. Greenwald, R. J., Freeman, G. J. & Sharpe, A. H. The B7 family revisited. *Annu. Rev. Immunol.* **23,** 515–548 (2005).

36. Watts, T. H. TNF/TNFR family members in costimulation of T cell responses. *Annu. Rev. Immunol.* **23,** 23–68 (2005).

37. Morishima, N., Mizoguchi, I., Okumura, M., Chiba, Y., Xu, M., Shimizu, M., Matsui, M., Mizuguchi, J. & Yoshimoto, T. A pivotal role for interleukin-27 in CD8+ T cell functions and generation of cytotoxic T lymphocytes. *J. Biomed. Biotechnol.* **2010,** 605483 (2010).

38. Collison, L. W., Workman, C. J., Kuo, T. T., Boyd, K., Wang, Y., Vignali, K. M., Cross, R., Sehy, D., Blumberg, R. S. & Vignali, D. A. A. The inhibitory cytokine IL-35 contributes to regulatory T-cell function. *Nature* **450,** 566–569 (2007).

39. Wu, W., Dietze, K. K., Gibbert, K., Lang, K. S., Trilling, M., Yan, H., Wu, J., Yang, D., Lu, M., Roggendorf, M., Dittmer, U. & Liu, J. TLR ligand induced IL-6 counter-regulates the anti-viral CD8(+) T cell response during an acute retrovirus infection. *Sci Rep* **5,** 10501 (2015).

40. Joshi, N. S., Cui, W., Chandele, A., Lee, H. K., Urso, D. R., Hagman, J., Gapin, L. & Kaech, S. M. Inflammation directs memory precursor and short-lived effector CD8(+) T cell fates via the graded expression of T-bet transcription factor. *Immunity* **27,** 281–295 (2007).

41. Smith, A. L. & Fazekas de St Groth, B. Antigen-pulsed CD8alpha+ dendritic cells generate an immune response after subcutaneous injection without homing to the draining lymph node. *J Exp Med* **189,** 593–598 (1999).

42. Ruedl, C. & Bachmann, M. F. CTL priming by CD8(+) and CD8(-) dendritic cells in vivo. *European journal of immunology* **29,** 3762–3767 (1999).

43. Colvin, B. L., Morelli, A. E., Logar, A. J., Lau, A. H. & Thomson, A. W. Comparative evaluation of CC chemokine-induced migration of murine CD8alpha+ and CD8alpha- dendritic cells and their in vivo trafficking. *Journal of Leukocyte Biology* **75,** 275–285 (2004).

44. Williams, M. A., Tyznik, A. J. & Bevan, M. J. Interleukin-2 signals during priming are required for secondary expansion of CD8+ memory T cells. *Nature* **441,** 890–893 (2006).

45. Kalia, V., Sarkar, S., Subramaniam, S., Haining, W. N., Smith, K. A. & Ahmed, R. Prolonged interleukin-2Ralpha expression on virus-specific CD8+ T cells favors terminal-effector differentiation in vivo. *Immunity* **32,** 91–103 (2010).

46. Kim, T. S., Gorski, S. A., Hahn, S., Murphy, K. M. & Braciale, T. J. Distinct Dendritic Cell Subsets Dictate the Fate Decision between Effector and Memory CD8+ T Cell Differentiation by a CD24-Dependent Mechanism. *Immunity* **40,** 400–413 (2014).

47. Sancho, D., Joffre, O. P., Keller, A. M., Rogers, N. C., Martínez, D., Hernanz-Falcón, P., Rosewell, I. & Reis e Sousa, C. Identification of a dendritic cell receptor that couples sensing of necrosis to immunity. *Nature* **458,** 899–903 (2009).

48. Germain, M. G. W. K. I. I. J. K. R., Kastenmuller, W., Ifrim, I., Kabat, J. & Germain, R. N. Histo-Cytometry: A Method for Highly Multiplex Quantitative Tissue Imaging Analysis Applied to Dendritic Cell Subset Microanatomy in Lymph Nodes. *Immunity* 1–13 (2012). doi:10.1016/j.immuni.2012.07.011

49. Eickhoff, S., Brewitz, A., Gerner, M. Y., Klauschen, F., Komander, K., Hemmi, H., Garbi, N., Kaisho, T., Germain, R. N. & Kastenmuller, W. Robust Anti-viral Immunity Requires Multiple Distinct T Cell-Dendritic Cell Interactions. *Cell* **162,** 1322–1337 (2015).

Chapter 3: CX_3CR1 distinguishes three antigen-experienced $CD8^+$ T cell subsets with a linear pedigree and distinct migratory patterns

3.1 Abstract

Viral infections induce pathogen-specific T-cell differentiation into diverse effector and memory subsets. These T-cell fate decisions and lineage relationships are poorly understood, in part, because available subset-defining markers do not adequately reflect existing heterogeneities. Moreover, inadequate subset-defining markers have made it difficult to assess the dynamic migratory patterns of T cell subsets into and through peripheral tissues. Here, we report that CX_3CR1 identifies three phenotypically and functionally distinct subsets among anti-viral $CD8^+$ effector and memory T-cells. Classical central memory (T_{CM}) and effector memory (T_{EM}) cells and their respective effector precursors were CX_3CR1^- and CX_3CR1^{high}, respectively. In addition, we identified a $CX_3CR1^{intermediate}$ subset, peripheral memory T-cells (T_{PM}), which shared features of both T_{CM} and T_{EM}. Lineage tracing indicated a unidirectional differentiation pedigree from T_{CM} to T_{PM} to T_{EM}. Interrogation of the migratory patterns of these subsets revealed that T_{PM} gradually acquired lymph node homing capability, but without assuming a *bone fide* T_{CM} phenotype. Further, T_{PM} surveyed peripheral tissues while T_{EM} did not.

3.2 Attributions

The following individuals contributed to the work described in this chapter: Carmen Gerlach (C.G.), E. Ashley Moseman (E.A.M.), Scott M. Loughhead (S.M.L.), David Alvarez (D.A.), , Lisette Waanders (L.W.), Juan C. de la Torre (J.C.d.l.T) and Ulrich H. von Andrian (U.H.v.A.).

S.M.L., C.G., E.A.M., and U.H.v.A. conceived the study design. S.M.L., C.G., and E.A.M. performed and analyzed experiments. D.A. performed parabiosis and thoracic duct lymph cannulations. L.W. characterized CX_3CL1 F_c and CX_3CR1 antibody staining. J.C.d.l.T. provided LCMV-OVA and technical advice. S.M.L., C.G., E.A.M., and U.H.v.A. wrote the chapter.

3.3 Introduction

When naïve $CD8^+$ T cells (T_N) encounter a viral infection, activation by cognate antigen (Ag) causes them to proliferate and differentiate, giving rise to effector cells (T_{Eff}) that are tasked with eradicating the offending pathogen. Following viral clearance, most T_{Eff} are eliminated, but a small fraction persists giving rise to long-lived memory cells (T_{Mem})[1]. It is well established that both the T_{Eff} and T_{Mem} populations are composed of distinct subsets[2,3], however, the fate decisions that are taken by T_N and T_{Eff} to generate these subsets are poorly understood, and the lineage relationships between different T_{Mem} classes have been a subject of debate[4,5]. Specifically, uncertainties exist surrounding the two major known T_{Mem} populations encountered in blood and spleen, the T_{CM} and T_{EM}, which are traditionally defined by their differential expression of CD62L and CCR7[4-6]. This combination of traffic molecules, which is absent from T_{EM}, enables T_N and T_{CM} to interact with high endothelial venules (HEV) in lymph nodes (LNs) and to survey these organs for recall Ag[7]. Since T_{Mem} are also present in afferent lymph draining peripheral tissues[8], it has been postulated, although never tested directly, that circulating T_{EM} continuously enter non-lymphoid tissues and return to the blood via draining lymphatics and the thoracic duct (TD)[6]. More recently, a third T_{Mem} subset, the tissue resident

memory cells (T_{RM}), have been identified[3]. This sessile T_{Mem} population is thought to be derived from T_{Eff} that seed non-lymphoid tissues during early effector responses. To date, the relationship between $T_{EM,}$ T_{CM} and T_{RM} remains poorly defined owing, at least in part, to the lack of specific markers that positively identify T_{EM} and allow the detection of phenotypic and functional heterogeneities among T_{Mem} and their precursors. Here, we report that the chemokine receptor CX_3CR1 represents such a marker, and we dissect the lineage relationships and trafficking properties of T_{Eff} and T_{Mem} subsets that are distinguishable by differential CX_3CR1 expression.

3.4 Methods

Mice - C57BL/6, *CX3CR1*$^{gfp/gfp}$*CD45.1*$^{+/+}$, *CD45.1*$^{+/+}$, OT-I, *rag1*$^{-/-}$ and *LTa*$^{-/-}$ mice (all on the C57BL/6 background) were purchased from the Jackson Laboratory. *LTa*$^{-/-}$ mice were also kindly provided by Dr. Nancy Ruddle (Yale School of Public Health). P14 mice were purchased from Taconic farms. All uninfected mice were housed, bred and crossed in a specific pathogen-free barrier facility of Harvard Medical School. Experiments using TCR-tg T cells were preformed either with *rag1*$^{+/+}$ or *rag1*$^{-/-}$ TCR-tg donor T cells, the latter to rule out any potential effects of TCRs with additional specificities. Whenever experiments were performed with *rag1*$^{+/+}$ and *rag1*$^{-/-}$ TCR-tg donor T cells, the results were comparable. Therefore, it is not specified which experiment was performed with *rag1*$^{+/+}$ and which with *rag1*$^{-/-}$ TCR-tg cells, and data from both types of experiments may be shown pooled if the experimental setup was otherwise the same. All animal experiments were performed in accordance with national and institutional guidelines.

T cell isolation from murine tissues - To obtain naïve TCR-tg $CD8^+$ T cells for adoptive transfer, blood was drawn from TCR-tg mice, erythrocytes were lysed and a small sample was analyzed by flow cytometry to quantify the fraction of p14 or OT-I cells ($V\alpha2^+CD8^+$). 10^4 $V\alpha2^+CD8^+$ T cells were transferred into naïve C57BL/6 recipient mice. If experiments required flow cytometric sorting of T_{Mem} or subsequent parabiosis, 1-$5x10^4$ naïve $V\alpha2^+CD8^+$ T cells were transferred.

Prior to flow cytometric analysis of antigen experienced T cells, tissues were treated as follows: Blood underwent erythrocyte lysis. Spleen, lymph nodes (iliac, axillary, brachial, deep & superficial cervical, lumbar and mesenteric) and livers were physically homogenized by forcing the organs through a cell strainer or metal mesh, followed by a density gradient (NycoPrepTM 1.077, Axis-Shield). Lungs, the female reproductive tract (FRT) and salivary glands were cut in small pieces followed by enzymatic digestion with 62.5µg/ml LiberaseTM (Roche) and 100µg/ml DNAseI (Roche) for 30 minutes at 37°C, before treating them, similar to livers. The FRT did not undergo a density gradient. Bone marrow was isolated from femurs. Small intestines were depleted of Peyer's Patches, cut in pieces, cleared of feces and incubated in HBSS / 2.5 mM EDTA for 20 min. to isolate IEL. The remaining small intestinal tissue was digested for 20 min. in HBSS / 2.5% FCS / 25µg/ml DNaseI (Roche) / 500µg/ml Collagenase D (Roche) to isolate LPL. IEL and LPL were further purified on a Percoll (GE Healthcare) density gradient. To label intravascular $CD8^+$ T cells, mice were i.v. injected with 1-3µg anti-CD8α or anti-CD8β 3 min. prior to sacrifice.

Prior to flow cytometric cell sorting, T cells were enriched by MACS technology (Miltenyi Biotec), using the $CD8\alpha^+$ T cell isolation kit (Miltenyi Biotec) for endogenous

T cells and CD45.1-biotin (BioLegend) staining followed by anti-biotin MicroBeads (Miltenyi Biotec) for adoptively transferred TCR-tg T cells. To quantify CX_3CR1 subset frequencies derived from these sorted and transferred cells, $CD45.1^+$ cells were enriched by CD45.1-biotin (BioLegend) staining followed by anti-biotin MicroBeads (Miltenyi Biotec) prior to flow cytometric analysis.

Parabiosis - Pairs of mice were matched by gender and body weight, and anesthetized i.p. with Ketamine (100mg/kg), 10 mg/kg Xylazine (10mg/kg), and Acepromazine (3mg/kg). Hair was removed from the opposing lateral flanks of both mice by shaving and depilatory cream. A longitudinal skin incision was made from the olecranon area to the knee joint on each mouse of the parabiotic pair, and the subcutaneous fascia was bluntly dissected to create ~0.5 cm skin flap. Animals were positioned side-by-side and the right olecranon and right knee joint of one animal was sutured to the corresponding left olecranon and left knee joint of the other. The dorsal and ventral skin flaps were then attached by continuous 6-0 suture at the olecranon and knee regions, and staples along the lateral abdominal aspect of the mice.

Thoracic duct lymph collection – Mice were administered ~0.5ml of olive oil by gavage approximately 1hr prior to surgery to better visualize lymphatic vessels and the cisterna chyli. Mice were then anesthetized by IP injection of 100 mg/kg Ketamine HCl, 10 mg/kg Xylazine and 3 mg/kg Acepromazine. After surgical site preparation, the mice received a heparinized polyethylene catheter in the left jugular vein for administration of fluids (Ringer's lactate, 1U/ml Heparin) prior to and throughout the thoracic duct

cannulation procedure. Next, an incision is made through the left abdominal wall exposing the intestines, spleen, left kidney, and adrenal gland, which are gently mobilized and held by hemostat clamps to expose the thoracic duct and cisterna chyli. The thoracic duct is then punctured and a heparinized cannula is inserted and fixed in place by adding a drop of tissue glue. Thoracic duct lymph was collected for 1-3h and assayed by flow cytometry. If thoracic duct cannulation was performed on one parabiotic partner, the parabiotic mice were surgically separated immediately prior to performing the thoracic duct cannulation procedure.

Flow cytometry - Antibodies were purchased from BioLegend or BD Biosciences. Intracellular cytokine staining was performed after 5 hours incubation with GolgiPlug™ (BD Biosciences) in the presence or absence of SIINFEKL peptide (Anaspec), using the Cytofix/Cytoperm™ Fixation/Permeabilization solution kit (BD Biosciences). The capacity of cells to bind fractalkine was assessed by incubating cells with fractalkine-Ig (1:3 diluted hybridoma supernatant), a fusion protein of fractalkine with a human IgG1 Fc fragment (Millennium) for 1h at 4°C, followed by staining with anti-human IgG Fc-biotin for 15 min at 4°C and subsequently streptavidin-APC for 15 min at 4°C. Gp33-specific T cells were detected by H-2 Db / KAVYNFATC / PE MHC Dextramer staining (Immudex). CX_3CR1 staining on human PBMCs was performed at 37°C.

Cells were sorted with a FACSAria™ and analyzed with a FACSCanto™ or LSR II (all BD Biosciences). Subsequent analysis was performed in FlowJo v10 (Tree Star) and GraphPad Prism 5/6.

Human blood - Human blood was obtained from anonymous human donors (Research Blood Components, LLC). Lymphocytes were enriched by density gradient (NycoPrepTM 1.077, Axis-Shield) and subsequently stained for flow cytomerty analysis.

Infections - Mice were infected intra-venously with 0.5-1x10^4 focus forming units (ffu) LCMV Armstrong strain (abbreviated LCMV), 0.5-1x10^4 ffu recombinant trisegmented LCMV Armstrong strain expressing the fluorescent protein katushka and ovalbumin (abbreviated LCMV-ova), 2x10^6 plaque forming units (pfu) recombinant VSV expressing ovalbumin (abbreviated VSV-ova), or 10^3 (primary infection) – 10^5 (secondary & tertiary infection) colony forming units (cfu) recombinant Listeria monocytogenes expressing ovalbumin[9] (abbreviated LM-ova). All infectious work was performed in accordance with national and institutional guidelines. LM-ova was kindly provided by Dr. Darren Higgins.

LCMV-ova was generated as follows: The OVA open reading frame (ORF) was amplified from cDNA using the PCR Extender System (5 Prime) and primers OVA-BbStart (TGAAGACAGCAAGATGGGCTCCATCGGTGCAGCA) and OVA-Bbstop (TGAAGACATGGTCTTAAGGGGAAACACATCTGCCA) containing the BbsI restriction site. After BbsI digestion, the PCR product was cloned into plasmid pol-I S-GPC/BbsI[10] to generate plasmid pol-I S-GPC/OVA. The Katushka ORF was amplified from cDNA using the PCR Extender System (5 Prime) and primers Katushka-BsStart (CGTCTCCAAGGATGGTGGGTGAGGATAGCGT) and Katushka_BsStop (CGTCTCATTCTTCAGTGCCCCAGTTTGCTAGGCA) containing BsmBI restriction sites. After BsmBI digestion the PCR product was cloned into the BsmBI site of plasmid

pol-I S-BsmBI/NP (*45*) to generate plasmid pol-I S-Katushka/NP. For subsequent virus rescue, subconfluent BHK-21 cells ($2x10^6$ cells/M6 well) were transfected for 5 h using 2.5 µl of Lipofectamine 2000 (Invitrogen) per µg of plasmid DNA. The plasmid cocktail included: pC-NP (0.8 µg) and pC-L (1 µg), together with plasmids pol-I L (1.4 µg), pol-I S-Katushka/NP (0.8 µg) and pol-I S-GPC/OVA (0.8 µg) that directed intracellular synthesis, via RNA pol-I, of the viral L and S genome RNA species. After 5 h transfection, cells were washed once with DMEM containing 2% FBS and fresh (3 ml/M6 well) DMEM containing 10% FBS added to cells and incubated for 72 h prior collecting the tissue culture supernatant for virus titration.

Transwell chemotaxis - T cell migration towards a recombinant mouse CCL19 (R&D systems) gradient was assessed using Transwell® 24-wells plates with 5µm pore size inserts (Corning Incorporated). 10^6 spleen-derived, MACS-enriched $CD8^+$ T cells ($CD8\alpha^+$ T cell isolation kit (Miltenyi Biotec)) were loaded in the upper chamber, while the lower chamber contained medium without or with indicated concentrations of CCL19. The absolute number of CX_3CR1^-, CX_3CR1^{int} and CX_3CR1^{hi} OT-I T_{Mem} that had migrated into the chemokine-containing lower chamber after 3 hours at 37°C was quantified and expressed relative to the corresponding populations' input numbers (% migrated) or numbers within the no chemokine-containing lower well (chemotactic index).

3.5 Results

CX_3CR1 is a differentiation marker for pathogen-specific $CD8^+$ T_{Eff} after viral infection

Murine CX_3CR1 has a single ligand, fractalkine (CX_3CL1), a chemokine that is upregulated on inflamed endothelium[11]. To date, murine CX_3CR1 has been primarily used to distinguish myeloid phagocyte subsets[12-14]. In humans, CX_3CR1 is found on a fraction of T_{Eff}-like T cells[15,16]; however, human CX_3CR1^+ T cells have not been systematically investigated. As there were, until very recently, no well-characterized antibodies to detect murine CX_3CR1, investigators have resorted to the use of *$CX_3CR1^{+/gfp}$* reporter mice in which green fluorescent protein (GFP) was 'knocked-in' to the *CX_3CR1* locus[12]. In healthy young *$CX_3CR1^{+/gfp}$* mice, which harbor mainly T_N, T-cells were essentially devoid of GFP expression (**Figure 3.1 A**), consistent with previous reports[12]. However, >80% of *$CX_3CR1^{+/gfp}$* T-cells expressed GFP on day 8 after acute systemic infection with lymphocytic choriomeningitis virus serotype Armstrong (LCMV). The majority of GFP-expressing T cells were $CD8^+$, whereas a minority expressing moderate levels of GFP were $CD4^+$ (**Figure 3.1 B**). Low expression of CX_3CR1 on a subset of $CD4^+$ T-cells had been previously noted in mouse models of allergic asthma and atopic dermatitis[17,18], but CX_3CR1 has been widely believed to be absent from murine $CD8^+$ T-cells.

GFP expression by *$CX_3CR1^{+/gfp}$* $CD8^+$ T-cells correlated closely with binding of soluble fractalkine and an anti-CX_3CR1 monoclonal antibody (MAb), but neither fractalkine nor the anti-CX_3CR1 MAb stained GFP^+ T-cells from *$CX_3CR1^{gfp/gfp}$* (*CX_3CR1* knock-out) mice, indicating that GFP fluorescence intensity in hemizygous T-cells specifically reported functional CX_3CR1 surface expression (**Figure 3.1 C**). Additionally, we tested Ag-dependence for CX_3CR1 acquisition using T cell receptor transgenic (TCR-tg) OT-I or P14 animals whose $CD8^+$ T-cells recognize the SIINFEKL peptide of

Figure 3.1: CX_3CR1 is a differentiation marker for pathogen-specific $CD8^+$ T_{Eff} after viral infection. Polyclonal (endogenous) or adoptively transferred TCR-tg $CD8^+$ T-cells were analyzed before and after viral infection. All experiments were performed with T-cells on a $CX_3CR1^{+/gfp}$ background unless stated otherwise. (**A**) Left: Composite FACS plots from one representative experiment showing GFP expression levels of peripheral blood T-cells from naive and LCMV-Armstrong infected mice. Right: Pooled data from 3 experiments (3-5 mice each). (**B**) Composite FACS plots of PBMC from 3-5 mice gated on $CD3^+CD8^+$ or $CD3^+CD4^{+.}$ **C**) Fractalkine fused to human IgG1 F_c (FKN-Ig) or an anti-CX_3CR1 monoclonal antibody (MAb) was used to stain $CD8^+$ T cells from $CX_3CR1^{+/gfp}$ and $CX_3CR1^{gfp/gfp}$ mice eight days following LCMV-infection. (**D-G**) Naïve $CX_3CR1^{+/gfp}$ $CD45.1^+$ OT-I cells ($1x10^4$) were transferred into C57BL/6 recipients followed by LCMV-ova or VSV-ova infection. (**D**) Composite plots of blood-derived OT-I cells from 2 mice (naïve) or 4 mice (day 6-10) at indicated timepoints. The gating strategy for GFP and CD27 was used to bin T_{Eff} in peripheral blood into CX_3CR1^-, CX_3CR1^{int}, and CX_3CR1^{hi} subsets (**E**), as well as for histograms of surface phenotype (**F**), and to monitor cytokine expression (mean + SD) in splenic T_{Eff} (**G**). $n = 2$ experiments (4-5 mice/each). ** $p<0.01$, *** $p<0.001$ by repeated measures one-way (F) or two-way (G) ANOVA with Tukey's (F) or Bonferroni (G) multiple comparisons test.

Figure 3.1 (Continued):

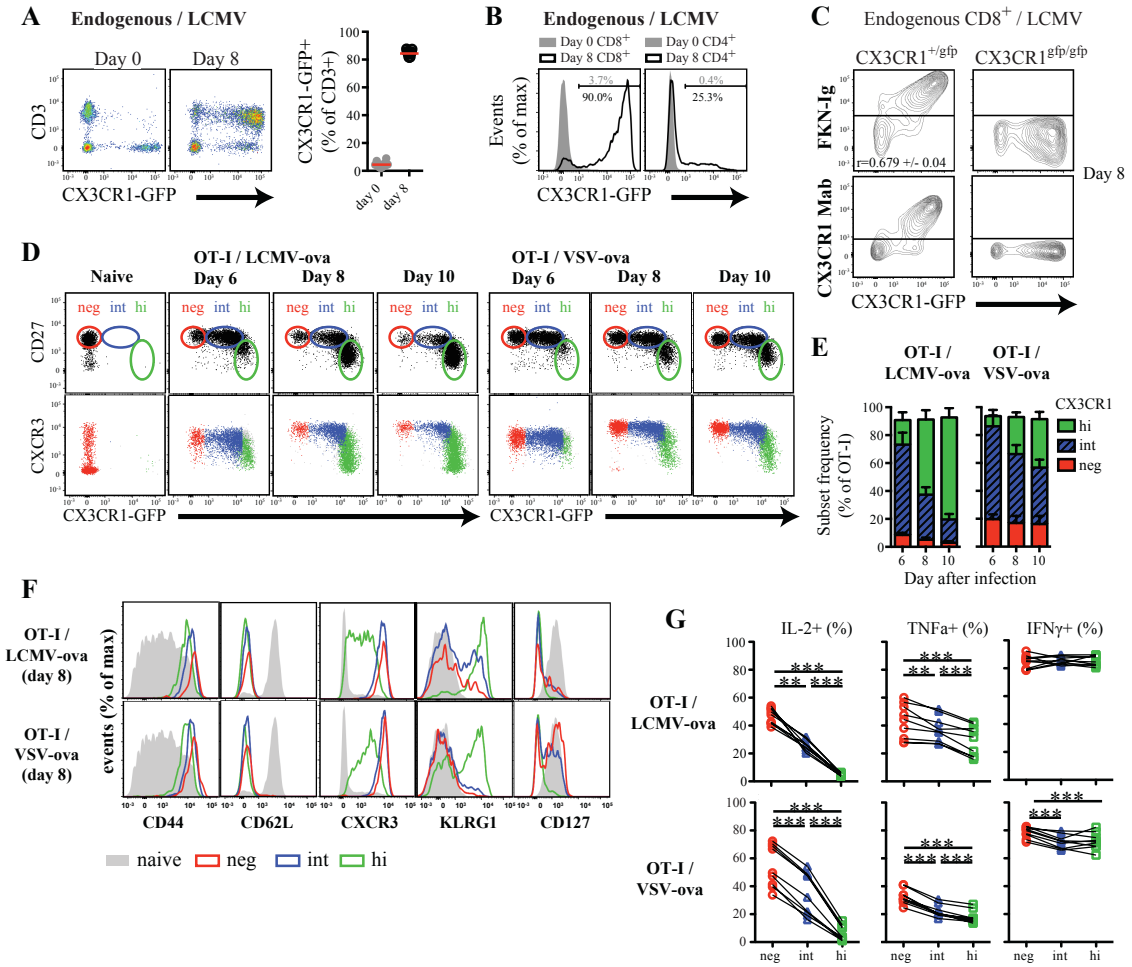

ovalbumin (OVA) or the immunodominant LCMV epitope, gp_{33-42}, respectively. During LCMV infection, virus-specific P14 cells, but not OT-I cells, upregulated GFP. In contrast, infection with LCMV-OVA drove upregulation of GFP on the majority of both OT-I and P14 cells. Thus, CX_3CR1 induction on $CD8^+$ T-cells required cognate TCR triggering and occurred in response to different Ags.

$CX_3CR1^{+/gfp}$ OT-I cells also upregulated GFP when animals were infected with other OVA expressing viruses or bacteria, although the kinetics and extent of CX_3CR1 induction was somewhat variable depending on the infectious agent (**Figure 3.1 D**). Regardless of the activating stimulus, CX_3CR1 induction was heterogeneous among Ag-specific T-cells, but always followed a typical time-course; starting on day 5 after challenge, a fraction of $CD8^+$ T-cells began to express intermediate levels of CX_3CR1, and expression subsequently intensified, reaching a peak on day 10. However, even when CX_3CR1 expression had peaked, three T_{Eff} subsets were always distinguishable: the bulk of cells were CX_3CR1^{hi}; a few cells remained CX_3CR1^{-}; while a substantial fraction displayed a CX_3CR1^{int} phenotype (**Figure 3.1 D,E**).

The differential regulation of CX_3CR1 prompted us to ask whether CX_3CR1 expression levels delineate distinct effector differentiation states. This is relevant because a T-cell's degree of T_{Eff} differentiation is thought to be inversely correlated with its potential to generate long-term memory[19]. Indeed, CX_3CR1^{-} and CX_3CR1^{int} $CD8^+$ T-cells expressed CD27 and moderate, but detectable levels of CD127, while the CX_3CR1^{hi} subset had lost both CD27 and CD127 and preferentially expressed killer cell lectin-like receptor G1 (KLRG1). Downregulation of CD27 and CD127 and upregulation of KLRG1 usually reflects terminal T_{Eff} differentiation[20-23]. Of note, the chemokine receptor

CXCR3, which is absent from T_N, was upregulated on CX_3CR1^- and CX_3CR1^{int} cells, but, similar to CD27 and CD127, was not expressed by CX_3CR1^{hi} cells. These phenotypic characteristics were observed with different immunization modalities (**Figure 3.1 D-F**). Taken together, these findings suggest a sequence of T_{Eff} differentiation, whereby the least differentiated CX_3CR1^- cells initially give rise to the CX_3CR1^{int} subset, which can progress to the CX_3CR1^{hi} state that displays a terminally differentiated phenotype.

As the magnitude of memory responses is thought to correlate with the fraction of T_{Eff} that produce the cytokine, interleukin-2 (IL-2), upon restimulation, in particular in conjunction with other cytokines[20,22], we compared each T_{Eff} subset's potential to produce IL-2, TNFα and IFNγ. Consistent with the sequence of differentiation from CX_3CR1^- to CX_3CR1^{int} to CX_3CR1^{hi} T_{Eff}, CX_3CR1^- and CX_3CR1^{int} T_{Eff} secreted IL-2, whereby the fraction of IL-2 producers was highest among CX_3CR1^- T_{Eff}, while IL-2 producers were rare among the CX_3CR1^{hi} subset (**Figure 3.1G**). Although CX_3CR1^- and CX_3CR1^{int} T_{Eff} were apparently less differentiated than CX_3CR1^{hi} cells, all three subsets secreted ample effector cytokines (IFNγ, TNFα) upon restimulation.

CX_3CR1 expression levels define three distinct memory $CD8^+$ T cell populations

Having determined that CX_3CR1 identifies three T_{Eff} subsets with distinct phenotypic and functional properties, we assessed the stability of this phenotype on T_{Mem}. CX_3CR1^{hi} T_{Mem} retained most of the phenotypic characteristics seen on CX_3CR1^{hi} T_{Eff} including lack of CD62L, CXCR3, and CD127 expression (**Figure 3.2 A**). KLRG-1 expression, however, was more heterogeneous on CX_3CR1^{hi} T_{Mem}. CX_3CR1^- and

Figure 3.2: CX_3CR1 expression levels identify three distinct memory $CD8^+$ T cell populations. Naïve OT-I *$CX_3CR1^{+/gfp}$* $CD45.1^+$ T cells were transferred into C57BL/6 followed by LCMV-OVA or VSV-OVA infection. (**A**) The phenotype of the OT-I T_{Mem} subsets was assessed >5 weeks after infection by staining for the indicated markers. (**B**) Chemotactic response of $CD8^+$ T_{Mem} subsets to CCL19 in a Transwell assay. Chemotactic index reflects the number of T_{Mem} that migrated towards CCL19 relative to the number of cells that migrated towards medium alone. Data depict mean ± SEM of 3-5 wells/group/experiment. *n* = 2 experiments (4 mice each). (**C**) Experimental protocol for serial adoptive transfer experiments (left) and absolute (middle) and relative (right) numbers of memory cells recovered from recipients of sorted T_{Eff} subsets. Results are from 2 independent experiments with 2-8 mice/group. Number of transferred T_{Eff}: $2x10^5$ (Exp.1) and $1.6x10^5$ (Exp. 2). *** $p<0.001$ by one-way ANOVA with Tukey's multiple comparisons test. (**D**) CX3CR1 expression phenotype of recovered OT-I memory cells. Same experiment as in A. Bars show mean + SD. (**E**) Experimental protocol for adoptive transfer of early T_{Mem} subsets (left). Pooled data from two experiments (2-5 mice/group) show subset frequency among splenic and LN resident OT-I T_{Mem}. Bars show mean + SD.

Figure 3.2 (Continued):

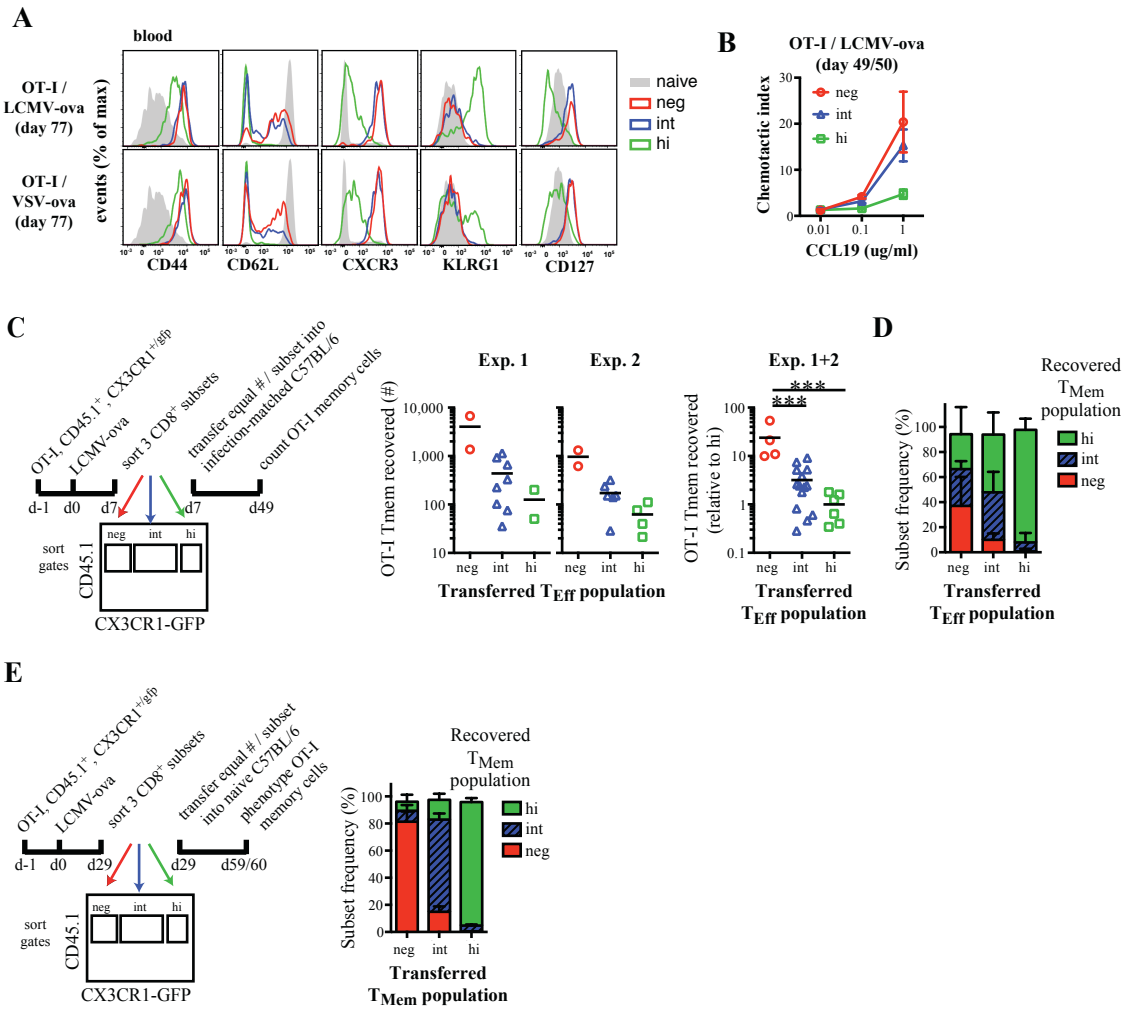

CX_3CR1^{int} T_{Mem} maintained CXCR3 expression and reacquired CD127 expression. To address how each of these three T_{Mem} populations relates to classical T_{CM} and T_{EM}, which were originally identified in human blood based on their differential expression of the chemokine receptor CCR7[6], we assessed the ability of T_{Mem} subsets to migrate towards a gradient of the CCR7 ligand, CCL19. CX_3CR1^{-} and CX_3CR1^{int} cells responded vigorously to this chemoattractant, whereas the CX_3CR1^{hi} subset showed poor chemotaxis (**Figure 3.2 B**), indicating that CX_3CR1^{hi} cells express little or no functional

CCR7. This implied that T_{CM}-like T-cells consist of at least two subsets distinguishable by CX_3CR1 expression.

To examine whether murine CX_3CR1 T cell subsets could inform dissection of human T cell subsets, T cells from human blood were analyzed for CX_3CR1 expression. Ag-experienced $CD8^+CD45RO^+$ T cells contained three subsets: CX_3CR1^-, CX_3CR1^{int} and CX_3CR1^{hi} at similar frequencies as in murine blood (**Figure 3.3**). Co-staining with CXCR3 closely paralleled mouse data while CD27 revealed at least three populations: $CX_3CR1^-CD27^+$, $CX_3CR1^+CD27^+$, and $CX_3CR1^+CD27^-$. Whereas the degree of conservation between CX_3CR1-defined human and murine T cells remains unclear, these data suggest that CX_3CR1 expression may aid in further dissection of $CD8^+$ T cell responses in humans as well.

To address whether differential CX_3CR1 expression might also predict the potential to generate long-lived memory, we sorted CX_3CR1^-, CX_3CR1^{int} and CX_3CR1^{hi} OT-I T_{Eff} from mice that had been infected with LCMV-OVA seven days prior and adoptively transferred equal numbers of each sorted subset into separate infection-matched congenic recipients. Six weeks later, there was a marked difference in the number of T_{Mem} that arose from each subset; few T_{Mem} were recovered from recipients of CX_3CR1^{hi} T_{Eff}, while CX_3CR1^{int} T_{Eff} gave rise to ~3x more T_{Mem}. Animals that had received CX_3CR1^- T_{Eff} generated by far the largest memory offspring, ranging in frequency from 10- to over 50-fold above the number of T_{Mem} that were recovered from CX_3CR1^{hi} recipients (**Figure 3.2 C**). Interestingly, the T_{Mem} populations that arose from each transferred T_{Eff} subset not only differed in number, but also in phenotype (**Figure 3.2 C,D**). Mice that had received CX_3CR1^- T_{Eff} on day 7 contained roughly equal

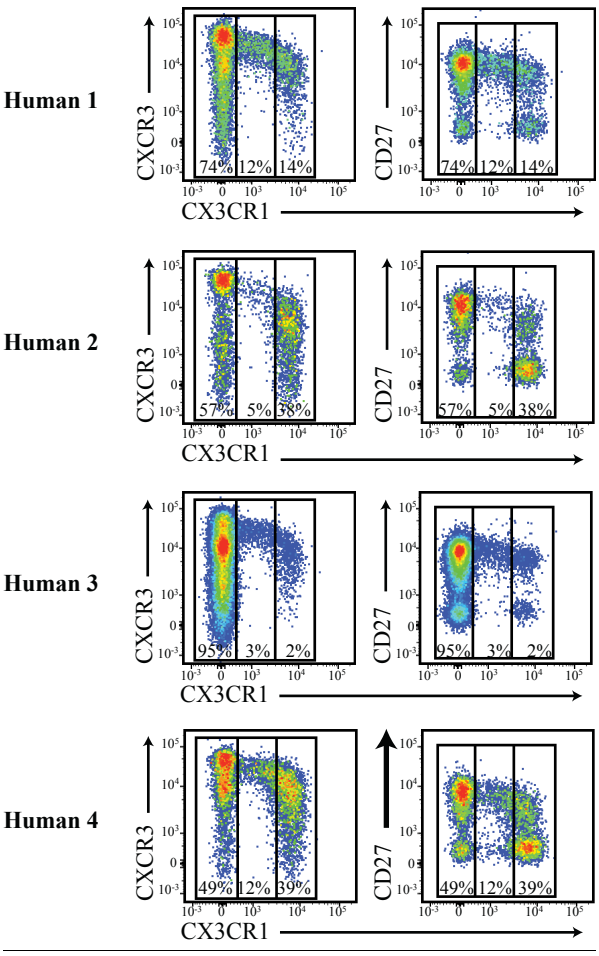

Figure 3.3: CX_3CR1 staining on human $CD8^+$ T cells. Blood from four anonymous human donors was stained for analysis of CX_3CR1^-, CX_3CR1^{int} and CX_3CR1^{hi} T_{Mem} subsets. Plots are pre-gated on $CD3^+CD8^+CD45RO^+$ T cells and are plotted as anti-CX_3CR1 against anti-CXCR3 or anti-CD27.

numbers of CX_3CR1^-, CX_3CR1^{int} and CX_3CR1^{hi} cells on day 49, whereas recipients of CX_3CR1^{int} T_{Eff} generated mainly CX_3CR1^{int} and CX_3CR1^{hi} cells, and CX_3CR1^{hi} T_{Eff} gave rise almost exclusively to CX_3CR1^{hi} offspring (**Figure 3.2 C,D**).

In the described experiments, T_{Eff} subsets were harvested and transferred at the peak of the anti-viral effector response, so the transferred cells likely encountered

cognate Ag in the host that promoted their further differentiation. Thus, we performed additional adoptive transfers with Ag-experienced CX_3CR1^-, CX_3CR1^{int} and CX_3CR1^{hi} OT-I cells that were purified during the early memory phase on day 29 and transferred to naive congenic recipients. One month later, the vast majority of cells in each transferred subset faithfully retained their original level of CX_3CR1 expression (**Figure 3.2 E**), indicating that each T_{Mem} population is phenotypically stable. This suggests that T_{Mem} can form even from CX_3CR1^{hi} precursors that underwent extensive effector differentiation.

CX_3CR1^{int} T_{Mem} re-express CD62L, but CX_3CR1^{hi} T_{EM} do not

Although most surface differentiation markers were similarly expressed on CX_3CR1^- and CX_3CR1^{int} T_{Mem}, the LN homing receptor, CD62L, was a notable exception; on day 77 post infection this marker was found on both subsets, but not on CX_3CR1^{hi} cells (**Figure 3.2 A)**, consistent with the differential appearance of each subset in LNs. However, the mean fluorescence intensity and frequency of $CD62L^+$ T_{Mem} was significantly higher among CX_3CR1^- cells than among the CX_3CR1^{int} subset. Moreover, the use of CD62L is further complicated by the fact that the vast majority of T_{Eff} are initially $CD62L^-$, and the frequency of Ag-experienced $CD62L^+$ cells increases gradually during the subsequent memory[4,25]. Whether and to what extent this reflects re-acquisition of CD62L by initially $CD62L^-$ memory precursors or selective outgrowth of a T_{Eff} subset that was *a priori* $CD62L^+$ has been a longstanding subject of debate[4,5].

To ask whether the progressive increase in $CD62L^+$ T_{Mem} resulted from CD62L re-acquisition or expansion of $CD62L^+$ precursors, we infected $CX_3CR1^{+/gfp}$ mice ($CD45.1^+$) with LCMV and, 30 days later, FACS-sorted four subsets of Ag-experienced

($CD44^{hi}$) $CD8^+$ T cells based on CD62L and CX_3CR1 expression as shown in **Figure 3.4 A**. Equal numbers of each of these early memory subsets were transferred into separate naïve C57BL/6 recipients ($CD45.2^+$), and 30 days later CD62L expression was analyzed on gp33-specific $CD45.1^+$ splenic and LN T-cells. One month after transfer of $CD62L^+$ CX_3CR1^- or $CD62L^-$ CX_3CR1^{hi} T_{Mem}, nearly all cells remained $CD62L^+$ or $CD62L^-$, respectively, indicating that these subsets maintain a stable phenotype at steady-state. By contrast, after transfer of $CD62L^-$ CX_3CR1^- or $CD62L^-$ CX_3CR1^{int} T_{Mem}, a sizeable fraction of cells acquired CD62L. Notably, CX_3CR1^- T_{Mem} were more efficient at re-expressing CD62L than CX_3CR1^{int} cells (**Figure 3.4 A**).

In aggregate, the above results indicate the presence of at least three discrete T_{Mem} populations: CX_3CR1^{hi} cells correspond to classical T_{EM} and retain a $CD62L^-$ $CCR7^-$ CX_3CR1^{hi} phenotype into the memory phase. In the early memory phase (around day 30), the CX_3CR1^- subset contained the largest percentage of $CD62L^+$ (i.e. LN homing) T_{CM}-like cells. During subsequent months, conversion of the highly plastic $CD62L^-$ CX_3CR1^- T_{Mem} (pre-T_{CM}) gives rise to additional $CD62L^+$ T_{Mem} (**Figure 3.4 A**). Because CX_3CR1^- T_{Mem} also express functional CCR7, they are equivalent to classical T_{CM}. The third subset, the CX_3CR1^{int} T_{Mem}, also express CCR7 and re-acquire CD62L, albeit more slowly and to a lesser extent than the CX_3CR1^- subset. However, even though many CX_3CR1^{int} cells appear T_{CM}-like, our adoptive transfer experiments show that the two subsets are not truly identical because the transferred CX_3CR1^{int} T_{Mem} maintain CX_3CR1 expression (**Figure 3.2 D,E**). These findings clearly show that during the early memory phase, a subset of T_{Mem} that initially expresses a $CD62L^-$ T_{EM} phenotype can contribute to the LN homing T_{Mem} pool (i.e. they became T_{CM}-like), however, this subset primarily

consisted of CX_3CR1^- pre-T_{CM} and CX_3CR1^{int} T_{Mem} that had not yet re-acquired CD62L. In contrast, CX_3CR1^{hi} T_{Mem}, the *bona fide* T_{EM}, were incapable of T_{CM} differentiation.

Our findings imply that T_{CM}, CX_3CR1^{int} T_{Mem}, and T_{EM} undergo homeostatic self-renewal (albeit with distinct efficiencies) with only minimal inter-subset conversion at steady-state and generate quantitatively and functionally divergent T_{Eff} progeny. This prompted us to ask whether each T_{Mem} population is locked in their individual differentiation program or can be re-educated by subsequent Ag challenge. Thus, we transferred sorted *CX₃CR1*$^{+/gfp}$ x OT-I T_{Mem} subsets from VSV-ova immunized donors to investigate the short- and long-term phenotype of T_{Eff} that arose after secondary challenge with LM-OVA (**Figure 3.4 B**). On day 6 and 7 post infection, each group of recipients contained a sizeable fraction of GFP^{dim} cells that had largely disappeared by day 9 and 35 when >80% and >90%, respectively, of the remaining T_{Eff} were CX_3CR1^{hi}. It is not clear if the early transient dip in apparent reporter expression reflected reduced CX_3CR1 biosynthesis or dilution of GFP in rapidly dividing lymphoblasts. Nevertheless, at every time-point analyzed there was a notable difference in the composition of progeny of each T_{Mem} subset: T_{CM} generated small but detectable populations of CX_3CR1^- and CX_3CR1^{int} cells, whereas CX_3CR1^{int} T_{Mem} did not produce CX_3CR1^- offspring, but generated persistent CX_3CR1^{int} progeny. T_{EM} (like T_{CM} and CX_3CR1^{int} T_{Mem}) gave rise to numerous CX_3CR1^{hi} T_{Eff}, but generated no other T_{Eff} subset.

Figure 3.4: CX_3CR1^{int} T_{Mem} re-express CD62L, but CX_3CR1^{hi} T_{EM} do not. (**A**) Experimental protocol for adoptive transfer of indicated endogenous T_{Mem} subsets (left). Pooled data from *n* = 3 experiments (1-4 mice/group/experiment) show frequency of CD62L+ cells (middle) and CX_3CR1 subset frequency (right) among splenic and LN resident OT-I T_{Mem}. Bar graphs depict mean + SD. (**B**) Left: Experimental protocol. Naïve OT-I $CX_3CR1^{+/gfp}$ $CD45.1^+$ T cells were transferred into naïve C57BL/6 followed by VSV-ova infection. Indicated populations of OT-I T_{Mem} were sorted from spleen and LNs on day 64 post infection and transferred into separate naïve C57BL/6 recipients. 3h after T_{Mem} transfer, recipients were infected with LM-ova (2° infection). Right: Phenotype of circulating OT-I T_{Mem} post 2° infection. Pooled data from two experiments (3-4 mice/group). Bars show mean + SD.

Figure 3.4 (Continued):

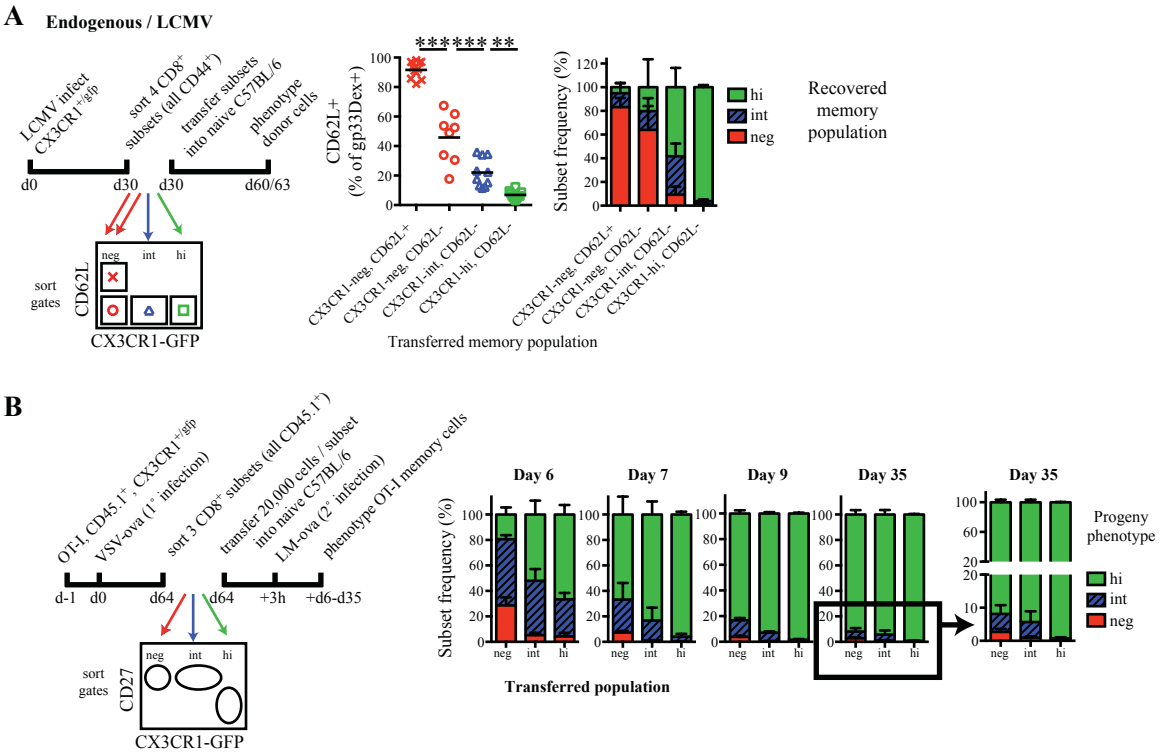

Distribution of CX_3CR1 T_{Mem} within peripheral tissues

Having determined the lineage relationships and lymph node homing properties of the three circulating T_{Mem} subsets, we set out to investigate each population's ability to survey non-lymphoid tissues and their relationship to resident memory T cells (T_{RM}). The non-migratory T_{RM} are believed to be derived, at least in part, from tissue-tropic T_{Eff} that arise during early effector responses[3,26,27]. However, it has also been suggested that at least some T_{RM} may be progeny of T_{EM}[28]. Indeed, when T_{EM} were first identified in human blood[6], it seemed reasonable to assume that T_{EM} may survey peripheral tissues because earlier studies had shown that substantial numbers of T_{Mem} can be harvested from afferent lymphatics that drain interstitial fluid from peripheral tissues[8]. Thus,

extravascular T_{Mem} comprise a mixture of sessile T_{RM} and migratory T_{Mem}. Most T_{RM} express CD69 and/or CD103[3], which retain T_{RM} within host tissues[29], although some T_{RM} do not express these markers[30]. The migratory T_{Mem}, which are phenotypically poorly defined, are thought to visit non-lymphoid tissues transiently and return to the blood via the draining lymphatics and thoracic duct.

To determine the relationship between T_{RM} and the circulating T_{Mem} subsets, we analyzed the phenotype of OT-I T_{Mem} that arose after LCMV-OVA infection within the extravascular compartment of several non-lymphoid tissues, including the salivary gland (SG), the female reproductive tract (FRT) and the intra-epithelial lymphocytes (IEL) as well as lamina propria lymphocytes (LPL) in the small intestine. Intra- and extravascular T_{Mem} in tissue cell suspensions were distinguished by flow cytometry after short-term intravenous (i.v.) injection of a fluorescent anti-CD8α MAb (**Figure 3.5 A**). This strategy allowed us to distinguish MAb-stained intravascular T cells from extravascular cells, which are inaccessible to the MAb and remain unstained[31].

There was considerable heterogeneity among extravascular OT-I T_{Mem}, with 70-80% expressing CD69 and roughly half co-expressing CD103, while 20-30% expressed neither marker (**Figure 3.5 B**). After gating on extravascular $CD69^{+}CD103^{+}$ OT-I T_{RM}, most (60-90%) were CX_3CR1^{-} and the remainder were CX_3CR1^{int}, while none were CX_3CR1^{hi} (**Figure 3.5 C**). This phenotype is consistent with previous findings that peripheral tissues in LCMV infected mice are seeded by T_{Eff} starting on or after day 4.5 and before day 7 post infection[26], a period during which most T_{Eff} are still CX_3CR1^{-} or CX_3CR1^{int} (**Figure 3.1 D**). Thus, T_{RM} precursors apparently do not upregulate CX_3CR1 once they have accessed a peripheral target tissue, even during an ongoing systemic

infection. Furthermore, the fact that T_{RM} were entirely devoid of CX_3CR1^{hi} cells strongly suggests that this population is neither derived from nor replenished by T_{EM}. Remarkably, even when we extended our analysis of non-lymphoid tissues to all extravascular T_{Mem} (i.e. without gating on CD69 or CD103), CX_3CR1^{hi} T-cells were almost completely absent, except in peritoneal lavage fluid where ~20% of T_{Mem} were CX_3CR1^{hi} (**Figure 3.5 D**). This exclusion from peripheral tissues was also observed following VSV-OVA infection (**Figure 3.5 E**)

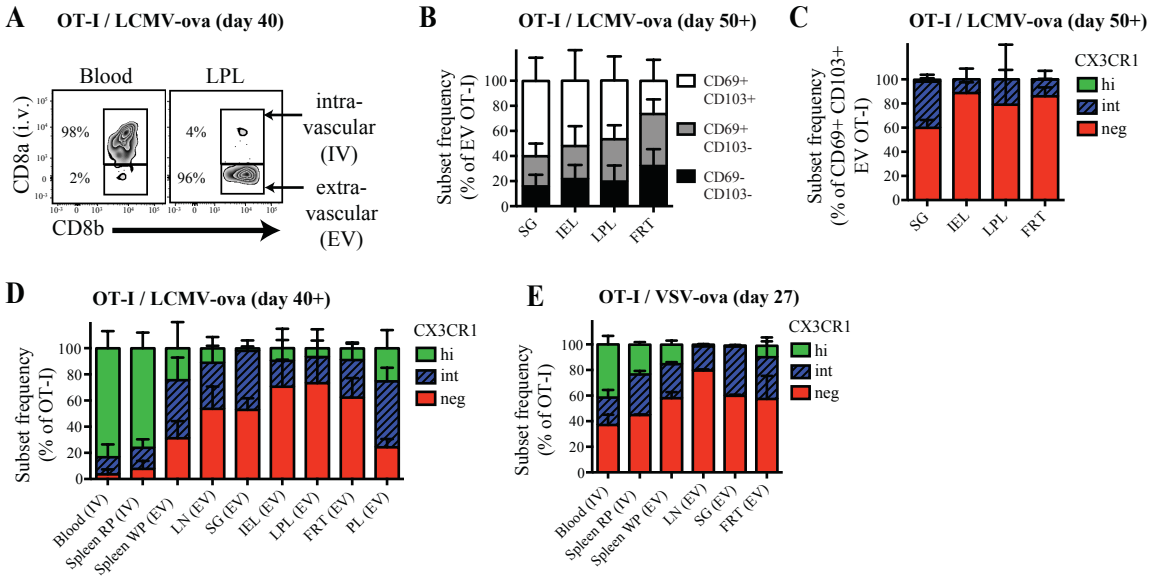

Figure 3.5: CX_3CR1^{hi} T_{EM} are largely excluded from peripheral tissues. (**A-D**) Naïve OT-I $CX_3CR1^{+/gfp}$ $CD45.1^+$ T cells were transferred into C57BL/6 mice prior to LCMV-ova infection. (**A**) Gating strategy for intra- and extra-vascular OT-I cells. Composite FACS plot from 4 mice. (**B**) CD69 and CD103 expression on extra-vascular OT-I T_{Mem} and (**C**) frequency of CX3CR1 subsets among extra-vascular $CD69^+CD103^+$ OT-I T_{Mem} in indicated tissues. (**B,C**) Bars show mean + SD. *n* = 2 experiments (2-5 mice/tissue/experiment). (**D**) Frequency of CX_3CR1-defined subsets among OT-I T_{Mem}. Bars show mean + SD. *n* = 4 experiments (Blood, Spleen, LN, SG) *n* = 3 experiments (IEL, LPL, FRT) (2-5 mice/tissue/experiment). (**E**) Naïve OT-I CX3CR1+/gfp CD45.1+ T cells were transferred into C57BL/6 followed by VSV-ova infection. Frequency of CX3CR1-defined subsets among OT-I TMem. Bars show mean + SD. n = 1 experiment (3 mice).

CX_3CR1^{int} T_{PM}, not T_{EM}, are the major T_{Mem} subset circulating between peripheral tissues and blood

The fact that T_{Mem} egress from peripheral tissues via the draining lymphatics has been documented in sheep[8] as well as humans[32], but the precise phenotype of these migratory T cells has been unclear. The finding that CX_3CR1^{hi} T_{Mem} are largely excluded from peripheral tissues seemed at odds with the idea that T_{EM} are the principal T_{Mem} subset surveying those tissues. Two scenarios seemed plausible to explain our findings: First, if T_{EM} were uniquely capable of accessing peripheral tissues, they would have to do so only rarely and/or spend very little time before departing via the draining lymphatics. Second, contrary to current belief, a T_{Mem} subset other than T_{EM} may be responsible for peripheral immune surveillance. To test these two alternatives, we collected thoracic duct lymph (TDL) from immunized mice to characterize the migratory T_{Mem} that are en route from tissues toward the blood stream.

The thoracic duct collects lymph from all tissues below the diaphragm and the left upper body. TDL contains abundant lymphocytes that recirculate through secondary lymphoid tissues (SLOs) via high endothelial venules (HEVs)[33]. In addition, the thoracic duct is also a conduit for migratory T_{Mem} that depart from peripheral tissues via the afferent lymph, pass through regional LNs and ultimately return to the blood. Homing via resting HEVs requires lymphocyte-expressed CD62L, while trafficking to most non-lymphoid tissues is CD62L independent[34]. Thus, we reasoned that it would be unlikely that any $CD62L^-$ T_{Mem} contained in TDL would have accessed the lymph via HEV entry into LNs and, therefore, $CD62L^-$ T_{Mem} would represent the migratory peripheral T_{Mem} subset.

Indeed, at 7 weeks after LCMV-OVA infection, the ratio of $CD62L^-$ and $CD62L^+$ OT-I T_{Mem} in TDL was ~1:1, suggesting that the number of T_{CM} that migrated through LNs was approximately equal to that of the peripheral migratory T_{Mem} (**Figure 3.6 A**). At this time point, peripheral blood T_{Mem} were strongly dominated by $CD62L^-$ $CX3CR1^{hi}$ T_{EM}, whereas the most abundant subset in TDL were CX_3CR1^{int} T_{Mem}. When OT-I T_{Mem} in TDL were subdivided based on CD62L expression, the $CD62L^+$ (i.e. LN homing) subset contained slightly more CX_3CR1^- T_{CM} than $CX3CR1^{int}$ T_{Mem} and was devoid of CX_3CR1^{hi} T_{EM}. In contrast, in the $CD62L^-$ (i.e. periphery derived) T_{Mem} subset, CX_3CR1^{int} cells were 3-4 times more frequent than CX_3CR1^- T_{CM} or CX_3CR1^{hi} T_{EM}.

While these results implied that CX_3CR1^{int} T_{Mem}, and not T_{EM}, are the predominant subset trafficking through peripheral tissues, it was important to verify that the $CD62L^-$ T_{Mem} in TDL were indeed a recirculating population. Conceivably, at least some of the thoracic duct-borne T_{Mem} might have represented progeny of *in situ* dividing T_{RM}. To address this issue, we performed parabiosis surgery to generate pairs of congenic mice, which establishes a shared circulatory system that allows genetically traceable hematopoietic cells from each animal to access the blood and tissues of a conjoined partner[35]. One animal (CD45.2) received OT-I *$CX_3CR1^{+/gfp}$* T_N (CD45.1/2) and was then infected with LCMV-OVA to generate T_{Mem} (**Figure 3.6 C**). After 5 weeks, the immunized animal was surgically joined to a naïve partner (CD45.1), which underwent thoracic duct cannulation 3-4 weeks later. Because the naïve parabiont does not harbor partner-derived T_{RM}[28], any OT-I T_{Mem} among its TDL should remain free of contaminating T_{RM} progeny and thus reflect exclusively migratory T_{Mem}. Consistent with our findings in non-parabiotic immune mice, the OT-I T_{Mem} population in blood of naïve

Figure 3.6: CX_3CR1^{int} T_{PM}, not T_{EM}, are the major T_{Mem} subset circulating between peripheral tissues and blood. (**A**) FACS plot of OT-I T_{Mem} concatenated from 3 mice. Frequency of CX_3CR1 subsets among total (top), $CD62L^+$ (middle) and $CD62L^-$ (bottom) OT-I T_{Mem} in blood and TDL. Bars show mean + SD. *n* = 2 experiments (3 mice/experiment). *** $p<0.001$ by one-way ANOVA with Tukey's multiple comparisons test. (**B**) Experimental setup for panels (**C**) and (**D**). Naïve OT-I $CX_3CR1^{+/gfp}$ $CD45.1^{+/-}$ T cells were transferred into C57BL/6 mice prior to LCMV-ova infection. Five weeks later, immune mice were joined to naïve congenic C57BL/6 (**C**) or $LTa^{-/-}$ (**D**) mice by parabiosis. 3-4 weeks later, blood and TDL were collected from the naïve partner. (**C, D**) 1st row: Frequency of $CD62L^+$ and $CD62L^-$ OT-I, and CX_3CR1 subsets among total (2nd row), $CD62L^+$ (3rd row) and $CD62L^-$ (4th row) OT-I T_{Mem} in blood and TDL. Bars show mean + SD. *n* = 2 experiments (1-2 mice/experiment). 3 mice total.

Figure 3.6 (Continued):

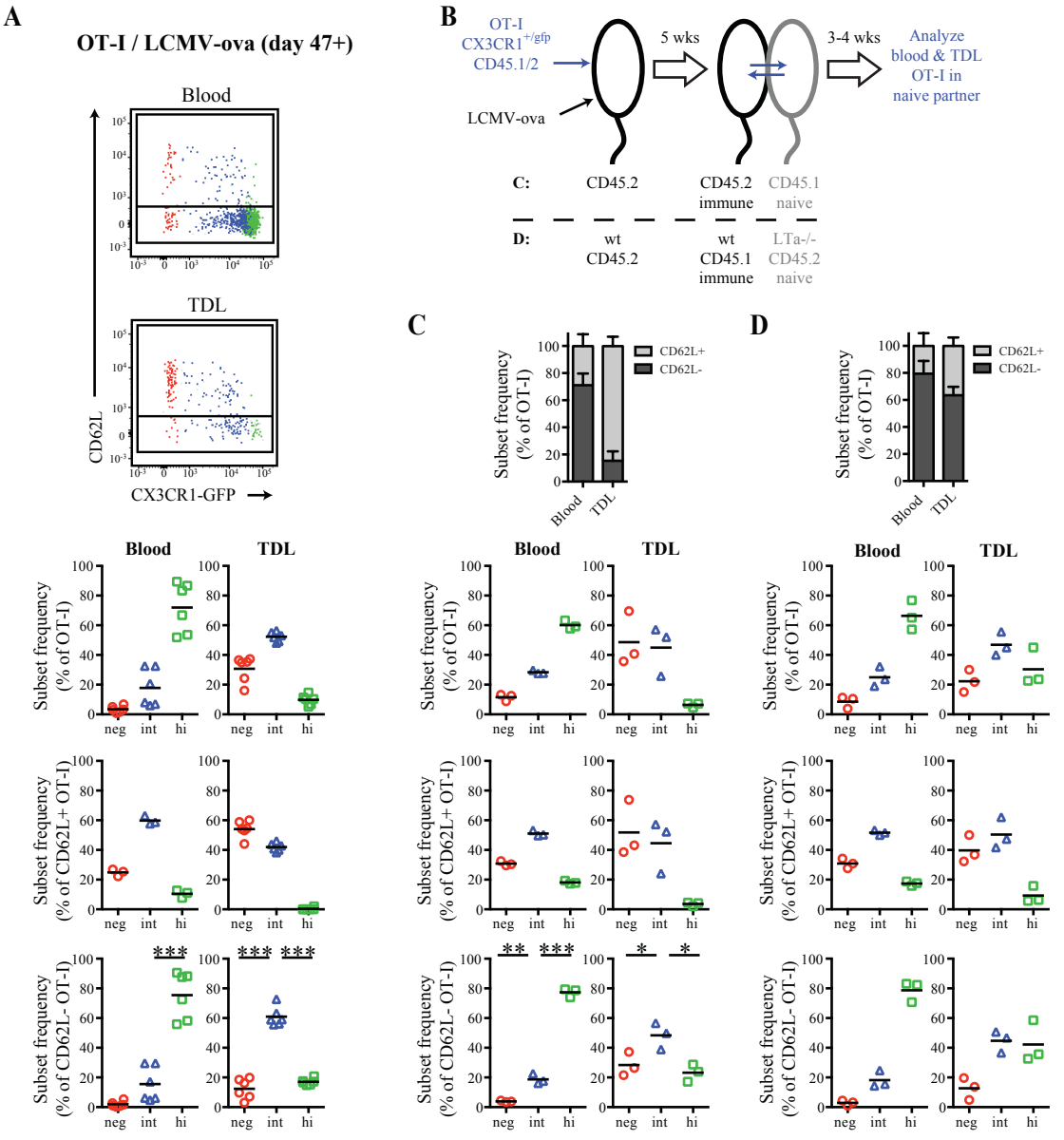

parabionts was dominated by CD62L^{-} CX$_3$CR1^{hi} T$_{EM}$ (**Figure 3.6 C**). However, ~80% of TDL T$_{Mem}$ in naïve parabionts were CD62L^{+}. This putative LN homing subset was composed of equal parts CX3CR1^{-} T$_{CM}$ and CX$_3$CR1^{int} T$_{Mem}$. By contrast, the CD62L^{-} T$_{Mem}$ in TDL were preferentially composed of CX$_3$CR1^{int} T$_{Mem}$, demonstrating that

blood-derived T_{Mem}, particularly the CX_3CR1^{int} subset, can traverse host tissues in a CD62L-independent fashion and return to the blood via the lymph.

Although CD62L is required for the vast majority of T cells to interact with HEVs, some mucosal lymphoid tissues, such as Peyer's patches, can support CD62L-independent lymphocyte homing[36]. To rigorously rule out that $CD62L^-$ T_{Mem} had entered the TDL pool after using alternate adhesion pathways to home to SLOs rather than migrating across peripheral tissues, we generated additional parabiotic pairs of immunized wildtype mice containing OT-I x *CX₃CR1*$^{+/gfp}$ T_{Mem} and naïve lymphotoxin-α deficient ($LT\alpha^{-/-}$) mice, which lack all SLOs except the spleen (**Figure 3.6 D**). In this setting, any T_{Mem} that could be recovered from TDL of $LT\alpha^{-/-}$ hosts must have accessed the lymph after trafficking from the blood through a non-lymphoid tissue, regardless of CD62L expression. Indeed, although the frequency of lymph-borne $CD62L^+$ T_{Mem} was higher in TDL of naïve WT parabionts (**Figure 3.6 C**, **top**) than in TDL of naïve $LT\alpha^{-/-}$ parabionts (**Figure 3.6 D**, **top**), the latter still contained ~40% $CD62L^+$ OT-I T_{Mem} that were composed in roughly equal parts of CX_3CR1^- T_{CM} and CX_3CR1^{int} T_{Mem} (**Figure 3.6 D, bottom**). These results reveal that T_{CM} have the capacity to recirculate through non-lymphoid tissues, at least in $LT\alpha^{-/-}$ mice where T_{CM} sequestration in SLOs is minimal. CX_3CR1^{int} T_{Mem} and CX_3CR1^{hi} T_{EM} occurred at similar frequency among the $CD62L^-$ T_{Mem} in TDL of $LT\alpha^{-/-}$ parabionts even though T_{EM} were ~5-fold more abundant in the blood. The somewhat higher proportion of T_{EM} in these experiments as compared to wildtype parabionts could potentially reflect a role for the LTα pathway in the regulation of peripheral lymphocyte trafficking. Notwithstanding, when T_{Mem} subset composition

was assessed in TDL of LTα$^{-/-}$ parabionts regardless of CD62L expression, the CX_3CR1^{int} subset predominated.

In aggregate, these experiments contradict the long-held paradigm that classical T_{EM} are specialized to survey non-lymphoid tissues at steady-state. Rather, our results show that the newly identified CX_3CR1^{int} T_{Mem} subset is the predominant population that recirculates between blood and peripheral tissues. Thus, we classify this subset as 'peripheral memory' T cells, or T_{PM}.

3.6 Discussion

In conclusion, we show that CX_3CR1 expression is induced on pathogen-specific $CD8^+$ T cells during viral and bacterial infections, and serves as a differentiation marker to subdivide $CD8^+$ T_{Eff} and T_{Mem} into three phenotypically, functionally and transcriptionally distinct subsets. The level of CX_3CR1 expression on T_{Eff} correlates with the degree of effector differentiation. Every T_{Eff} subset can produce at least some T_{Mem}, suggesting that even a 'terminal' T_{Eff} differentiation state does not preclude a memory fate. However, only the relatively rare CX_3CR1^- subset has the capacity to produce long-lived CX_3CR1^- T_{Mem} most of which differentiate into classical $CD62L^+CCR7^+$ LN homing T_{CM}. CX_3CR1^{hi} T_{Eff} can produce only CX_3CR1^{hi} T_{EM}, which are permanently $CD62L^-$ and completely excluded from resting LNs. As such, high expression of CX_3CR1 constitutes a unique marker to positively identify $CD8^+$ T_{EM}. Finally, T_{RM} that permanently reside within non-lymphoid tissues arise from early CX_3CR1^- and CX_3CR1^{int} T_{Eff} and remain largely CX_3CR1^-.

CX_3CR1^- and CX_3CR1^{int} T_{Eff} also give rise to a hitherto unrecognized T_{Mem} subset, the T_{PM}, which are CX_3CR1^{int} and gradually re-acquire LN homing receptors. At steady-state, each T_{Mem} population is phenotypically stable with minimal exchange between subsets, however, Ag rechallenge experiments reveal a uni-directional $T_{CM} \rightarrow T_{PM} \rightarrow T_{EM}$ pedigree. The newly identified T_{PM} possess phenotypic, functional, and migratory properties that clearly distinguish them from classical T_{CM} and T_{EM}. We define T_{PM} as a long-lived, phenotypically stable population of Ag-experienced CX_3CR1^{int} T cells that express CD27, CXCR3 and CCR7, as well as variable levels of CD62L. Like T_{CM}, the $CCR7^+CD62L^+$ T_{PM} subset is capable of homing to LNs, but can also access peripheral tissues, whereas $CD62L^-$ T_{PM} preferentially survey the periphery. CCR7 expression on $CD62L^-$ T_{PM} presumably enables these cells to access afferent lymphatics and return to the blood[37,38]. Our findings revealed that current concepts of T_{Mem} subset distribution and trafficking require revision. T_{CM}, as described earlier, circulate between blood and SLOs[7], while T_{PM} survey the periphery. By contrast, T_{EM}, which had traditionally been thought to circulate between blood and peripheral tissues, are actually excluded from most extravascular compartments, except the spleen. Further study is needed to clarify the functional consequences of this apparent restriction of T_{EM} to the intravascular space.

3.7 References

1. Williams, M. A. & Bevan, M. J. Effector and memory CTL differentiation. *Annu. Rev. Immunol.* **25,** 171–192 (2007).
2. Jameson, S. C. & Masopust, D. Diversity in T cell memory: an embarrassment of riches. *Immunity* **31,** 859–871 (2009).

3. Mueller, S. N., Gebhardt, T., Carbone, F. R. & Heath, W. R. Memory T cell subsets, migration patterns, and tissue residence. *Annu. Rev. Immunol.* **31,** 137–161 (2013).

4. Wherry, E. J., Teichgräber, V., Becker, T. C., Masopust, D., Kaech, S. M., Antia, R., Andrian, von, U. H. & Ahmed, R. Lineage relationship and protective immunity of memory CD8 T cell subsets. *Nat Immunol* **4,** 225–234 (2003).

5. Marzo, A. L., Klonowski, K. D., Le Bon, A., Borrow, P., Tough, D. F. & Lefrançois, L. Initial T cell frequency dictates memory CD8+ T cell lineage commitment. *Nat Immunol* **6,** 793–799 (2005).

6. Sallusto, F., Lenig, D., Förster, R., Lipp, M. & Lanzavecchia, A. Two subsets of memory T lymphocytes with distinct homing potentials and effector functions. *Nature* **401,** 708–712 (1999).

7. Andrian, von, U. H. & Mempel, T. R. Homing and cellular traffic in lymph nodes. *Nat Rev Immunol* **3,** 867–878 (2003).

8. Mackay, C. R., Marston, W. L. & Dudler, L. Naive and memory T cells show distinct pathways of lymphocyte recirculation. *J Exp Med* **171,** 801–817 (1990).

9. Dudani, R., Chapdelaine, Y., Faassen Hv, H. V., Smith, D. K., Shen, H., Krishnan, L. & Sad, S. Multiple mechanisms compensate to enhance tumor-protective CD8(+) T cell response in the long-term despite poor CD8(+) T cell priming initially: comparison between an acute versus a chronic intracellular bacterium expressing a model antigen. *The Journal of*

Immunology **168,** 5737–5745 (2002).

10. Emonet, S. F., Garidou, L., Mcgavern, D. B. & la Torre, de, J. C. Generation of recombinant lymphocytic choriomeningitis viruses with trisegmented genomes stably expressing two additional genes of interest. *Proceedings of the National Academy of Sciences* **106,** 3473–3478 (2009).
11. Bazan, J. F., Bacon, K. B., Hardiman, G., Wang, W., Soo, K., Rossi, D., Greaves, D. R., Zlotnik, A. & Schall, T. J. A new class of membrane-bound chemokine with a CX3C motif. *Nature* **385,** 640–644 (1997).
12. Jung, S., Aliberti, J., Graemmel, P., Sunshine, M. J., Kreutzberg, G. W., Sher, A. & Littman, D. R. Analysis of fractalkine receptor CX(3)CR1 function by targeted deletion and green fluorescent protein reporter gene insertion. *Mol Cell Biol* **20,** 4106–4114 (2000).
13. Palframan, R. T., Jung, S., Cheng, G., Weninger, W., Luo, Y., Dorf, M., Littman, D. R., Rollins, B. J., Zweerink, H., Rot, A. & Andrian, von, U. H. Inflammatory chemokine transport and presentation in HEV: a remote control mechanism for monocyte recruitment to lymph nodes in inflamed tissues. *J Exp Med* **194,** 1361–1373 (2001).
14. Geissmann, F., Jung, S. & Littman, D. R. Blood monocytes consist of two principal subsets with distinct migratory properties. *Immunity* **19,** 71–82 (2003).
15. Imai, T., Hieshima, K., Haskell, C., Baba, M., Nagira, M., Nishimura, M., Kakizaki, M., Takagi, S., Nomiyama, H., Schall, T. J. & Yoshie, O. Identification and molecular characterization of fractalkine receptor

CX3CR1, which mediates both leukocyte migration and adhesion. *Cell* **91,** 521–530 (1997).

16. Nishimura, M., Umehara, H., Nakayama, T., Yoneda, O., Hieshima, K., Kakizaki, M., Dohmae, N., Yoshie, O. & Imai, T. Dual functions of fractalkine/CX3C ligand 1 in trafficking of perforin+/granzyme B+ cytotoxic effector lymphocytes that are defined by CX3CR1 expression. *The Journal of Immunology* **168,** 6173–6180 (2002).

17. Mionnet, C., Buatois, V., Kanda, A., Milcent, V., Fleury, S., Lair, D., Langelot, M., Lacoeuille, Y., Hessel, E., Coffman, R., Magnan, A., Dombrowicz, D., Glaichenhaus, N. & Julia, V. CX3CR1 is required for airway inflammation by promoting T helper cell survival and maintenance in inflamed lung. *Nat Med* **16,** 1305–1312 (2010).

18. Staumont-Sallé, D., Fleury, S., Lazzari, A., Molendi-Coste, O., Hornez, N., Lavogiez, C., Kanda, A., Wartelle, J., Fries, A., Pennino, D., Mionnet, C., Prawitt, J., Bouchaert, E., Delaporte, E., Glaichenhaus, N., Staels, B., Julia, V. & Dombrowicz, D. CX_3CL1 (fractalkine) and its receptor CX_3CR1 regulate atopic dermatitis by controlling effector T cell retention in inflamed skin. *Journal of Experimental Medicine* **211,** 1185–1196 (2014).

19. Gerlach, C., van Heijst, J. W. J. & Schumacher, T. N. M. The descent of memory T cells. *Ann N Y Acad Sci* **1217,** 139–153 (2011).

20. Sarkar, S., Kalia, V., Haining, W. N., Konieczny, B. T., Subramaniam, S. & Ahmed, R. Functional and genomic profiling of effector CD8 T cell subsets with distinct memory fates. *Journal of Experimental Medicine* **205,** 625–640

(2008).

21. Kaech, S. M., Tan, J. T., Wherry, E. J., Konieczny, B. T., Surh, C. D. & Ahmed, R. Selective expression of the interleukin 7 receptor identifies effector CD8 T cells that give rise to long-lived memory cells. *Nat Immunol* **4,** 1191–1198 (2003).

22. Hintzen, R. Q., de Jong, R., Lens, S. M., Brouwer, M., Baars, P. & van Lier, R. A. Regulation of CD27 expression on subsets of mature T-lymphocytes. *The Journal of Immunology* **151,** 2426–2435 (1993).

23. Voehringer, D., Blaser, C., Brawand, P., Raulet, D. H., Hanke, T. & Pircher, H. Viral infections induce abundant numbers of senescent CD8 T cells. *The Journal of Immunology* **167,** 4838–4843 (2001).

24. Graef, P., Buchholz, V. R., Stemberger, C., Flossdorf, M., Henkel, L., Schiemann, M., Drexler, I., Höfer, T., Riddell, S. R. & Busch, D. H. Serial transfer of single-cell-derived immunocompetence reveals stemness of CD8(+) central memory T cells. *Immunity* **41,** 116–126 (2014).

25. Badovinac, V. P., Haring, J. S. & Harty, J. T. Initial T cell receptor transgenic cell precursor frequency dictates critical aspects of the CD8(+) T cell response to infection. *Immunity* **26,** 827–841 (2007).

26. Masopust, D., Choo, D., Vezys, V., Wherry, E. J., Duraiswamy, J., Akondy, R., Wang, J., Casey, K. A., Barber, D. L., Kawamura, K. S., Fraser, K. A., Webby, R. J., Brinkmann, V., Butcher, E. C., Newell, K. A. & Ahmed, R. Dynamic T cell migration program provides resident memory within intestinal epithelium. *Journal of Experimental Medicine* **207,** 553–564

(2010).

27. Stary, G., Olive, A., Radovic-Moreno, A. F., Gondek, D., Alvarez, D., Basto, P. A., Perro, M., Vrbanac, V. D., Tager, A. M., Shi, J., Yethon, J. A., Farokhzad, O. C., Langer, R., Starnbach, M. N. & Andrian, von, U. H. VACCINES. A mucosal vaccine against Chlamydia trachomatis generates two waves of protective memory T cells. *Science* **348,** aaa8205 (2015).

28. Jiang, X., Clark, R. A., Liu, L., Wagers, A. J., Fuhlbrigge, R. C. & Kupper, T. S. Skin infection generates non-migratory memory CD8+ TRM cells providing global skin immunity. *Nature* 1–6 (2012).

29. Mackay, L. K., Rahimpour, A., Ma, J. Z., Collins, N., Stock, A. T., Hafon, M.-L., Vega-Ramos, J., Lauzurica, P., Mueller, S. N., Stefanovic, T., Tscharke, D. C., Heath, W. R., Inouye, M., Carbone, F. R. & Gebhardt, T. The developmental pathway for CD103(+)CD8(+) tissue-resident memory T cells of skin. *Nat Immunol* **14,** 1294–1301 (2013).

30. Steinert, E. M., Schenkel, J. M., Fraser, K. A., Beura, L. K., Manlove, L. S., Igyarto, B. Z., Southern, P. J. & Masopust, D. Quantifying Memory CD8 T Cells Reveals Regionalization of Immunosurveillance. *Cell* **161,** 737–749 (2015).

31. Anderson, K. G., Sung, H., Skon, C. N., Lefrançois, L., Deisinger, A., Vezys, V. & Masopust, D. Cutting edge: intravascular staining redefines lung CD8 T cell responses. *J Immunol* **189,** 2702–2706 (2012).

32. Hunger, R. E., Yawalkar, N., Braathen, L. R. & Brand, C. U. The HECA-452 epitope is highly expressed on lymph cells derived from human skin. *Br. J.*

Dermatol. **141,** 565–569 (1999).

33. Gowans, J. L. & Knight, E. J. The route of re-circulation of lymphocytes in the rat. *Proc. R. Soc. London (Biol.).* **159**, 257-282, (1964).

34. Andrian, von, U. H. & Mackay, C. R. T-cell function and migration. Two sides of the same coin. *N Engl J Med* **343,** 1020–1034 (2000).

35. Wright, D. E., Wagers, A. J., Gulati, A. P., Johnson, F. L. & Weissman, I. L. Physiological migration of hematopoietic stem and progenitor cells. *Science* **294,** 1933–1936 (2001).

36. Bargatze, R. F., Jutila, M. A. & Butcher, E. C. Distinct roles of L-selectin and integrins α4β7 and LFA-1 in lymphocyte homing to Peyer's patch-HEV in situ: The multistep model confirmed and refined. *Immunity* **3,** 99–108 (1995).

37. Debes, G. F., Arnold, C. N., Young, A. J., Krautwald, S., Lipp, M., Hay, J. B. & Butcher, E. C. Chemokine receptor CCR7 required for T lymphocyte exit from peripheral tissues. *Nat Immunol* **6,** 889–894 (2005).

38. Bromley, S. K., Thomas, S. Y. & Luster, A. D. Chemokine receptor CCR7 guides T cell exit from peripheral tissues and entry into afferent lymphatics. *Nat Immunol* **6,** 895–901 (2005).

Chapter 4: Intravascular surveillance by terminally differentiated effector and memory $CD8^+$ T cells

4.1 Abstract

Following infection, pathogen-specific T cells proliferate and divide in a heterogeneous manner, giving rise to effector and memory T cells with distinct migratory patterns. This migratory division of labor ensures that the host is efficiently scanned for ongoing or recurring infections. Recent evidence (**Chapter 3**) suggests that the presumed migratory behavior of the classical effector memory T cell (T_{EM}) subset needs revision. Here, we report that terminally differentiated effector and memory T cells adhere to and patrol dermal endothelium, while less differentiated T cells do not. This behavior is enriched within arterioles and migration tends to be retrograde to blood flow. Further, patrolling T cells survey endothelium for antigen (Ag) as injection of cognate Ag results in rapid stopping. Together, this suggests that terminally differentiated effector and memory T cells engage in a migratory behavior that supports protective scanning of endothelium.

4.2 Attributions

The following individuals contributed to the work described in this chapter: Scott M. Loughhead (S.M.L.), Carmen Gerlach (C.G.), Lisette Wanders (L.W.), Zimeng Zhang (Z.Z.), and Ulrich H. von Andrian (U.H.v.A.).

S.M.L. and U.H.v.A. conceived the study design. S.M.L. performed and analyzed experiments. C.G. performed experiments and provided technical advice. L.W. sorted T_{Mem} CX_3CR1 subsets for transfer. Z.Z. performed confocal microscopy of ear dermis. S.M.L. wrote the chapter.

4.3 Introduction

During a viral infection, naïve $CD8^+$ T cells (T_N) proliferate rapidly in response to cognate antigen (Ag) and give rise to effector cells (T_{Eff}) that must clear the rapidly replicating pathogen. Guided by inflammatory chemokines and adhesion molecules, T_{Eff} extravasate into tissues and mediate protection through cytokine production and direct cytotoxicity. Following viral clearance, contraction begins and most T_{Eff} are eliminated, but a small fraction of long-lived memory cells (T_{Mem}) persist. Given that cytotoxic T lymphocytes (CTLs) require contact in order to exert their protective function, the tissue distribution of T_{Mem} is critical for effective protection of the host upon secondary infection. Three subsets of T_{Mem} have been described: central memory T cells (T_{CM}), effector memory T cells (T_{EM}), and tissue-resident memory T cells (T_{RM}). T_{CM} and T_{EM} circulate within the blood and are distinguished by the presence of the lymph node (LN)-trafficking molecules CCR7 and CD62L on T_{CM} and their absence on T_{EM}[1], which functionally relates to their migration patterns[2]. In contrast, T_{RM} do not circulate and generally express CD103 and CD69, which help to retain the cells within peripheral tissues[3-6]. T_{RM} therefore act locally to provide rapid protection to tissues[7-9] while T_{CM} circulate through LNs, survey Ag-laden DCs arriving from peripheral tissues, and expand into T_{Eff} upon antigenic stimulation[10]. Prior to the discovery of T_{RM}, a population of T_{Mem} was described that migrated through peripheral tissues and could be found in the afferent lymph[11]. Given that T_{EM} lack the requisite trafficking molecules for LN-homing, T_{EM} were ascribed to be this population that migrates through peripheral tissues. However, as described in **Chapter 3**, T_{EM} do not form the majority of T_{Mem} circulating through

peripheral tissues. Instead, the newly defined peripheral memory T cell (T_{PM}) dominates the T_{Mem} subsets migrating through peripheral tissues. This implied that the migration pattern of T_{EM} was restricted to the vasculature as they are excluded from LNs and do not migrate through peripheral tissues. We therefore sought to address the ramifications of this apparent vascular restriction.

4.4 Methods

Mice - C57BL/6, B6-albino, $CX_3CR1^{gfp/gfp}CD45.1^{+/+}$, $CD45.1^{+/+}$, $CCR2^{rfp/rfp}$, $CCR5^{-/-}$, OT-I, and β-Actin TdTomato mice (all on the C57BL/6 background) were purchased from the Jackson Laboratory. P14 mice were purchased from Taconic farms. All uninfected mice were housed, bred and crossed in a specific pathogen-free barrier facility of Harvard Medical School. All animal experiments were performed in accordance with national and institutional guidelines.

T cell isolation from murine tissues - To obtain naïve TCR-tg $CD8^+$ T cells for adoptive transfer, blood was drawn from TCR-tg mice, erythrocytes were lysed and a small sample was analyzed by flow cytometry to quantify the fraction of p14 or OT-I cells ($Va2^+CD8^+$). $5x10^3$ $Va2^+CD8^+$ T cells were transferred into naïve C57BL/6 recipient mice. If experiments were for analysis of T_{Mem} populations, $2.5x10^4$ naïve $Va2^+CD8^+$ T cells were transferred.

Prior to flow cytometric analysis of antigen experienced T cells, tissues were treated as follows: Blood underwent erythrocyte lysis. Ears were physically split along collagen plate into dorsal and ventral halves, then cut into small pieces. Minced ears were

enzymatically digested with 62.5µg/ml LiberaseTM (Roche) and 100µg/ml DNAseI (Roche) for 60 minutes at 37°C on a rotisserie. Spleens were physically homogenized by forcing the organs through a cell strainer or metal mesh. Lungs, the female reproductive tract (FRT) and salivary glands were cut in small pieces followed by enzymatic digestion with 62.5µg/ml LiberaseTM (Roche) and 100µg/ml DNAseI (Roche) for 30 minutes at 37°C, before application of a density gradient (NycoPrepTM 1.077, Axis-Shield). The FRT did not undergo a density gradient.

Prior to flow cytometric cell sorting, T cells were enriched by MACS technology (Miltenyi Biotec), using CD45.1-biotin (BioLegend) staining followed by anti-biotin MicroBeads (Miltenyi Biotec) for adoptively transferred TCR-tg T cells.

Flow cytometry and antibodies - Cells were sorted with a FACSAria^{TM} and analyzed with a FACSCanto^{TM} (all BD Biosciences). Subsequent analysis was performed in FlowJo (Tree Star) and Prism 6 (GraphPad) for statistics.

Antibodies for flow cytometry were purchased from BioLegend. CD8α (53-6.7), CD11b (M1/70), CD45.1 (A20), CD45.2 (104), CD45 (30-F11), Vα2 (B20.1), CX_3CR1 (SA011F11), KLRG-1 (2F1), CD11a (M17/4), CD18 (C71/16), CD49d (9C10), CD29 (HmB1-1), CD31 (MEC13.3), ICAM-1 (3E2), ICAM-2 (3C4), VCAM-1 (429). *In vivo* blocking antibodies were purchased from Bio X Cell. Mac-1 (M1/70), LFA-1 (M17/4), VLA-4 (PS/2), Rat IgG2a control (2A3).

Infections - Mice were infected intra-venously with 0.5-1x10^4 focus forming units (ffu) LCMV Armstrong strain (abbreviated LCMV), 0.5-1x10^4 ffu recombinant trisegmented

LCMV Armstrong strain expressing the fluorescent protein katushka and ovalbumin (abbreviated LCMV-ova), $2x10^6$ plaque forming units (pfu) recombinant VSV expressing ovalbumin (abbreviated VSV-OVA). For intra-dermal ear infections, mice were anesthetized, then ear gently placed on styrofoam block using double-sided tape. Using a nano-fill syringe with 35G needle, 5ul bolus was injected into the ear. For subcutaneous footpad infections, mice were anesthetized, then infected with 20ul LCMV-OVA. All infectious work was performed in accordance with national and institutional guidelines.

Intravascular staining - Mice were intravenously injected via the tail vein with 100ul PBS containing 3ug fluorescent antibody. 3min after injection, mice were sacrificed and organs collected. Antibodies used (CD8β PE or APC-Cy7, CD45 APC-Cy7)

Photo-conversion of kaede tg - Mice were anesthetized using vaporized isoflurane, delivered in 100ml/min ambient air using SomnoSuite® (Kent Scientific). For photoconversion, mice were placed face down and the ear gently attached to a styrofoam block using double-sided tape. The ear was then exposed to violet light (405nm; sustained power 200-249mW) using a portable hand-held laser (Electra Pro Series; Laserglow technologies). The ear was exposed to the beam for 4min at a distance of 5cm. Mice were subsequently allowed to recover from anesthesia prior to intravascular staining.

Intra-vital multi-photon microscopy - B6-albino mice were anesthetized with vaporized isoflurane, delivered in 100ml/min ambient air using a SomnoSuite® (Kent Scientific).

Ears were gently attached to an aluminum block using double-sided tape. Ear temperature was maintained at 33^{o} C using a heat pad. GenTeal (Novartis) eye gel was pooled over the ear to permit immersion of 20X objective (0.95 numerical aperture). Images were acquired using Prairie Technologies Ultima Two Photon Microscope using a Tsunami Ti:sapphire laser with a 10-W MilleniaXs pump laser (Spectra-Physics). To visualize vasculature, mice were i.v. injected with 50ul 1:20 Q655 vascular label (Molecular Probes) in PBS. Images were acquired with a laser wavelength of 970nm to permit sufficient excitation of TdTomato. Dermal vasculature was analyzed by excitation of ~70um optical stacks every 30s for 15-60min with 4-5um spacing. For injection of peptide during imaging, the left carotid artery was cannulated with PE 10 tubing (VWR) and the right ear was imaged. Images were transformed into four-dimensional time lapse movies and analyzed using Imaris software.

Transwell chemotaxis - T cell migration towards recombinant mouse CXCL9, CCL2, CCL3, CCL5, and CX_3CL1 (R&D systems) gradient was assessed using Transwell® 24-wells plates with 5μm pore size inserts (Corning Incorporated). $5x10^5$ spleen-derived, MACS-enriched $CD8^+$ T cells ($CD8a^+$ T cell isolation kit (Miltenyi Biotec)) from day 12 LCMV-OVA infected mice were loaded in the upper chamber. The lower chamber contained medium without or with indicated concentrations of chemokines. The absolute number of CX_3CR1^-, CX_3CR1^{int} and CX_3CR1^{hi} OT-I T_{Mem} that had migrated into the chemokine-containing lower chamber after 2 hours at 37°C was quantified and expressed relative to the corresponding populations' numbers within the no chemokine-containing lower well (chemotactic index).

Confocal microscopy - Ears were fixed overnight in 4% paraformaldehyde at 4^{o} C. Ears were then split along collagen plate into dorsal and ventral halves. The dorsal half was then stained with antibodies in PBS containing 0.3% Triton X-100. After overnight staining, ears were placed on slides, and images were acquired using Olympus FV1000 confocal microscope.

4.5 Results

Terminally differentiated, CX_3CR1^{hi}, T_{Eff} are retained within the intravascular space and are not blood-borne contaminants

The chemokine receptor, CX_3CR1, distinguishes three distinct subsets of Ag-experienced T cells that have a linear pedigree of differentiation from $CX_3CR1^{neg} \rightarrow CX_3CR1^{int} \rightarrow CX_3CR1^{hi}$. In the memory phase, CX_3CR1 defines the following relationships: $T_{CM} \rightarrow T_{PM} \rightarrow T_{EM}$. To assess the intravascular and extravascular localization of CX_3CR1-expressing T cells, we crossed $CX_3CR1^{gfp/+}$ reporter mice in which green fluorescent protein (GFP) has been 'knocked in' to the *CX_3CR1* locus[12] to CD45.1-expressing T cell receptor transgenic (TCR-tg) OT-I mice, whose $CD8^{+}$-T cells recognize ovalbumin (OVA)-derived SIINFEKL. Small numbers of $CX_3CR1^{gfp/+}$ OT-I CD45.1 cells were transferred into naïve C57BL/6 mice and subsequently infected intravenously (i.v.) with lymphocytic choriomeningitis virus serotype Armstrong (LCMV) expressing OVA. At the peak of the T cell response on day 8, >50% of OT-I cells in the blood are CX_3CR1^{hi} (**Figure 4.1 A-C**). Intra- and extra-vascular populations of T_{Eff} from tissue cell suspensions of the ear, kidney, lung, and salivary gland (SG) were

Figure 4.1: CX_3CR1^{hi} T_{Eff} are retained within the intravascular space and are not blood-borne contaminants. OT-I $CX_3CR1^{gfp/+}$ CD45.1 cells were transferred prior to intravenous LCMV-OVA infection. 8 days post-infection (p.i.), intra-vascular cells were labeled by i.v. injection of fluorescently labeled anti-CD8β (**A**). Representative FACS plot and histogram of intra-vascular staining and $CX_3CR1^{gfp/+}$ expression in the ear (**B**). Percentage of $CX_3CR1^{hi}KLRG\text{-}1^{+}$ among intra- and extra-vascular OT-I cells in blood, ear, kidney (kid), lung, and salivary gland (SG), as well as their vascular distribution within tissues (**C,D**). Ears were intra-dermally (i.d.) infected with a small bolus of LCMV-OVA. Day 8 p.i., the percentage of $CX_3CR1^{hi}KLRG\text{-}1^{+}$ in blood and ear was analyzed following intra-vascular staining with CD8β (**E,F**). OT-I Kaede tg cells were transferred into C57BL/6 albino mice and i.v. infected with LCMV-OVA. On day 8 p.i., OT-I Kaede tg cells in the ear were photo-converted by exposure to a violet laser beam (405nm). 15min after photo-conversion, intra-vascular cells were labeled with fluorescently labeled anti-CD8β (**G**). Representative FACS plots of intra-vascular and extra-vascular OT-I Kaede tg cells from ipsilateral and contralateral ears (**H**). Representative FACS plots and quantification of CX_3CR1 and KLRG-1 staining among OT-I Kaede tg cells in the blood or converted and non-converted populations within the intravascular compartment of the ear (**I,J**). After photo-conversion, indicated amounts of time were waited prior to intravascular staining and harvest. Shown is the percentage of converted cells among OT-I Kaede tg cells within the intra- or extra-vascular space of the ear (**K**). (* indicates $p<0.05$, ** indicates $p<0.01$)

Figure 4.1 (Continued):

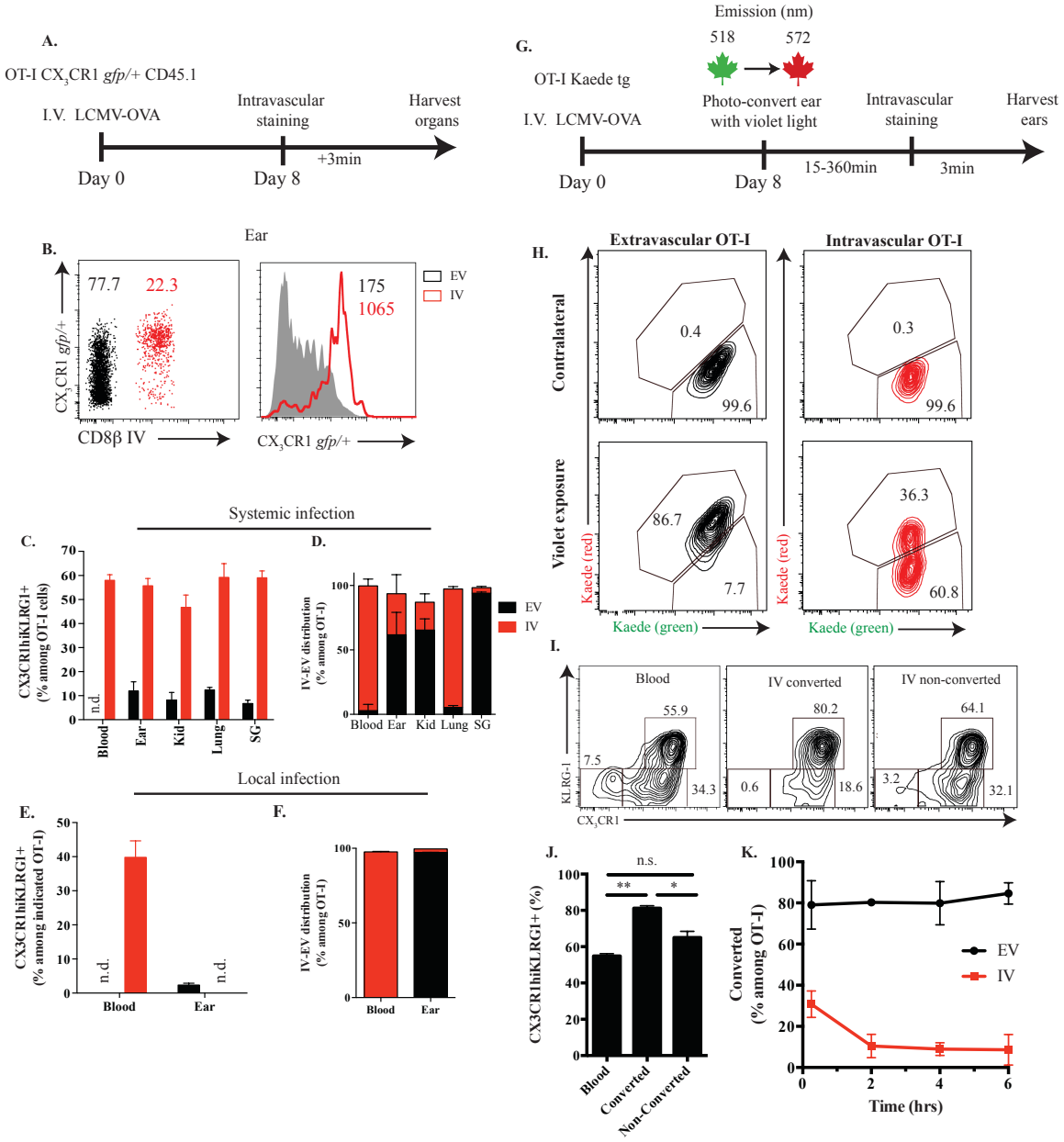

distinguished by flow cytometry after short-term injection of anti-CD8β (**Figure 4.1 A-D**). This procedure allowed separation of intravascular MAb-stained cells from extravascular cells, which are inaccessible to the MAb and are therefore not stained[13]. For greater resolution of subsets, we used KLRG-1 instead of the previously characterized

markers of CD27 or CXCR3 because these epitopes were cleaved by enzymes used to generate single cell suspensions from tissues. As had been seen for T_{Mem}, extravascular T_{Eff} were largely CX_3CR1^{neg} or CX_3CR1^{int}. In contrast, the majority of intravascular T_{Eff} were CX_3CR1^{hi} (**Figure 4.1 C,D**). In the context of this systemic infection, it is possible that insufficient inflammation or Ag exists within the tissues tested to effectively recruit CX_3CR1^{hi} T cells. To address this point, the ear was directly infected by intra-dermal (i.d.) injection of LCMV-OVA. On day 8, despite >10-fold recruitment of T_{Eff} compared to systemic infection, CX_3CR1^{hi} T cells were exceedingly rare in the extravascular space of the ear (**Figure 4.1 E,F**). This exclusion from tissues was independent of the virus used as infection with vesicular stomatitis virus (VSV) expressing OVA failed to recruit CX_3CR1^{hi} T cells by systemic infection or local infection of the ear (data not shown).

To date, i.v. staining with fluorescent antibodies has been used to distinguish intra- and extra-vascular T cells, with the extra-vascular fraction being analyzed and the intravascular fraction discarded as blood-borne contaminants [6,14,15]. To address whether these CX_3CR1^{hi} T_{Eff} were indeed just 'passersby', we crossed OT-I TCR-tg mice to mice expressing the photo-convertible kaede fluorescent protein (Kaede tg)[16]. When exposed to violet light, the kaede fluorophore undergoes a stable conformational change that alters its emission wavelength from green (518nm) to red (575nm), which can be detected by flow cytometry. In this way, photo-conversion by violet light exposure to a particular tissue can provide a temporal 'stamp' of cellular localization. The ear was chosen as an optimal tissue to examine intravascular persistence since it is well vascularized and does not require surgical manipulation for exposure to light. Following OT-I kaede tg transfer and i.v. infection with LCMV-OVA, intra- and extravascular OT-I cells of the ear were

photo-converted on day 8 post-infection (p.i.). Cells restricted to the vasculature could then be tracked by intravascular staining at various times after photo-conversion. To allow photo-converted non-adherent and rolling cells to pass through the dermal vasculature, i.v. staining was performed fifteen minutes after photo-conversion. As expected, the majority (~80%) of extra-vascular OT-I cells were photo-converted. Surprisingly, ~30% of intravascular OT-I cells persisted in dermal vascular beds, suggesting that a subset of cells were not blood-borne contaminants (**Figure 4.1 G,H**). Phenotypically, these persisting photo-converted cells were significantly enriched for the CX_3CR1^{hi} T_{Eff} subset compared to circulating T_{Eff} cells (**Figure 4.1 I**). To address the kinetics of this persistence, i.v. staining was performed varying amounts of time after photo-conversion. Over time, the number of lingering cells steadily declined with less than half the initial number remaining two hours after photo-conversion (**Figure 4.1 J**). Notably, there was no further enrichment for the CX_3CR1^{hi} subset over time. Together, this suggested that not all intravascularly labeled cells were blood-borne and that a subset of T_{Eff} cells was capable of this persistence.

CX_3CR1^{hi} T_{Eff} cells patrol arteriolar endothelium

To address the behavior of these persisting CX_3CR1-expressing T cells within the vasculature, we crossed OT-I $CX_3CR1^{gfp/+}$ mice to β-Actin TdTomato animals for transfer into recipients and subsequent visualization by intravital multi-photon microscopy (IV-MPM). To avoid photo-toxicity from melanocytes and enable better imaging contrast, C57BL/6 albino mice were used for imaging[17]. This permitted visualization of all OT-I cells by expression of TdTomato, as well as discernment of

differentiation status by variable expression of $CX_3CR1^{gfp/+}$. In addition, the vasculature was visualized by i.v. injection of fluorescent quantum dots. This revealed a fraction of T cells with an amoeboid morphology migrating through the extravascular space of the ear, as well as a population of T cells with an elongated morphology that could be observed patrolling along endothelium without extravasating (**Figure 4.2 A; Video 4.1**). To determine CX_3CR1 expression, 3-dimensional surfaces for each cell were created and the mean intensity of $CX_3CR1^{gfp/+}$ expression, as well as TdTomato expression, was calculated for each surface. Calculating the expression of GFP relative to TdTomato ensured that evaluation of GFP expression was not biased by insufficient optical sampling or inefficient photon recovery. This ratiometric quantification revealed that patrolling cells were exclusively $CX_3CR1^{gfp/+}$ bright cells while cells outside of the vasculature were low or intermediate, which is in concordance with the data from intravascular staining and OT-I kaede tg experiments (**Figure 4.2 B-E**). To our knowledge, this is the first time that $CD8^+$ T cell differentiation states have been visualized in a dynamic manner. Additionally, T cells within the vasculature migrated with a velocity of ~18um/min, which is similar to that described for monocytes[18] (**Figure 4.2 F**). In contrast to monocytes, T cells patrolled along arteriolar endothelium and were even enriched in arterioles compared to venules when normalized for endothelial surface area (**Figure 4.2 G**). Additionally, patrolling T cells displayed preferential migration against blood flow (**Figure 4.2 H; Video 4.2**). This kind of rheotactic behavior has been observed previously using *in vitro* flow chambers[19], but its mechanism remains unclear.

Figure 4.2: CX_3CR1^{hi} T_{Eff} patrol arteriolar endothelium and migrate against flow. Representative image of IV-MPM of the ear dermis on day 8 p.i. showing tracks of OT-I β-Actin TdTomato $CX_3CR1^{gfp/+}$ cells. Arteriolar tracks are shown in red, venular tracks in green, and extravascular tracks in white. Dermal vasculature is visualized in blue (**A;** see also **Video 4.1**). Representative tracks at 5min intervals show quantification of TdTomato and GFP mean intensity over time and ratiometric quantficiation of $CX_3CR1^{gfp/+}$ intensity (**B-D**). Summation of ratiometric quantification of $CX_3CR1^{gfp/+}$ and average velocity over multiple experiments within different vascular compartments of the ear. Each dot represents one track (**E,F**). Track density within arteriolar and venular compartments; calculated by normalizing the number of tracks within vascular segments by the surface area of that vascular segment (**G**). Directionality of movement was calculated by summing the instantaneous directionality of arteriolar tracks relative to blood flow within a particular movie. A ratio of cells migrating with or against the flow was then calculated and is plotted. Each dot represents the summed directionality for one 30min imaging period (**H;** see also **Video 4.2**). (* indicates $p<0.05$, *** indicates $p<0.005$, **** indicates $p<0.0001$).

Figure 4.2 (Continued):

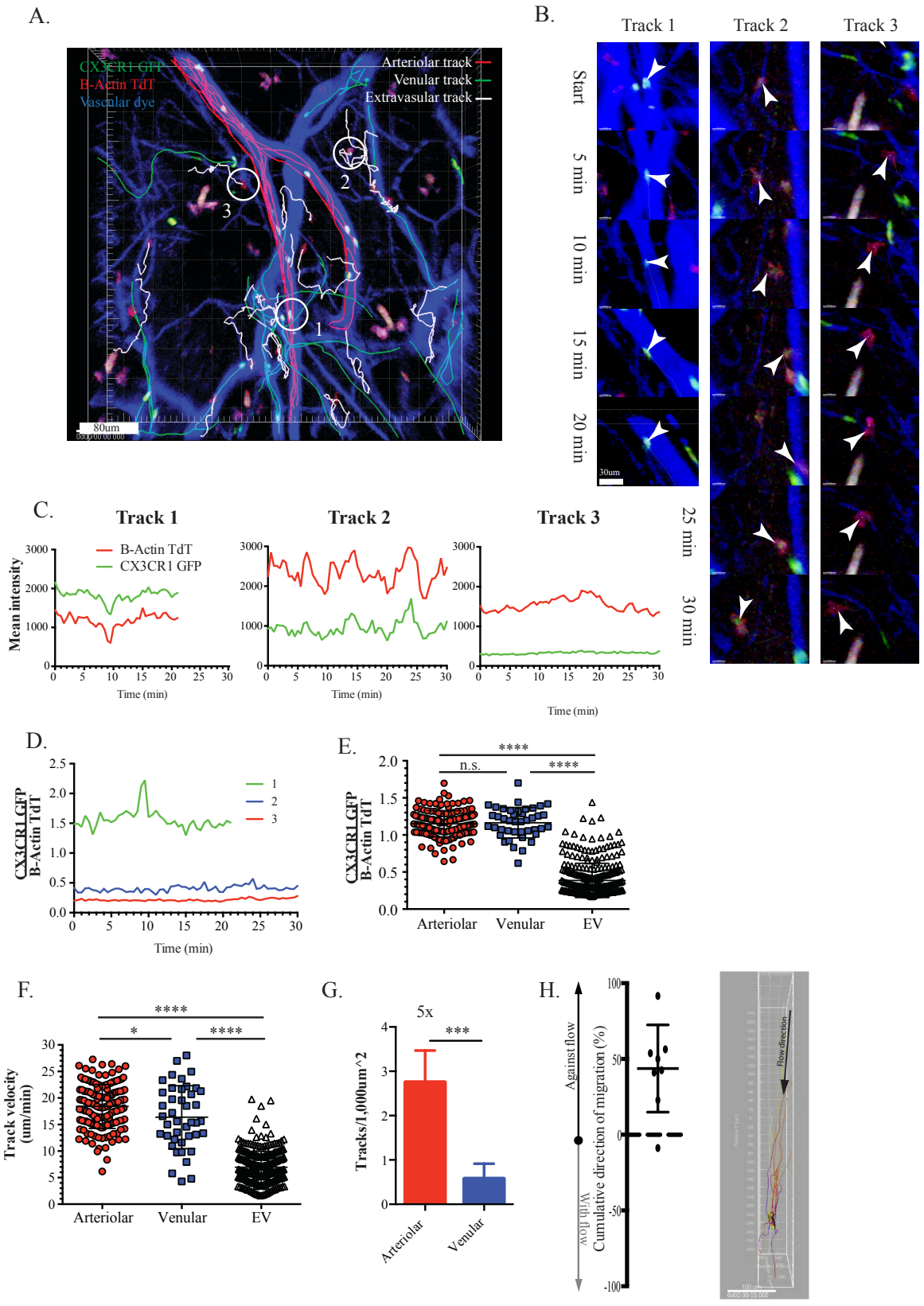

Requirements for patrolling by CX_3CR1^{hi} T_{Eff} cells

While OT-I TCR-tg cells were capable of patrolling during systemic infection with LCMV-OVA, it was unclear whether this behavior was unique to this infectious route, pathogen, or TCR-tg. Following subcutaneous (s.c.) infection of the footpad with LCMV-OVA or i.v. infection with VSV-OVA, CX_3CR1^{hi} OT-I T_{Eff} cells could be observed patrolling arterioles by IV-MPM (**Videos 4.3,4**). To test a different TCR-tg, we crossed P14 TCR-tg mice, which recognize the immunodominant LCMV epitope, gp_{33-41}, to β-actin TdTomato mice expressing $CX_3CR1^{gfp/+}$. After transfer of these P14 TCR-tg cells, naïve recipients were infected i.v. with LCMV and patrolling of arterioles on day 8 could still be seen by IV-MPM (**Figure 4.5 A; Videos 4.3-5**). Together, this suggests that patrolling is generally associated with virally induced inflammation that drives Ag-specific expansion and generation of CX_3CR1^{hi} T_{Eff}.

At day 8 following infection with LCMV or VSV, each expressing GFP, no ongoing replication could be seen in the ear, using GFP as a surrogate (data not shown). This indicated that Ag-recognition was not required for patrolling, but did not rule out the possibility that ongoing inflammation promoted an activated endothelium that could support adhesion of CX_3CR1^{hi} T_{Eff} through expression of chemokines or adhesion molecules. To address this, OT-I TdT $CX_3CR1^{gfp/+}$ from the spleens of mice infected 8 days prior with LCMV-OVA were transferred into naïve recipients. The dermal vasculature was monitored by IV-MPM for two hours following transfer. Even in this small time frame, CX_3CR1^{hi} T_{Eff} patrolled endothelium and were again enriched within arterioles (**Figure 4.5 B; Video 4.6**). While this system permitted visualization of vascular localization and behavior, it was difficult to assess whether the vascular context

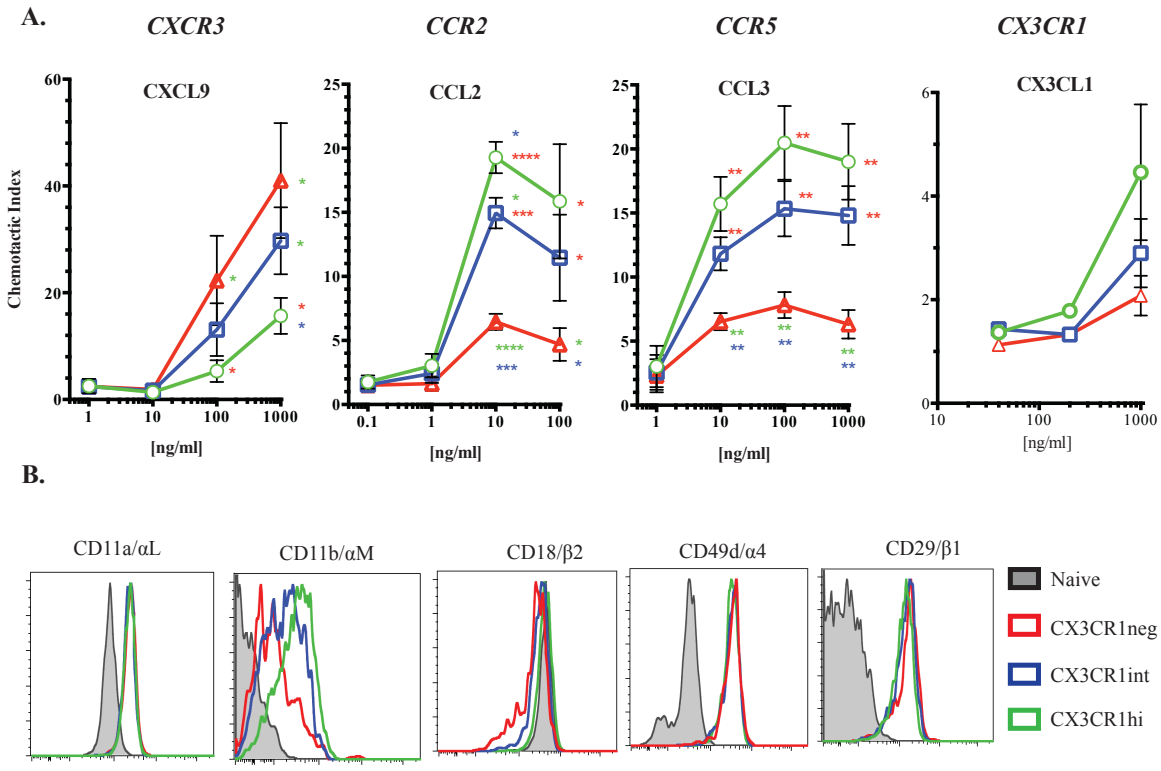

Figure 4.3: Chemokine receptor and integrin expression by T_{Eff} subsets. Chemotactic response of $CD8^+$ T_{Eff} subsets to indicated chemokines in a Transwell assay. Chemotactic index reflects the number of T_{Eff} that migrated towards chemokine relative to the number of cells that migrated towards medium alone. Asterisk color indicates compared subset. Chemokine receptor mediating responsiveness at top (**A**). Flow cytometry staining of indicated integrin subunits on $CD8^+$ T_{Eff} subsets, as well as naïve $CD8^+$ T cells (**B**).

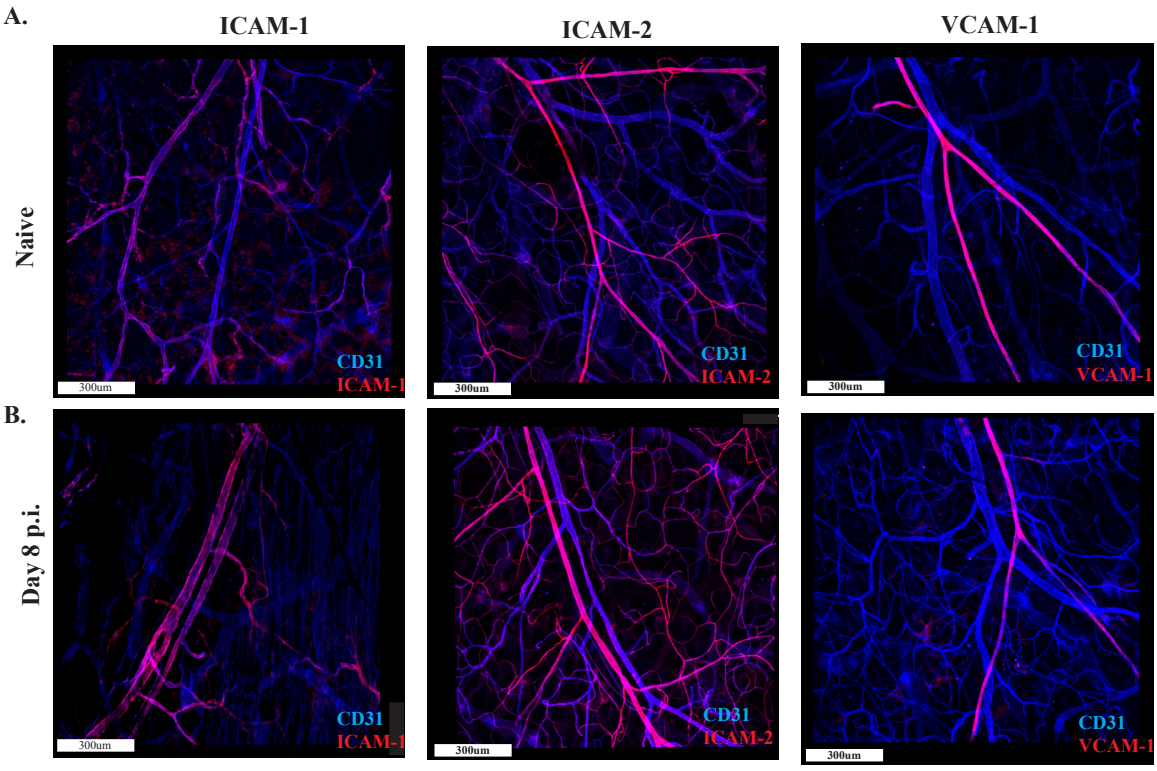

Figure 4.4: Cell adhesion molecule expression by dermal endothelium. Ears from naïve and mice that had been infected 8 days prior with LCMV-OVA were stained for indicated cell adhesion molecules and counter-stained with CD31 (**A,B**).

in naïve mice was more or less permissive of patrolling than that of mice with ongoing inflammation. To investigate this point, OT-I kaede tg cells from the spleens of mice i.v. infected with LCMV-OVA 7 days previously were transferred into infection-matched or naïve recipients. The next day, patrolling OT-I kaede tg cells in the ear were identified by photo-conversion and i.v. staining. Surprisingly, significantly more patrolling OT-I cells were recovered from the ears of naïve mice, compared to infection-matched mice (**Figure 4.5 C**). This could not be attributed to differences in the frequency of transferred cells in the blood, but may be the result of inflammation-induced retention within specific tissue

compartments. While this apparent increase is difficult to resolve, it is clear that an inflammatory context is not required to support patrolling by CX_3CR1^{hi} T_{Eff}.

Leukocyte adhesion to endothelium generally requires a cascade of adhesive events that ultimately result in firm adhesion[20]. Selectin-mediated tethering causes rolling, which then permits chemokine receptor-mediated activation of integrins, which bind to cell adhesion molecules (CAMs) on the endothelium and result in firm adhesion and resistance to the shear stress of blood flow[21]. Given that patrolling behavior was enriched in the CX_3CR1^{hi} subset and along arteriolar endothelium, the expression of adhesion molecules on T_{Eff} and their counter-receptors on dermal endothelium was interrogated. Guided by immgen analysis of chemokine receptor correlates of CX_3CR1 expression during memory formation by T cells [22], CX_3CR1^{hi} T_{Eff} were found to be most responsive to CCR2, CCR5, and CX_3CR1 ligands and less responsive to CXCR3 ligands (**Figure 4.3 A**). Comparison of integrin expression revealed no differences in expression of LFA-1 or VLA-4 expression, but higher expression of Mac-1 by CX_3CR1^{hi} T_{Eff} cells (**Figure 4.3 B**). Adhesion molecules on dermal endothelium were visualized by confocal microscopy, which demonstrated enriched expression of ICAM-2 on arteriolar endothelium and capillaries and restricted VCAM-1 expression by arterioles (**Figure 4.4 A**). ICAM-2 did not appear significantly altered by inflammation while VCAM-1 appeared to be induced on venular endothelium. ICAM-1, in contrast, was expressed by venular endothelium and was induced on arteriolar endothelium following infection (**Figure 4.4 B**).

Guided by this information, the mechanism of patrolling behavior was interrogated by injecting blocking antibodies prior to photoconversion and intravascular

Figure 4.5: Requirements for patrolling by CX_3CR1^{hi} T_{Eff}. Arteriolar track velocity of OT-I β-Actin TdT $CX_3CR1^{gfp/+}$ cells at day 8 p.i. by the indicated route for VSV-OVA and LCMV-OVA. P14 β-Actin TdT $CX_3CR1^{gfp/+}$ cells were tracked 8 days following infection with LCMV-Armstrong (**A**). Track velocities within arterioles and venules following transfer of T_{Eff} into naïve mice, as measured by IV-MPM (**B**). OT-I Kaede tg T_{Eff} were transferred into infection-matched or naïve mice. 16 hours later, ears were photo-converted and converted intra-vascular cells were enumerated by flow cytometry (**C**). Day 8 p.i. with LCMV-OVA, blocking antibodies were injected 1 hour prior to photo-conversion and intravascular staining. Recovered intra-vascular converted OT-I Kaede tg cells is shown (**D**). Arteriolar track velocity for various OT-I TCR-tg cells that lack the indicated chemokine receptor day 8 p.i. with LCMV-OVA. T cells from the following strains were transferred for imaging by IV-MPM: OT-I β-Actin TdT $CX_3CR1^{gfp/+}$ (WT), OT-I β-Actin TdT $CX_3CR1^{gfp/gfp}$ ($CX_3CR1^{-/-}$), OT-I $CX_3CR1^{gfp/+}$ $CCR2^{rfp/rfp}$ ($CCR2^{-/-}$), OT-I β-Actin TdT $CCR5^{-/-}$ ($CCR5^{-/-}$) (**E**). Kaede tg mice were either infected i.v. with LCMV-OVA (day 8 p.i.) or left uninfected (steady state). Ears were photo-converted and intravascular lymphocytes identified by anti-CD45 staining. Representative plots for CD8β and CD11b among converted intra-vascular $CD45^+$ cells (**F**). Enumeration of recovered intra-vascular converted cells from the ears (**G**). During IV-MPM imaging, 100ng SIINFEKL was injected via the carotid artery and behavior of OT-I β-Actin TdT $CX_3CR1^{gfp/+}$ cells was monitored (**H-J**). Tracks represent the previous 10min of migration. Arteriolar tracks are shown in white, venular tracks in green (**H**). Average arteriolar track velocity for indicated time points (**I**). Summary of arteriolar track velocity for three separate mice pre- and post-injection of 100ng SIINFEKL (**J**).

Figure 4.5 (Continued):

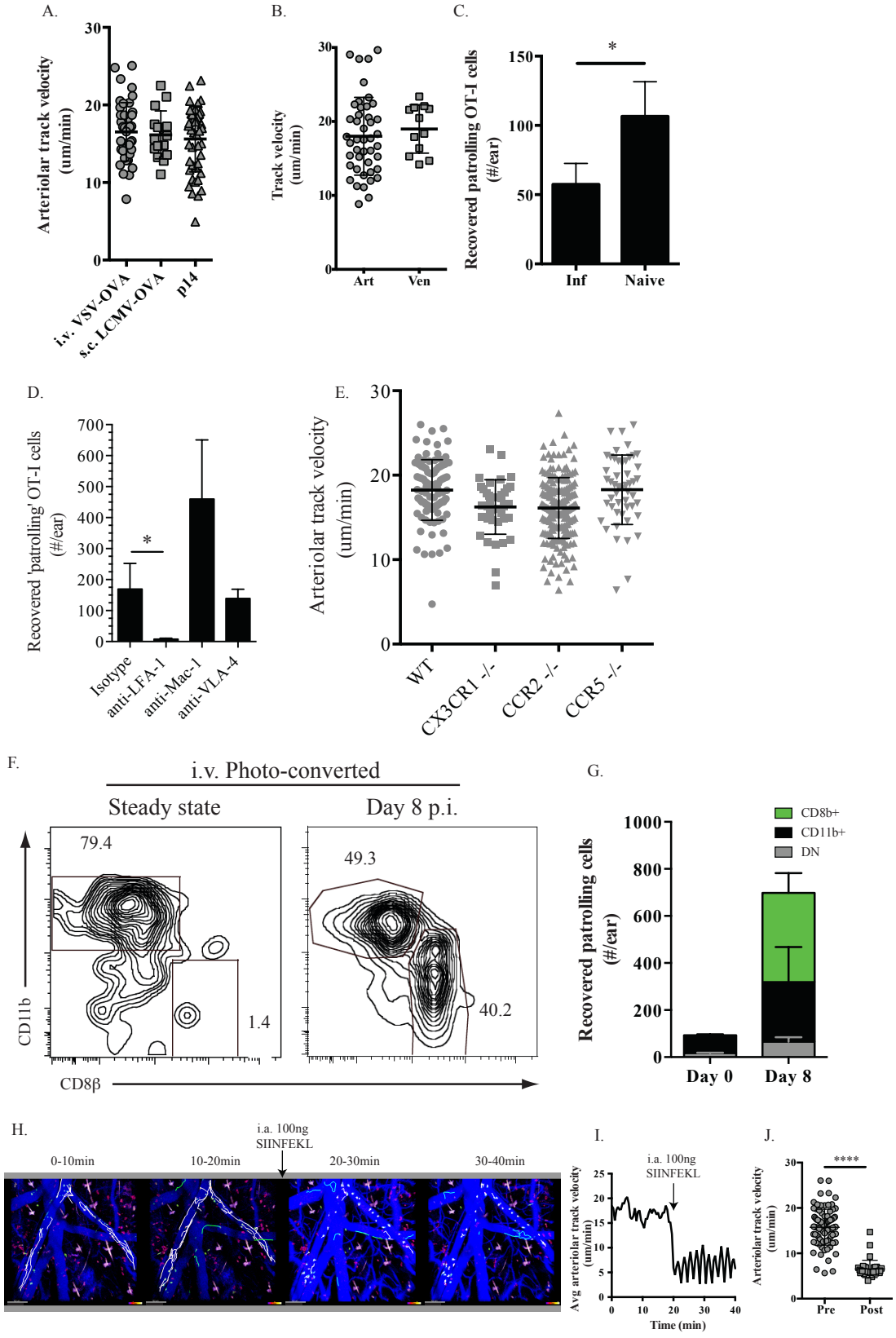

staining. Following blockade of the integrin, LFA-1, intravascular photo-converted cells were significantly reduced, demonstrating dependence on this integrin for patrolling. In contrast, blockade of the integrin VLA-4 did not significantly affect the number of photo-converted cells while Mac-1 blockade appeared to increase the frequency of patrolling (**Figure 4.5 D**). Although no increase in OT-I cells was observed in the blood after Mac-1 blockade, this increased patrolling may be the result of release of cells from elsewhere in the host.

Terminally differentiated, CX_3CR1^{hi}, T cells were enriched for patrolling behavior compared to less terminally differentiated, CX_3CR1^{neg} or CX_3CR1^{int}, T cells, which indicated that CX_3CR1^{hi} T cells expressed distinct trafficking molecules that permitted adhesion for patrolling. As CX_3CR1 expression defined the subset capable of patrolling, we used cells from OT-I β-Actin TdT $CX_3CR1^{gfp/gfp}$ mice for adoptive transfer, as these cells lack functional CX_3CR1. On day 8, by IV-MPM, $CX_3CR1^{gfp/gfp}$ T cells were seen patrolling arteriolar endothelium with a velocity similar to that seen for $CX_3CR1^{gfp/+}$ T cells (**Figure 4.5 E; Video 4.7**). This data demonstrates that while CX_3CR1 expression correlates with a subset of T cells that are capable of patrolling, it is not required for patrolling behavior. On T_{Eff}, CX_3CR1 expression correlates with increased chemotactive responsiveness to CCR2 and CCR5 ligands (**Figure 4.3 A**). To test whether T cells used these chemokine receptors to engage in adhesive interactions with the endothelium, mice were crossed to generate OT-I $CX_3CR1^{gfp/+}CCR2^{rfp/rfp}$ and OT-I β-Actin RFP $CCR5^{-/-}$ mice, which lack functional CCR2 and CCR5, respectively. Adoptively transferred OT-I cells from these mice also patrolled endothelium in the

effector phase, and with velocities similar to wild-type OT-I cells (**Figure 4.5 E; Videos 4.8,9**).

Given that CX_3CR1-expressing monocytes have been described to patrol dermal endothelium in the steady state[18], we sought to characterize the frequency of patrolling monocytes to T cells under steady state and inflammatory conditions, as well as identify whether other previously unidentified cells were capable of this behavior. Previous methods for identifying intravascular patrolling cells in different organs have relied on fluorescent reporters or *ex vivo* labeling of cells[18,23-25], which severely limits the ability to fully characterize patrolling cells in a tissue, as the assay will be inherently biased by the reporter used or cell type labeled. By photo-converting the ears of kaede tg mice, followed by intravascular staining with the pan-lymphocyte marker, anti-CD45 MAb, patrolling lymphocytes will be marked in an unbiased manner. Subsequently, the intravascular photo-converted cell types can be distinguished by flow cytometry. Therefore, the ears of naïve or infected kaede tg mice were photo-converted, in conjunction with anti-CD45 MAb staining to define intravascular lymphocytes. In naïve mice, $CD8^+$ T cells were no longer found in the i.v. converted fraction, while a population of $CD11b^+$ CX_3CR1-expressing monocytes made up 90% of i.v. converted cells (**Figure 4.5 F**). In the effector phase (8 days p.i.), the number of i.v. converted cells per ear had increased five-fold, with half of the cells being made up of CX_3CR1-expressing T_{Eff} and the other half CX_3CR1-expressing monocytes (**Figure 4.5 F,G**). Notably, <10% of i.v. converted cells were $CD11b^-CD8\beta^-$, suggesting that monocytes and $CD8^+$ T cells form the majority of cells capable of this behavior. Furthermore, while CX_3CR1 may not be required for patrolling on either cell type, its expression is tightly

correlated with patrolling capacity, as naïve mice, which lack Ag-experienced CX_3CR1-expressing T cells also lack patrolling T cells.

Patrolling CX_3CR1^{hi} T cells intimately interact with arteriolar endothelium. The contact created by patrolling may therefore be a scanning behavior to permit recognition of cognate Ag presented by the endothelium. Given that Ag recognition by T cells results in rapid arrest[26,27], we tested whether patrolling velocity could be altered by intra-arterial (i.a.) injection of cognate Ag. On day 8 p.i., the carotid artery was cannulated to enable injection of SIINFEKL peptide during imaging. In this way, presentation to OT-I cells is rapid and independent of Ag presentation as the peptide displaces existing pMHC complexes. Prior to injection, OT-I β-Actin TdT $CX_3CR1^{gfp/+}$ cells patrolled arteriolar endothelium at ~16um/min. After i.a. injection of SIINFEKL, T cells responded rapidly (<1min) and their velocity was reduced to ~5um/min (**Figure 4.5 H-J; Video 4.10**). This suggests that T cells are indeed capable of seeing Ag presented by arteriolar endothelium.

Effector memory T cells scan vascular endothelium

Following the peak of the T cell response to viral infection, contraction begins wherein 90-95% of pathogen-specific T cells will die, leaving behind a population of memory T cells. Given this steep contraction as well as minor histocompatibility antigens that result in the rejection of many of the adoptively transferred T cells used, many aspects of patrolling were assessed in the effector phase to provide sufficient cells for analysis. However, T_{Eff} and T_{Mem} differ in many ways and thus, it cannot be inferred that patrolling by CX_3CR1^{hi} T_{Eff} indicates that CX_3CR1^{hi} T_{Mem} will also patrol. To formally address patrolling in the memory phase, cells from OT-I $CX_3CR1^{gfp/+}$ mice, which had

been extensively backcrossed to mitigate rejection by the host, were used for adoptive transfer. Notably, T cells from these mice lack expression of TdTomato, which prevents identification of OT-I cells that do not express CX_3CR1 and ratiometric quantification of CX_3CR1 intensity. Nonetheless, 39 days post-infection, CX_3CR1-expressing T cells could reliably be found patrolling arteriolar endothelium, albeit with lower frequency than observed in the effector phase (**Figure 4.6 A; Video 4.11**). Furthermore, patrolling velocity was comparable to that seen for T_{Eff} (**Figure 4.6 B**).

These results demonstrated that T_{Mem}, specifically T_{EM} (CX_3CR1-expressing), were capable of patrolling, but did not rule out the possibility that T_{CM} (non-CX_3CR1-expressing) could patrol, since these were not visualized in this experimental setup. To examine patrolling of T_{Mem} subsets, as well as patrolling by other cell types, kaede tg mice were i.v. infected with LCMV-OVA. 43 days later, cells within the ear were photo-converted and intravascular lymphocytes were identified by i.v. injection of anti-CD45 MAb. Phenotyping intravascular photo-converted cells revealed that $CD8^+$ T cells and $CD11b^+$ monocytes formed the majority of patrolling cells (>90%) and were roughly equal in frequency (**Figure 4.6 C,D**). Both $CD8^+$ T cells and $CD11b^+$ monocytes were significantly enriched for CX_3CR1 expression (~90%) compared to their counterparts in the blood (20-30%) (**Figure 4.6 E**). This disequilibrium indicated that patrolling was restricted to T_{EM} and did not occur with any appreciable frequency on T_{CM}.

Patrolling of endothelium by T_{EM} places these cells in an ideal location for sensing local tissue inflammation compared to T_{CM}, which have a short half-life in blood and circulate through LNs. However, arteriolar endothelium is surrounded by a dense

Figure 4.6: T_{EM} scan dermal endothelium. OT-I $CX_3CR1^{gfp/+}$ T_{Mem} were visualized by IV-MPM 90 days p.i. with LCMV-OVA. Tracks of CX_3CR1-expressing cells are shown in both arterioles and venules (**A**). Average track velocity within arterioles and venules is shown for three mice (**B**). 37 days after infection with LCMV-OVA, the ears of Kaede tg mice were photo-converted and intra-vascular lymphocytes identified by fluorescent anti-CD45. Representative FACS plots of IV-labeled $CD45^+$ cells is shown (**C**). Relative frequencies of cell subsets within indicated compartments and percentage of CX_3CR1^+ cells within these subsets (**D,E**). OT-I $CX_3CR1^{gfp/+}$ CD45.1 T_{Mem} subsets were FACS-sorted from mice infected 90 days previously and equal numbers transferred into separate infection-matched mice, which had been infected i.v. and i.d. in the ear with LCMV-OVA. One day after transfer, mice were infected i.v. and i.d. in the ear with VSV-OVA. Four days after secondary infection, blood and ears were harvested and distribution of subsets was evaluated. Frequency of transferred subsets in blood and abundance of transferred subsets in infected and contralateral ears is shown (**F**).

Figure 4.6 (Continued):

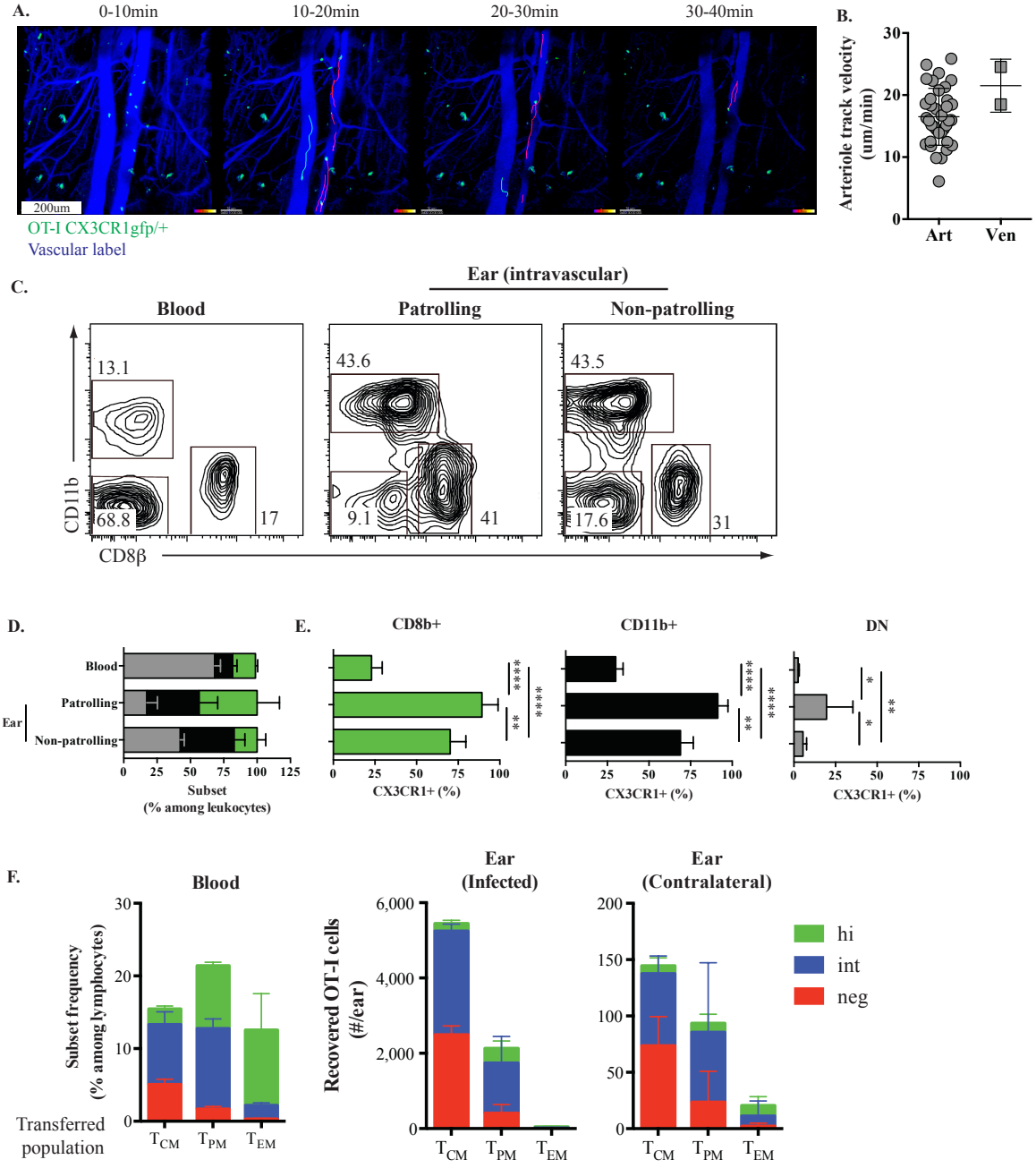

layer of smooth muscle cells and extravasation through arterioles has not been described.

To test the kinetics of tissue entry by different T_{Mem} subsets, T_{CM}, T_{PM}, and T_{EM} OT-I cells were sorted based on $CX_3CR1^{gfp/+}$ expression from mice that had been infected

90 days previously with LCMV-OVA. Equal numbers of T_{CM}, T_{PM}, or T_{EM} were then transferred into infection-matched mice. Subsequently, mice were i.v. infected with VSV-OVA, as well as infected i.d. in the right ear with VSV-OVA. Thus, cross-protection was provided by recognition of OVA. Early after this secondary infection (day 4 p.i.), mice which had T_{CM} or T_{PM} transferred accumulated substantial numbers of extravasated T cells in the infected ear with significantly fewer in the contralateral ear (**Figure 4.6 F**). Surprisingly, despite significant expansion of transferred T_{EM} in the blood, transferred T_{EM} failed to enter the infected ear. This indicates that T_{EM} are likely not poised to enter tissues and are retained within the vasculature by unknown mechanisms, despite expression of inflammatory chemokine receptors.

4.6 Discussion

Here, we sought to resolve the enigmatic migratory behavior of terminally differentiated $CD8^+$ T cells, which are restricted to the vasculature and excluded from LNs and peripheral tissues. Using a novel application of the photo-convertible fluorescent protein, kaede, we have shown that CX_3CR1^{hi} T cells in the dermal vasculature are not blood-borne contaminants, but rather are capable of persisting in vascular beds for hours. Furthermore, using $CX_3CR1^{gfp/+}$ reporter mice, we were able to discern the differentiation status of effector and memory T cells in the ear dermis by IV-MPM. This revealed that persisting CX_3CR1^{hi} T cells were patrolling along dermal endothelium and were enriched within arterioles. Moreover, patrolling T cells tended to migrate against blood flow. Patrolling could be seen with different viral infections and routes of infection. Patrolling T cells were not observed in naive, uninfected mice, but could be found in roughly equal

numbers to CX_3CR1-expressing monocytes in the effector and memory phase following infection. Notably, we found that CX_3CR1-expressing $CD8^+$ T cells and monocytes formed the majority (~90%) after infection. Despite the correlation between CX_3CR1 expression and patrolling behavior, functional CX_3CR1 was not required for patrolling to occur. However, blockade of LFA-1 resulted in rapid detachment of patrolling T cells while blockade of the integrins VLA-4 and Mac-1 did not abrogate patrolling.

Interestingly, upon secondary infection, T_{EM} (CX_3CR1^{hi}) failed to extravasate into tissues compared to T_{CM} (CX_3CR1^{neg}) or T_{PM} (CX_3CR1^{int}). This suggests that patrolling T cells are not poised for rapid entry into tissues, but rather exert their function within the vasculature. As T cell function depends on cellular contact, patrolling of arteriolar endothelium may serve as a mechanism by which T cells scan endothelium for recurring infection. This concept is supported by the observation that recognition of cognate Ag on arteriolar endothelium results in rapid arrest of patrolling T cells. It remains unclear, however, what effector functions are deployed following recognition, as a cytotoxic outcome would lead to rapid hemorrhage. Local cytokine production, however, may be more productive as it would quell further replication within arteriolar endothelial cells.

Endothelial cells act as conduits of blood, which convey nutrients as well as cells systemically throughout the body. As such, infected endothelial cells will shed virus into the blood where it will rapidly redistribute throughout the body. It is therefore of critical importance to prevent infection and viral shedding within endothelial cells. In particular, arteriolar endothelium, as it is sheathed by a dense layer of smooth muscle cells, which constrict blood vessels, but also prevent scanning of arteriolar endothelium from the tissue parenchyma. Without scanning of the arteriolar lumen, arteriolar endothelial cells

would represent an immunological 'blind spot' not scanned by Ag-experienced $CD8^+$ T cells. We therefore propose that scanning of arterioles by terminally differentiated $CD8^+$ T cells serves to protect what would otherwise be a vulnerable tissue.

4.7 Videos

Video 4.1: Patrolling of OT-I CX_3CR1^{hi} T_{Eff} cells along dermal endothelium. OT-I β-Actin TdTomato $CX_3CR1^{gfp/+}$ cells were adoptively transferred into C57BL/6 albino mice and subsequently infected i.v. with LCMV-OVA. On day 8 post-infection (p.i.), mouse ear dermis was imaged by IV-MPM. Vasculature was visualized by i.v. injection of Q655 Vascular label (Molecular probes). On the right, close-up views of tracks with extended analysis in **Figures 4.2 B-D**.

Video 4.2: Patrolling T cells preferentially migrate against blood flow. Imaging preparation similar to **Video 4.1**. Arteriolar tracks from two representative movies are plotted from a single origin. Arteriolar blood flow is from top to bottom. Cumulative data plotted in **Figure 4.2 H**.

Video 4.3: Patrolling by CX_3CR1^{hi} T_{Eff} cells following i.v. VSV-OVA infection. OT-I β-Actin TdTomato $CX_3CR1^{gfp/+}$ cells were adoptively transferred into C57BL/6 albino mice and subsequently infected i.v. with VSV-OVA. On day 8 p.i., mouse ear dermis was imaged by IV-MPM. Vasculature was visualized by i.v. injection of Q655 Vascular label (Molecular probes). Quantification in **Figure 4.5 A**.

Video 4.4: Patrolling by CX_3CR1^{hi} T_{Eff} cells following s.c. LCMV-OVA infection. OT-I β-Actin TdTomato $CX_3CR1^{gfp/+}$ cells were adoptively transferred into C57BL/6 albino mice and subsequently infected s.c. in the footpad with LCMV-OVA. On day 8 p.i., mouse ear dermis was imaged by IV-MPM. Vasculature was visualized by i.v. injection of Q655 Vascular label (Molecular probes). Quantification in **Figure 4.5 A**.

Video 4.5: Patrolling by p14 CX_3CR1^{hi} T_{Eff} cells following LCMV-Armstrong infection. p14 β-Actin TdTomato $CX_3CR1^{gfp/+}$ cells were adoptively transferred into C57BL/6 albino mice and subsequently infected i.v. with LCMV-Armstrong. On day 8 p.i., mouse ear dermis was imaged by IV-MPM. Vasculature was visualized by i.v. injection of Q655 Vascular label (Molecular probes). Quantification in **Figure 4.5 A**.

Video 4.6: CX_3CR1^{hi} T_{Eff} cells patrol steady state endothelium. OT-I β-Actin TdTomato $CX_3CR1^{gfp/+}$ cells were adoptively transferred into C57BL/6 mice and subsequently infected i.v. with LCMV-OVA. On day 8 p.i., T_{Eff} cells were enriched from spleens by magnetic sorting. T_{Eff} cells were i.v. transferred into naïve C57BL/6 albino mice and mouse ear dermis was imaged by IV-MPM indicated times after transfer. On left, video begins 75 minutes after transfer. Video on right is from a separate mouse and is 25 minutes after transfer. Vasculature was visualized by i.v. injection of Q655 Vascular label (Molecular probes). Data plotted in **Figure 4.5 B**.

Video 4.7: CX_3CR1 is not required for patrolling behavior. OT-I β-Actin TdTomato $CX_3CR1^{gfp/gfp}$ cells were adoptively transferred into C57BL/6 albino mice and

subsequently infected i.v. with LCMV-OVA. On day 8 p.i., mouse ear dermis was imaged by IV-MPM. Vasculature was visualized by i.v. injection of Q655 Vascular label (Molecular probes). Summarized in **Figure 4.5 E**.

Video 4.8: CCR2 is not required for patrolling behavior. OT-I $CX_3CR1^{gfp/+}$ $CCR2^{rfp/rfp}$ cells were adoptively transferred into C57BL/6 albino mice and subsequently infected i.v. with LCMV-OVA. On day 8 p.i., mouse ear dermis was imaged by IV-MPM. Notably, RFP expression by T_{Eff} was not bright enough for detection. Vasculature was visualized by i.v. injection of Q655 Vascular label (Molecular probes). Summarized in **Figure 4.5 E**.

Video 4.9: CCR5 is not required for patrolling behavior. OT-I $CX_3CR1^{gfp/+}$ and OT-I β-Actin TdTomato $CCR5^{-/-}$ cells were co-transferred into C57BL/6 albino mice and subsequently infected i.v. with LCMV-OVA. On day 8 p.i., mouse ear dermis was imaged by IV-MPM. Vasculature was visualized by i.v. injection of Q655 Vascular label (Molecular probes). CCR5-sufficient T cells outnumbered CCR5-deficient T cells in the blood at the time of imaging. This difference is reflected in the imaging volume, but does not reflect deficient patrolling by $CCR5^{-/-}$ T cells. Summarized in **Figure 4.5 E**.

Video 4.10: Ag-dependent stopping of patrolling CX_3CR1^{hi} T cells. OT-I β-Actin TdTomato $CX_3CR1^{gfp/+}$ cells were adoptively transferred into C57BL/6 albino mice and subsequently infected i.v. with LCMV-OVA. On day 8 p.i., the carotid artery was cannulated to permit intra-arterial (i.a.) injection during the imaging period. Mouse ear

dermis was imaged by IV-MPM and vasculature was visualized by i.v. injection of Q655 Vascular label (Molecular probes). At ~32 minutes, 100ng SIINFEKL was i.a. injected along with a small bolus of Q655 vascular label to identify timing of injection. Still images shown and quantification of velocity in **Figure 4.5 H-J**.

Video 4.11: Effector memory T cells patrol dermal endothelium. Backcrossed OT-I $CX_3CR1^{gfp/+}$ cells were adoptively transferred into C57BL/6 albino mice and subsequently infected i.v. with LCMV-OVA. On day 39 p.i.,, mouse ear dermis was imaged by IV-MPM and vasculature was visualized by i.v. injection of Q655 Vascular label (Molecular probes). Still images and track velocity shown in **Figure 4.6 A,B**.

4.8 References

1. Sallusto, F., Lenig, D., Förster, R., Lipp, M. & Lanzavecchia, A. Two subsets of memory T lymphocytes with distinct homing potentials and effector functions. *Nature* **401,** 708–712 (1999).
2. Andrian, von, U. H. & Mempel, T. R. Homing and cellular traffic in lymph nodes. *Nat Rev Immunol* **3,** 867–878 (2003).
3. Gebhardt, T., Wakim, L. M., Eidsmo, L., Reading, P. C., Heath, W. R. & Carbone, F. R. Memory T cells in nonlymphoid tissue that provide enhanced local immunity during infection with herpes simplex virus. *Nat Immunol* **10,** 524–530 (2009).
4. Jiang, X., Clark, R. A., Liu, L., Wagers, A. J., Fuhlbrigge, R. C. & Kupper, T. S. Skin infection generates non-migratory memory CD8+ TRM cells providing global skin immunity. *Nature* 1–6 (2012). doi:10.1038/nature10851
5. Mackay, L. K., Rahimpour, A., Ma, J. Z., Collins, N., Stock, A. T., Hafon, M.-L.,

Vega-Ramos, J., Lauzurica, P., Mueller, S. N., Stefanovic, T., Tscharke, D. C., Heath, W. R., Inouye, M., Carbone, F. R. & Gebhardt, T. The developmental pathway for CD103(+)CD8(+) tissue-resident memory T cells of skin. *Nat Immunol* **14,** 1294–1301 (2013).

6. Skon, C. N., Lee, J.-Y., Anderson, K. G., Masopust, D., Hogquist, K. A. & Jameson, S. C. Transcriptional downregulation of S1pr1 is required for the establishment of resident memory CD8(+) T cells. *Nat Immunol* **14,** 1285–1293 (2013).

7. Schenkel, J. M., Fraser, K. A., Vezys, V. & Masopust, D. Sensing and alarm function of resident memory CD8+ T cells. *Nat Immunol* **14,** 509–513 (2013).

8. Schenkel, J. M., Fraser, K. A., Beura, L. K., Pauken, K. E., Vezys, V. & Masopust, D. T cell memory. Resident memory CD8 T cells trigger protective innate and adaptive immune responses. *Science* **346,** 98–101 (2014).

9. Ariotti, S., Hogenbirk, M. A., Dijkgraaf, F. E., Visser, L. L., Hoekstra, M. E., Song, J.-Y., Jacobs, H., Haanen, J. B. & Schumacher, T. N. T cell memory. Skin-resident memory $CD8^+$ T cells trigger a state of tissue-wide pathogen alert. *Science* **346,** 101–105 (2014).

10. Sallusto, F., Geginat, J. & Lanzavecchia, A. Central memory and effector memory T cell subsets: function, generation, and maintenance. *Annu. Rev. Immunol.* **22,** 745–763 (2004).

11. Mackay, C. R., Marston, W. L. & Dudler, L. Naive and memory T cells show distinct pathways of lymphocyte recirculation. *J Exp Med* **171,** 801–817 (1990).

12. Jung, S., Aliberti, J., Graemmel, P., Sunshine, M. J., Kreutzberg, G. W., Sher, A.

& Littman, D. R. Analysis of fractalkine receptor CX(3)CR1 function by targeted deletion and green fluorescent protein reporter gene insertion. *Mol Cell Biol* **20,** 4106–4114 (2000).

13. Anderson, K. G., Sung, H., Skon, C. N., Lefrançois, L., Deisinger, A., Vezys, V. & Masopust, D. Cutting edge: intravascular staining redefines lung CD8 T cell responses. *J Immunol* **189,** 2702–2706 (2012).

14. Schenkel, J. M. & Masopust, D. Tissue-Resident Memory T Cells. *Immunity* **41,** 886–897 (2014).

15. Anderson, K. G., Mayer-Barber, K., Sung, H., Beura, L., James, B. R., Taylor, J. J., Qunaj, L., Griffith, T. S., Vezys, V., Barber, D. L. & Masopust, D. Intravascular staining for discrimination of vascular and tissue leukocytes. *Nat Protoc* **9,** 209–222 (2014).

16. Tomura, M., Yoshida, N., Tanaka, J., Karasawa, S., Miwa, Y., Miyawaki, A. & Kanagawa, O. Monitoring cellular movement in vivo with photoconvertible fluorescence protein 'Kaede' transgenic mice. *Proceedings of the National Academy of Sciences* **105,** 10871–10876 (2008).

17. Li, J. L., Goh, C. C., Keeble, J. L., Qin, J. S., Roediger, B., Jain, R., Wang, Y., Chew, W. K., Weninger, W. & Ng, L. G. Intravital multiphoton imaging of immune responses in the mouse ear skin. *Nat Protoc* **7,** 221–234 (2012).

18. Auffray, C., Fogg, D., Garfa, M., Elain, G., Join-Lambert, O., Kayal, S., Sarnacki, S., Cumano, A., Lauvau, G. & Geissmann, F. Monitoring of blood vessels and tissues by a population of monocytes with patrolling behavior. *Science* **317,** 666–670 (2007).

19. Valignat, M.-P., Theodoly, O., Gucciardi, A., Hogg, N. & Lellouch, A. C. T lymphocytes orient against the direction of fluid flow during LFA-1-mediated migration. *Biophysical Journal* **104,** 322–331 (2013).

20. Ley, K., Laudanna, C., Cybulsky, M. I. & Nourshargh, S. Getting to the site of inflammation: the leukocyte adhesion cascade updated. *Nat Rev Immunol* **7,** 678–689 (2007).

21. Andrian, von, U. H. & Mackay, C. R. T-cell function and migration. Two sides of the same coin. *N Engl J Med* **343,** 1020–1034 (2000).

22. Best, J. A., Blair, D. A., Knell, J., Yang, E., Mayya, V., Doedens, A., Dustin, M. L., Goldrath, A. W. & Immunological Genome Project Consortium. Transcriptional insights into the CD8(+) T cell response to infection and memory T cell formation. *Nat Immunol* **14,** 404–412 (2013).

23. Geissmann, F., Cameron, T. O., Sidobre, S., Manlongat, N., Kronenberg, M., Briskin, M. J., Dustin, M. L. & Littman, D. R. Intravascular immune surveillance by CXCR6+ NKT cells patrolling liver sinusoids. *PLoS Biol* **3,** e113 (2005).

24. Carlin, L. M., Stamatiades, E. G., Auffray, C., Hanna, R. N., Glover, L., Vizcay-Barrena, G., Hedrick, C. C., Cook, H. T., Diebold, S. & Geissmann, F. Nr4a1-dependent Ly6C(low) monocytes monitor endothelial cells and orchestrate their disposal. *Cell* **153,** 362–375 (2013).

25. Guidotti, L. G., Inverso, D., Sironi, L., Di Lucia, P., Fioravanti, J., Ganzer, L., Fiocchi, A., Vacca, M., Aiolfi, R., Sammicheli, S., Mainetti, M., Cataudella, T., Raimondi, A., Gonzalez-Aseguinolaza, G., Protzer, U., Ruggeri, Z. M., Chisari, F. V., Isogawa, M., Sitia, G. & Iannacone, M. Immunosurveillance of the liver by

intravascular effector CD8(+) T cells. *Cell* **161,** 486–500 (2015).

26. Dustin, M. L. Stop and go traffic to tune T cell responses. *Immunity* **21,** 305–314 (2004).

27. Honda, T., Egen, J. G., Lämmermann, T., Kastenmuller, W., Torabi-Parizi, P. & Germain, R. N. Tuning of Antigen Sensitivity by T Cell Receptor-Dependent Negative Feedback Controls T Cell Effector Function in Inflamed Tissues. *Immunity* (2014). doi:10.1016/j.immuni.2013.11.017

Chapter 5: Conclusions and future directions

5.1 Discussion of results

Naïve $CD8^+$ T cells circulate through secondary lymphoid organs (SLOs) in search of cognate antigen (Ag). Upon Ag recognition and activation, $CD8^+$ T cells are 'licensed' to take on a number of other migratory patterns, including entry into peripheral tissues[1]. These migratory patterns vary depending on the differentiation state and subset of the $CD8^+$ T cell[2] and are determined by the accumulation of antigenic and inflammatory signals[3]. How DC subsets differentially influence these fate decisions, as well as phenotypic markers that define novel subsets and migratory patterns of $CD8^+$ T cell subsets have been investigated here.

DC subsets differentially affect $CD8^+$ T cell fate decisions in vitro

Naïve $CD8^+$ T cells are activated within SLOs, where they engage in durable interactions with DCs presenting their cognate Ag[4]. Here, we have explored how a subset of DCs, CD8 DCs, captures antigen for subsequent presentation to $CD8^+$ T cells, and whether the context surrounding this pMHC presentation may influence $CD8^+$ T cell fates differently depending on the presenting DC subset. In particular, the role of the phosphatidylserine (PS) receptor, TIM-4[5,6], in the capture of apoptotic cells by CD8 DCs was explored. Following maturation, CD8 DCs strongly upregulated expression of TIM-4, whereas CD11b DCs failed to do so. Using DCs from TIM-4 KO mice or blocking antibodies *in vitro*, engulfment of apoptotic cells was found to be largely dependent on TIM-4. Furthermore, this deficient uptake affected subsequent cross-presentation of apoptotic cell-associated Ags. However, *in vivo* exploration of apoptotic cell capture and ensuing presentation to $CD8^+$ T cells did not implicate TIM-4 in either infectious or

model settings. This indicates that there are redundancies in the mechanisms by which CD8 DCs recognize apoptotic cells *in vivo*. This may occur via bridging molecules that recognize PS, which are present *in vivo*, but not *in vitro*. For example, the bridging molecules, MFG-E8[7] or C1q[8], may be produced by cells not present in *in vitro* assays, which then force apoptotic cell recognition by molecules like TIM-4. When these bridging molecules are present during *in vivo* assays, TIM-4 dependence may be masked.

Beyond pMHC interactions, DC subsets may influence $CD8^+$ T cell fates based on the molecular context in which Ag is presented. Costimulatory and co-inhibitory molecules, as well as soluble cytokines serve to amplify or dampen signal strength and skew cell fate decisions. Whether and how these signals differ between DC subsets and their subsequent effect on $CD8^+$ T cell fate had not been adequately explored. Using peptide-pulsed DC subsets, we have shown that CD8 DCs promote enhanced generation of terminally differentiated $CD8^+$ T cells when priming occurs *in vitro* and following adoptive transfer of *in vitro*-primed $CD8^+$ T cells. Additionally, CD11b DCs promoted greater IL-2 production by $CD8^+$ T cells. However, when primed *in vivo*, peptide-pulsed DC subsets failed to alter $CD8^+$ T cell fate decisions. This was not due to differential DC subset migration, as both subsets arrived in draining LNs. It is likely that $CD8^+$ T cells integrate signals derived from both the Ag-presenting DC subset, as well as accessory cells within the draining LN, which could mask any differences observed *in vitro*.

Together, the findings of **Chapter 2** highlight that, in isolation, immune cells may become dependent on particular processes for optimal responses, but when placed in the complex environment of an organism, redundancies are revealed that prevent excessive dependence on a particular process or pathway.

CX_3CR1 distinguishes three subsets of $CD8^+$ T cells and redefines migration of T_{EM} and effector precursors

The study of $CD8^+$ T cell fate decisions has, to date, been limited by inadequate subset-defining markers. In particular, the markers that define the classical subsets: T_{EM} and T_{CM}, CCR7 and CD62L[9], are lost upon restimulation. Here, we have shown that the chemokine receptor, CX_3CR1, defines three subsets of $CD8^+$ T cells. CX_3CR1^- cells have been identified as classical T_{CM} while CX_3CR1^{hi} cells are equivalent to T_{EM}. The third subset of cells, heretofore not described, express an intermediated level of CX_3CR1 (CX_3CR1^{int}) and has been termed peripheral memory T cell (T_{PM}). Notably, when CX_3CR1-expressing subsets were restimulated after transfer, CX_3CR1 expression was never lost. Instead, increasing levels of CX_3CR1 were associated with terminal differentiation and implied a linear pedigree of differentiation: T_{CM} to T_{PM} to T_{EM}. Furthermore, analysis of re-acquisition of CD62L expression by CX_3CR1 subsets resolved a long-standing issue in the field[10,11] concerning identification of the effector subsets that re-acquire CD62L during progression into the memory phase. We found that CX_3CR1^- and CX_3CR1^{int} both re-acquired CD62L, albeit with differing efficiency, while CX_3CR1^{hi} T cells failed to re-acquire CD62L (**Figure 5.1**).

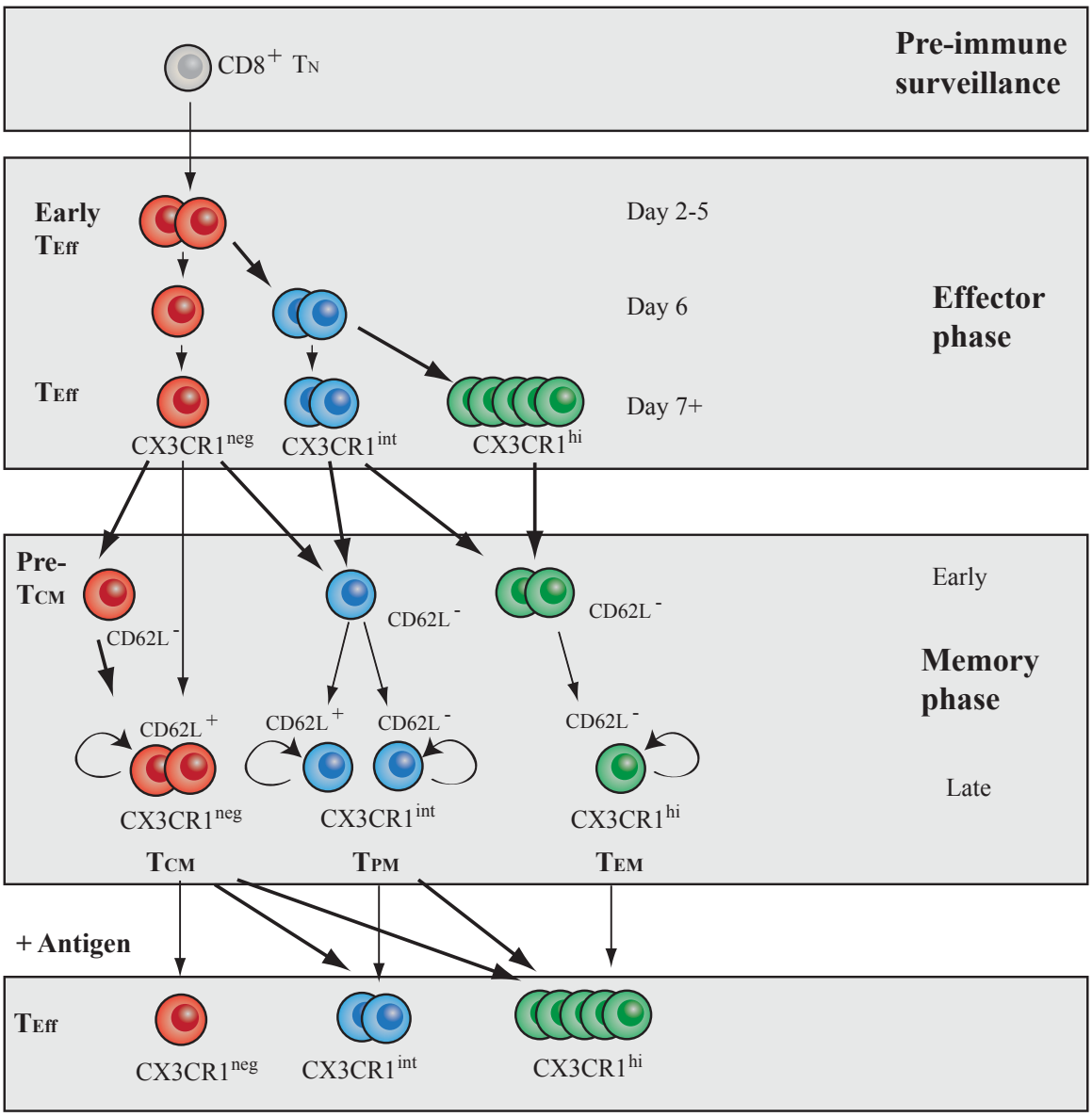

Figure 5.1: Linear pedigree of CD8$^+$ T cell differentiation as defined by CX$_3$CR1 expression. Schematic of CD8+ T cell differentiation into CX3CR1$^-$, CX3CR1^{int} and CX3CR1^{hi} T_{Eff} and T_{Mem} subsets. The number of depicted cells represents the relative abundance of the subsets. The thickness of the arrows indicates the relative dominance of the particular differentiation pathway.

T_{EM} have long been believed to survey peripheral tissues[12], but direct evidence of this behavior has been lacking. Using CX_3CR1 to define memory T cell subsets, we established that CX_3CR1^{int} cells are, in fact, the predominant subset migrating through peripheral tissues. Hence, we have termed these cells peripheral memory T cells (T_{PM}). In contrast, CX_3CR1^{hi} T_{EM} did not appear to migrate through peripheral tissues and were, instead, generally restricted to the intravascular space of tissues. This prompted us to investigate what function T_{EM} and their effector precursors could serve considering that they were excluded from LNs and peripheral tissues. Intravital multi-photon microscopy (IV-MPM), together with a novel application of photo-convertible kaede tg mice, revealed that CX_3CR1^{hi} T cells scanned arteriolar endothelium in both the effector and memory phase after viral infection. Patrolling was independent of activated endothelium and functional CX_3CR1, but was highly dependent on the integrin, LFA-1. Thus, the data presented in **Chapter 3** and **Chapter 4** significantly alter the current paradigm for T_{EM} migration and identifies a novel endothelial scanning behavior for this subset (**Figure 5.2**).

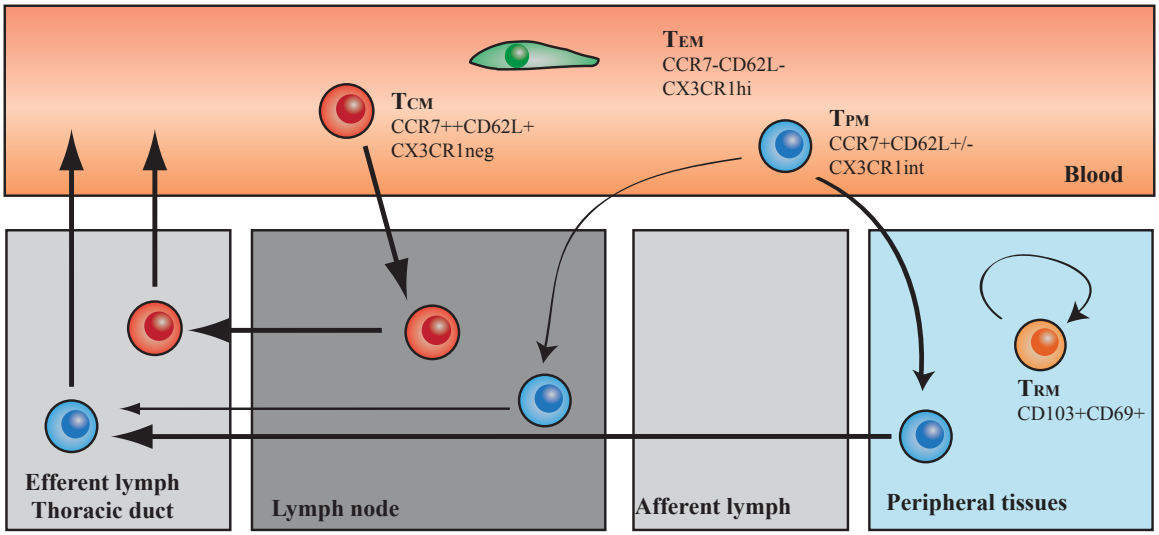

Figure 5.2: T_{Mem} migratory properties and tissue distribution. Representation of the migratory properties of T_{CM} (red), T_{PM} (blue), T_{EM} (green), and T_{RM} (orange). Thickness of line indicates relative prevalence of migration behavior. Elongated T_{EM} represents patrolling of vascular endothelium.

5.2 Future work

Transcriptional analysis of physiologically relevant DCs

Our studies in **Chapter 2** demonstrated that subsets of DCs could influence $CD8^+$ T cell responses through mechanisms related to Ag capture, as well as ancillary cytokines. Whereas these studies revealed redundancies when applied *in vivo*, they nevertheless identified novel processes that may be explored further.

Differences in IFNγ production between $CD8^+$ T cells primed by CD8 DCs (T_{8DC}) and $CD8^+$ T cells primed by CD11b DCs (T_{11bDC}) could largely be attributed to greater IL-12 production by CD8 DCs, but the finding that T_{11bDC} produced more IL-2 than their T_{8DC} counterparts was never resolved (**Figure 2.6**). IL-2 production by CD8 T cells during priming is correlated with high secondary expansion potential[13,14] and

understanding how to promote generation of these cells is of great interest for vaccine strategies. Transcriptional analysis of the co-stimulatory molecules and cytokines variably induced by maturation of CD11b DCs and CD8 DCs may shed light on the differential signals being integrated by T cells during our *in vitro* experiments. Surprisingly, a rigorous analysis of DC subset transcriptional changes following maturation has not been undertaken. Instead, many studies have sorted subsets of DCs from steady state environments, which have helped to clarify the lineage relationships of DC precursors and the differentiated subsets[15-17]. However, the transcriptional landscape of DCs in the steady state is one that promotes tolerance. Studies that have deeply explored transcriptional changes following maturation have been done with bone marrow derived DCs (BMDCs)[18]. Whereas these *in vitro* studies yield novel insights into certain aspects of DC biology[19], their translation to physiological DCs remains unclear. Furthermore, other cellular contaminants in BMDC cultures[20] can complicate interpretations[21]. Therefore, analysis of transcriptional changes following DC subset maturation, even *in vitro*, will be informative. Additionally, new sequencing technologies allow for analysis of DCs sorted from an *in vivo* environment where cell numbers have previously limited interrogation. In this way, subsets of DCs could be sorted based on some functional criterion to enrich for DCs with particular attributes. For example, subsets of DCs that capture apoptotic cells in model settings[22] could be compared to those that fail to capture apoptotic cells to evaluate whether there are particular transcripts associated with this ability. Alternatively, in *in vitro* settings where T_{11bDC} produced more IL-2 than their T_{8DC} counterparts, transcriptional analysis of the T cells themselves will uncover signaling nodes[23] that are involved in IL-2 production and perhaps other

attributes that have been associated with IL-2 production[14]. Together, these kinds of analyses will shed light on how maturing DC subsets differ from their immature counterparts and point to receptors that may mediate apoptotic cell capture in inflammatory settings, as well as the cytokines produced by DC subsets and how T cells integrate these signals.

Understanding the cellular sources that mask differential in vivo priming of CD8$^+$ T cells by DC subsets

Priming of T cells *in vitro* by CD11b DCs or CD8 DCs drove differential cytokine production and differentiation when T cells were subsequently transferred *in vivo.* During priming, CD8$^+$ T cells engage in durable interactions with DCs[4] and therefore it was hypothesized that DC subsets may differentially affect CD8$^+$ T cell differentiation *in vivo* as well. However, the differences seen *in vitro* were masked when priming occurred *in vivo*, thus highlighting the importance of accessory cells that produce signals which are integrated by Ag-specific T cells. To uncover the sources and signals that minimize differential priming effects, resident CD8 DCs could be punctually ablated using XCR1$^{DTR\text{-}venus}$ mice[24] prior to immunization. This would minimize potential Ag handover[25] as well as local IL-12 production. Additionally, IL-12p40$^{-/-}$ mice could be used to limit IL-12 production to immunizing DC subsets. Ag handover could also be ruled out using H-2K^{bm1} mice, where H-2K^b has a single point mutation that prevents binding of SIINFEKL and thus activation of OT-I cells[26]. This limits presentation of SIINFEKL-loaded H-2K^b to injected DC subsets. However, in this case, cross-dressing[27] cannot be ruled out since membrane transfer of SIINFEKL-loaded H-2K^b complexes

would permit activation of OT-I cells by resident DCs. To investigate the role of plasmacytoid DCs (pDCs) and type I interferons (IFN-I) as potential contributors to $CD8^+$ T cell differentiation, E2-2$^{-/-}$ mice[28] or BDCA-2^{DTR} mice[29] could be used to deplete pDCs constitutively or punctually. Alternatively, OT-I cells crossed to IFNAR$^{-/-}$ mice could be used to assess whether IFN-I from any source may influence T cell differentiation during priming in LNs. Together, these approaches may address the cell types and molecules that shape $CD8^+$ T cell responses during priming in LNs.

Ubiquity of T_{EM} patrolling

Our studies described in **Chapter 3** and **Chapter 4** demonstrate that CX_3CR1^{hi} $CD8^+$ T cells were rarely found in peripheral tissues and instead, could be found patrolling along endothelium within the dermal vasculature. The ear was chosen as an ideal organ to investigate this behavior because it can be exposed to violet light for photo-conversion of kaede protein or IV-MPM without surgical manipulation. However, the patrolling behavior of CX_3CR1^{hi} $CD8^+$ T cells on the endothelium of other tissues has not been investigated here. Patrolling by CX_3CR1^{hi} monocytes has been shown within the microvasculature of the dermis, kidney, and mesentery[30,31] and for $CXCR6^+$ NKT cells within liver sinusoids[32,33]. This would suggest that CX_3CR1^{hi} T_{Eff} and T_{EM} might patrol the vasculature of these tissues as well. Furthermore, *in vitro* IL-2-differentiated effector $CD8^+$ T cells patrol liver sinusoids following adoptive transfer[34]. However, the relationship between these *in vitro* differentiated cells and CX_3CR1^{hi} T_{Eff} and T_{EM} is unclear as $CD8^+$ T cells stimulated in the presence of IL-2 or IL-15 *in vitro* failed to induce CX_3CR1 expression (data not shown). *In vitro* stimulated $CD4^+$ T cells have also

been shown to adhere to and migrate along the meningeal vasculature prior to onset of experimental autoimmune encephalomyelitis (EAE)[35]. Whereas these data do not directly address patrolling by CX_3CR1^{hi} T_{Eff} or T_{EM}, they highlight other organs where these cells may exhibit similar patrolling behaviors.

Previously, methods to study patrolling have been limited to direct visualization by intravital microscopy and reliance on fluorescent reporters[30-34]. This confines study to organs that can be effectively stabilized and imaged over long time periods. Additionally, fluorescent reporters permit identification only of cells that have been tagged. If the reporter is promiscuous or broad, specific discernment of patrolling cell types can be challenging. Conversely, if the reporter is specific and narrow, some patrolling cell types may not be detected. Using a novel method of intravascular staining in conjunction with photo-convertible kaede tg mice, identification of patrolling is limited only by the ability to expose the tissue to violet light and available antibodies for flow cytometric analysis. This can be used to query organs where patrolling by particular cell types has already been established and identify additional patrolling cell types in different inflammatory contexts. Furthermore, this approach could be applied to organs where intravital visualization proves particularly challenging. Intravital imaging of the lung and portions of the intestinal tract are possible, but require significant surgical manipulation to expose and stabilize[36-38]. Less invasive methods like endoscopy with violet light could potentially be used for photo-conversion in these tissues, similar to methods for photo-conversion of colonic cells[39]. In conjunction with intravascular staining, these techniques may unveil evidence of patrolling in hard to reach tissues, which could both provide support for and guide further efforts to image patrolling in these tissues in real time.

Molecular mechanisms for patrolling

Previous studies[30], in addition to our work using intravascular staining in combination with photo-convertible kaede tg mice have established CX_3CR1^{hi} $CD8^+$ T cells and CX_3CR1^{hi} monocytes as the major cell types capable of patrolling along dermal endothelium. However, the mechanistic underpinnings for this process are poorly understood. The integrin, LFA-1, is required for attachment of both monocytes[30] and $CD8^+$ T cells to endothelium (**Figure 4.3 D**), but LFA-1 is broadly expressed by lymphocytes[40] and cannot explain the specificity of patrolling behavior. CX_3CR1 was initially described to be partially required for monocyte patrolling[30], but this is more likely the result of decreased monocyte survival in $CX_3CR1^{gfp/gfp}$ mice[31,41]. CX_3CR1^{hi} $CD8^+$ T cells also did not require functional CX_3CR1 for patrolling (**Figure 4.5 E**). Nor did they require the chemokine receptors CCR2 or CCR5. Given that LFA-1 is required for attachment, the cell adhesion molecules (CAMs) with which LFA-1 interacts should guide future interrogation. The two prominent LFA-1 ligands ICAM-1 and ICAM-2 have been shown to be dually required for monocyte patrolling[31]. While ICAM-1 deficient mice had partially reduced patrolling, this reduction was significantly enhanced in ICAM-1/-2 double deficient mice[31]. ICAM-2 expression on dermal arteriolar endothelium in steady state (**Figure 4.4 A**) suggests that patrolling CX_3CR1^{hi} $CD8^+$ T cells may depend on ICAM-2 for attachment. However, studies to dissect ICAM-2 dependent adhesion may require transfer of CX_3CR1^{hi} T_{Eff} into naïve mice or waiting for the development of T_{EM} prior to antibody blockade of ICAM-2. This may be necessary as ICAM-1 is induced by inflammation (**Figure 4.4 B**), which could mediate cellular

attachment and would mask a role for ICAM-2 during the effector phase of the response. Alternatively, an intermediate adhesion step in the form of tethering to platelets may be required for adherence to endothelium, as *in vitro* differentiated $CD8^+$ effector T cells have been shown to be partially dependent on platelets for adherence to liver sinusoids[34]. In this model, effector T cells did not require LFA-1 for adherence, which may indicate a mechanism distinct from that in dermal endothelium. Nonetheless, further investigation into platelets as contributors to patrolling behavior by CX_3CR1^{hi} $CD8^+$ T cells is warranted for a better understanding of the patrolling mechanism.

Transcriptional analysis of patrolling T cells may also provide clues as to the molecular requirements for this process. Of the three $CD8^+$ T cell subsets defined by CX_3CR1 expression, CX_3CR1^{hi} $CD8^+$ T cells are significantly enriched among patrolling cells (**Figure 4.1 I,J**). Thus, identification of adhesion molecules selectively upregulated by CX_3CR1^{hi} $CD8^+$ T cells compared to CX_3CR1^- and CX_3CR1^{int} $CD8^+$ T cells will help point to relevant molecules for investigation in future experiments. Recently, subsets of $CD8^+$ T cells defined by CX_3CR1 expression were subjected to microarray analysis[42], and these data could be mined for differential expression patterns of potential adhesive molecules. However, in the published study, CX_3CR1 subsets were divided into four groups by CX_3CR1^+/CX_3CR1^- and $CD62L^+/CD62L^-$, as opposed to separating intermediate and high expressers of CX_3CR1. Our extensive characterization of variable CD62L expression (**Figure 3.4 A**) would suggest that $CX_3CR1^+CD62L^-$ $CD8^+$ T cells would be enriched for being CX_3CR1^{hi}, but may also include CX_3CR1^{int} cells that have not yet reacquired CD62L. However, even with the potential noise from this CX_3CR1^{int} contamination, CX_3CR1^{hi} transcripts would likely still be enriched. Beyond sorting

subsets based purely on CX_3CR1 expression, there may be unidentified subsets within the CX_3CR1^{hi} population that are uniquely capable of patrolling compared to other CX_3CR1^{hi} $CD8^+$ T cells. Direct identification of patrolling cells using the photo-convertible kaede tg system would enable separation of patrolling CX_3CR1^{hi} $CD8^+$ T cells versus non-patrolling CX_3CR1^{hi} $CD8^+$ T cells for transcriptional analysis.

Functional significance of patrolling T_{EM}

Perhaps the most intriguing unanswered question to address concerns the functional significance of the patrolling behavior observed. To adequately address this question, a mechanism by which patrolling behavior can be inhibited must be identified. Furthermore, this mechanism must be relatively specific for patrolling behavior as inhibition of cell adhesion pathways like LFA-1 will mediate effects too broad to be interpreted as arising solely from defective patrolling[43]. ICAM-2 is a promising candidate as ICAM-2 expression is restricted to arteriolar endothelium (**Figure 4.4**), its expression is not altered by inflammation[44], and its absence is not currently known to have major consequences for T cell responses. Transcriptional analysis, as described above, may provide additional clues as to the relevant molecules to target.

Alternatively, systems wherein CX_3CR1^{hi} T cells could be constitutively deleted may reveal functional consequences associated with their absence. This could be done using the recently described CX_3CR1^{CreER} mouse[45] crossed to the R-DTA mouse[46], which expresses the lethal diphtheria toxin α subunit upon cre-mediated excision of a stop sequence. Using these mice, tamoxifen administration would result in the punctual ablation of CX_3CR1-expressing cells. To avoid global ablation of CX_3CR1-expressing

cells, which would include microglia, monocytes, macrophages[47], as well as T_{EM}, bone marrow (BM) chimeras could be generated by co-transferring CX_3CR1^{CreER}R-DTA BM and $RAG^{-/-}$ BM into lethally irradiated wild-type mice. Thus, following tamoxifen administration, T_{EM} would be completely absent whereas the CX_3CR1-expressing myeloid compartment would remain intact. Such mice would prove useful for interrogating the functional consequences of patrolling behavior, as well as determining the broader implications of constitutively lacking T_{EM}.

In addition to being able to specifically perturb patrolling behavior, the right model system must be chosen to interrogate the physiological consequences of this perturbation. Considering that patrolling T cells are in intimate contact with endothelium, it is tempting to speculate that patrolling cells serve to mitigate pathogenic replication and dissemination within and from endothelial cells. Therefore, pathogens that infect endothelial cells may not be effectively controlled when patrolling is inhibited. Hemorrhagic fever viruses, as well as the bacteria, *Toxoplasma gondii*[48] and *Borrelia burgdorferi*[49] have been suggested to infect endothelial cells. To avoid significant biosafety issues with hemorrhagic fever viruses, glycoproteins from these viruses may be used to psuedotype VSV, which may promote similar tropisms, but are no longer lethal[50]. VSV is, however, particularly susceptible to type I interferon-mediated control[51] and may limit prolonged replication. To avoid this problem, $IFNAR^{-/-}$ mice may be infected with these pseudotyped viruses and thus open up alternative mechanisms of control that may include patrolling T cells. *Toxpoplasma gondii* and *Borrelia burgdorferi* are also intriguing candidates, where infection of the blood microvasculature and subsequent invasion of the brain is thought to be a potential mechanism for crossing the blood brain

barrier[52-54]. During this passage, microbially derived Ags may be presented for activation of patrolling $CD8^+$ T cells. Thus activated, patrolling $CD8^+$ T cells would subsequently deploy a number of effector functions in order to limit further replication and consequent invasion of the brain.

This raises another interesting question regarding the function of patrolling T cells: what effector functions are utilized following Ag recognition? Perforin and granzyme-mediated cytotoxicity directed towards endothelial cells would result in loss of vascular integrity and be deleterious to the host. In contrast, secretion of cytokines like IFNγ may promote an anti-viral or anti-microbial state in endothelial cells that would limit replication and further dissemination[55]. To visualize cytokine production following activation, Ag-specific IFNγ yellow fluorescent protein (YFP) reporter mice could be used[56]. Alternatively and perhaps more informative, the anti-microbial state promoted in endothelial cells could be measured using the REX3 mouse, which is a dual reporter mouse that expresses red fluorescent protein (RFP) under the control of the CXCL9 promoter and blue fluorescent protein (BFP) under the control of CXCL10[57]. Both CXCL9 and CXCL10 are strongly induced by IFNγ[58,59] and could therefore be used as surrogates for IFNγ-sensing by endothelium during intravital imaging. If degranulation and cytotoxicity are occurring, this process can be measured by i.v. injection of a fluorescent antibody against CD107, which is exposed during degranulation and marks cytolytic T cells[60,61].

In summary, $CD8^+$ T cell differentiation is the result of multiple cellular players that contribute to the overall Ag density and cytokine milieu interpreted by T cells. Rarely are $CD8^+$ T cells wholly dependent on stimuli from a single cellular subset for

their differentiation. However, dissection of these dependencies in model settings may reveal signaling pathways that aid our understanding of T cell biology and can be wielded for therapeutic purposes. Furthermore, understanding how $CD8^+$ T cell fate decisions are made is important given the distinct functional properties and migratory patterns of the $CD8^+$ T cell subsets that result. Analysis of these subsets using CX_3CR1 as a marker of terminal differentiation has redefined the migration of T_{EM} and the newly described T_{PM}. CX_3CR1 and the experimental tools described herein have thus opened up new hypotheses regarding effective surveillance of the body by $CD8^+$ T cell subsets.

5.3 References

1. Andrian, von, U. H. & Mackay, C. R. T-cell function and migration. Two sides of the same coin. *N Engl J Med* **343,** 1020–1034 (2000).
2. Sallusto, F., Geginat, J. & Lanzavecchia, A. Central memory and effector memory T cell subsets: function, generation, and maintenance. *Annu. Rev. Immunol.* **22,** 745–763 (2004).
3. Cui, W. & Kaech, S. M. Generation of effector CD8+ T cells and their conversion to memory T cells. *Immunol Rev* **236,** 151–166 (2010).
4. Mempel, T. R., Henrickson, S. E. & Andrian, von, U. H. T-cell priming by dendritic cells in lymph nodes occurs in three distinct phases. *Nature* **427,** 154–159 (2004).
5. Kobayashi, N., Karisola, P., Peña-Cruz, V., Dorfman, D. M., Jinushi, M., Umetsu, S. E., Butte, M. J., Nagumo, H., Chernova, I., Zhu, B., Sharpe, A. H., Ito, S., Dranoff, G., Kaplan, G. G., Casasnovas, J. M., Umetsu, D. T., DeKruyff, R. H. &

Freeman, G. J. TIM-1 and TIM-4 glycoproteins bind phosphatidylserine and mediate uptake of apoptotic cells. *Immunity* **27,** 927–940 (2007).

6. Miyanishi, M., Tada, K., Koike, M., Uchiyama, Y., Kitamura, T. & Nagata, S. Identification of Tim4 as a phosphatidylserine receptor. *Nature* **450,** 435–439 (2007).

7. Hanayama, R., Tanaka, M., Miwa, K., Shinohara, A., Iwamatsu, A. & Nagata, S. Identification of a factor that links apoptotic cells to phagocytes. *Nature* **417,** 182–187 (2002).

8. Païdassi, H., Tacnet-Delorme, P., Garlatti, V., Darnault, C., Ghebrehiwet, B., Gaboriaud, C., Arlaud, G. J. & Frachet, P. C1q binds phosphatidylserine and likely acts as a multiligand-bridging molecule in apoptotic cell recognition. *The Journal of Immunology* **180,** 2329–2338 (2008).

9. Sallusto, F., Lenig, D., Förster, R., Lipp, M. & Lanzavecchia, A. Two subsets of memory T lymphocytes with distinct homing potentials and effector functions. *Nature* **401,** 708–712 (1999).

10. Wherry, E. J., Teichgräber, V., Becker, T. C., Masopust, D., Kaech, S. M., Antia, R., Andrian, von, U. H. & Ahmed, R. Lineage relationship and protective immunity of memory CD8 T cell subsets. *Nat Immunol* **4,** 225–234 (2003).

11. Marzo, A. L., Klonowski, K. D., Le Bon, A., Borrow, P., Tough, D. F. & Lefrançois, L. Initial T cell frequency dictates memory CD8+ T cell lineage commitment. *Nat Immunol* **6,** 793–799 (2005).

12. Mackay, C. R., Marston, W. L. & Dudler, L. Naive and memory T cells show distinct pathways of lymphocyte recirculation. *J Exp Med* **171,** 801–817 (1990).

13. Williams, M. A., Tyznik, A. J. & Bevan, M. J. Interleukin-2 signals during priming are required for secondary expansion of CD8+ memory T cells. *Nature* **441,** 890–893 (2006).

14. Feau, S., Arens, R., Togher, S. & Schoenberger, S. P. Autocrine IL-2 is required for secondary population expansion of CD8(+) memory T cells. *Nat Immunol* **12,** 908–913 (2011).

15. Miller, J. C., Brown, B. D., Shay, T., Gautier, E. L., Jojic, V., Cohain, A., Pandey, G., Leboeuf, M., Elpek, K. G., Helft, J., Hashimoto, D., Chow, A., Price, J., Greter, M., Bogunovic, M., Bellemare-Pelletier, A., Frenette, P. S., Randolph, G. J., Turley, S. J., Merad, M., the Immunological Genome Consortium, Jakubzick, C., Best, A. J., Knell, J., Goldrath, A., Miller, J., Brown, B., Koller, D., Cohen, N., Brennan, P., Brenner, M., Regev, A., Fletcher, A., Elpek, K., Malhotra, D., Turley, S., Jianu, R., Laidlaw, D., Collins, J., Narayan, K., Sylvia, K., Kang, J., Gazit, R., Rossi, D. J., Kim, F., Rao, T. N., Wagers, A., Shinton, S. A., Hardy, R. R., Monach, P., Bezman, N. A., Sun, J. C., Kim, C. C., Lanier, L. L., Heng, T., Kreslavsky, T., Painter, M., Ericson, J., Davis, S., Mathis, D. & Benoist, C. Deciphering the transcriptional network of the dendritic cell lineage. *Nat Immunol* (2012). doi:10.1038/ni.2370

16. Satpathy, A. T., KC, W., Albring, J. C., Edelson, B. T., Kretzer, N. M., Bhattacharya, D., Murphy, T. L. & Murphy, K. M. Zbtb46 expression distinguishes classical dendritic cells and their committed progenitors from other immune lineages. *Journal of Experimental Medicine* **209,** 1135–1152 (2012).

17. Meredith, M. M., Liu, K., Darrasse-Jeze, G., Kamphorst, A. O., Schreiber, H. A.,

Guermonprez, P., Idoyaga, J., Cheong, C., Yao, K. H., Niec, R. E. & Nussenzweig, M. C. Expression of the zinc finger transcription factor zDC (Zbtb46, Btbd4) defines the classical dendritic cell lineage. *Journal of Experimental Medicine* **209,** 1153–1165 (2012).

18. Amit, I., Garber, M., Chevrier, N., Leite, A. P., Donner, Y., Eisenhaure, T., Guttman, M., Grenier, J. K., Li, W., Zuk, O., Schubert, L. A., Birditt, B., Shay, T., Goren, A., Zhang, X., Smith, Z., Deering, R., McDonald, R. C., Cabili, M., Bernstein, B. E., Rinn, J. L., Meissner, A., Root, D. E., Hacohen, N. & Regev, A. Unbiased reconstruction of a mammalian transcriptional network mediating pathogen responses. *Science* **326,** 257–263 (2009).

19. Chevrier, N., Mertins, P., Artyomov, M. N., Shalek, A. K., Iannacone, M., Ciaccio, M. F., Gat-Viks, I., Tonti, E., DeGrace, M. M., Clauser, K. R., Garber, M., Eisenhaure, T. M., Yosef, N., Robinson, J., Sutton, A., Andersen, M. S., Root, D. E., Andrian, von, U., Jones, R. B., Park, H., Carr, S. A., Regev, A., Amit, I. & Hacohen, N. Systematic discovery of TLR signaling components delineates viral-sensing circuits. *Cell* **147,** 853–867 (2011).

20. Helft, J., Böttcher, J., Chakravarty, P., Zelenay, S., Huotari, J., Schraml, B. U., Goubau, D. & Reis e Sousa, C. GM-CSF Mouse Bone Marrow Cultures Comprise a Heterogeneous Population of CD11c(+)MHCII(+) Macrophages and Dendritic Cells. *Immunity* **42,** 1197–1211 (2015).

21. Shalek, A. K., Satija, R., Shuga, J., Trombetta, J. J., Gennert, D., Lu, D., Chen, P., Gertner, R. S., Gaublomme, J. T., Yosef, N., Schwartz, S., Fowler, B., Weaver, S., Wang, J., Wang, X., Ding, R., Raychowdhury, R., Friedman, N., Hacohen, N.,

Park, H., May, A. P. & Regev, A. Single-cell RNA-seq reveals dynamic paracrine control of cellular variation. *Nature* **510,** 263–269 (2015).

22. Iyoda, T., Shimoyama, S., Liu, K., Omatsu, Y., Akiyama, Y., Maeda, Y., Takahara, K., Steinman, R. M. & Inaba, K. The CD8+ dendritic cell subset selectively endocytoses dying cells in culture and in vivo. *J Exp Med* **195,** 1289–1302 (2002).

23. Wu, C., Yosef, N., Thalhamer, T., Zhu, C., Xiao, S., Kishi, Y., Regev, A. & Kuchroo, V. K. Induction of pathogenic TH17 cells by inducible salt-sensing kinase SGK1. *Nature* **496,** 513–517 (2013).

24. Yamazaki, C., Sugiyama, M., Ohta, T., Hemmi, H., Hamada, E., Sasaki, I., Fukuda, Y., Yano, T., Nobuoka, M., Hirashima, T., Iizuka, A., Sato, K., Tanaka, T., Hoshino, K. & Kaisho, T. Critical roles of a dendritic cell subset expressing a chemokine receptor, XCR1. *J Immunol* **190,** 6071–6082 (2013).

25. Allan, R. S., Waithman, J., Bedoui, S., Jones, C. M., Villadangos, J. A., Zhan, Y., Lew, A. M., Shortman, K., Heath, W. R. & Carbone, F. R. Migratory dendritic cells transfer antigen to a lymph node-resident dendritic cell population for efficient CTL priming. *Immunity* **25,** 153–162 (2006).

26. Kurts, C., Kosaka, H., Carbone, F. R., Miller, J. F. & Heath, W. R. Class I-restricted cross-presentation of exogenous self-antigens leads to deletion of autoreactive CD8(+) T cells. *J Exp Med* **186,** 239–245 (1997).

27. Wakim, L. M. & Bevan, M. J. Cross-dressed dendritic cells drive memory CD8+ T-cell activation after viral infection. *Nature* **471,** 629–632 (2011).

28. Cisse, B., Caton, M. L., Lehner, M., Maeda, T., Scheu, S., Locksley, R.,

Holmberg, D., Zweier, C., Hollander, den, N. S., Kant, S. G., Holter, W., Rauch, A., Zhuang, Y. & Reizis, B. Transcription factor E2-2 is an essential and specific regulator of plasmacytoid dendritic cell development. *Cell* **135,** 37–48 (2008).

29. Swiecki, M., Gilfillan, S., Vermi, W., Wang, Y. & Colonna, M. Plasmacytoid Dendritic Cell Ablation Impacts Early Interferon Responses and Antiviral NK and CD8+ T Cell Accrual. *Immunity* **33,** 955–966 (2010).

30. Auffray, C., Fogg, D., Garfa, M., Elain, G., Join-Lambert, O., Kayal, S., Sarnacki, S., Cumano, A., Lauvau, G. & Geissmann, F. Monitoring of blood vessels and tissues by a population of monocytes with patrolling behavior. *Science* **317,** 666–670 (2007).

31. Carlin, L. M., Stamatiades, E. G., Auffray, C., Hanna, R. N., Glover, L., Vizcay-Barrena, G., Hedrick, C. C., Cook, H. T., Diebold, S. & Geissmann, F. Nr4a1-dependent Ly6C(low) monocytes monitor endothelial cells and orchestrate their disposal. *Cell* **153,** 362–375 (2013).

32. Geissmann, F., Cameron, T. O., Sidobre, S., Manlongat, N., Kronenberg, M., Briskin, M. J., Dustin, M. L. & Littman, D. R. Intravascular immune surveillance by CXCR6+ NKT cells patrolling liver sinusoids. *PLoS Biol* **3,** e113 (2005).

33. Lee, W.-Y., Moriarty, T. J., Wong, C. H. Y., Zhou, H., Strieter, R. M., Van Rooijen, N., Chaconas, G. & Kubes, P. An intravascular immune response to Borrelia burgdorferi involves Kupffer cells and iNKT cells. *Nat Immunol* **11,** 295–302 (2010).

34. Guidotti, L. G., Inverso, D., Sironi, L., Di Lucia, P., Fioravanti, J., Ganzer, L., Fiocchi, A., Vacca, M., Aiolfi, R., Sammicheli, S., Mainetti, M., Cataudella, T.,

Raimondi, A., Gonzalez-Aseguinolaza, G., Protzer, U., Ruggeri, Z. M., Chisari, F. V., Isogawa, M., Sitia, G. & Iannacone, M. Immunosurveillance of the liver by intravascular effector CD8(+) T cells. *Cell* **161,** 486–500 (2015).

35. Bartholomäus, I., Kawakami, N., Odoardi, F., Schläger, C., Miljkovic, D., Ellwart, J. W., Klinkert, W. E. F., Flügel-Koch, C., Issekutz, T. B., Wekerle, H. & Flügel, A. Effector T cell interactions with meningeal vascular structures in nascent autoimmune CNS lesions. *Nature* **462,** 94–98 (2009).

36. Looney, M. R., Thornton, E. E., Sen, D., Lamm, W. J., Glenny, R. W. & Krummel, M. F. Stabilized imaging of immune surveillance in the mouse lung. *Nat Methods* **8,** 91–96 (2010).

37. McDole, J. R., Wheeler, L. W., McDonald, K. G., Wang, B., Konjufca, V., Knoop, K. A., Newberry, R. D. & Miller, M. J. Goblet cells deliver luminal antigen to CD103+ dendritic cells in the small intestine. *Nature* **483,** 345–349 (2012).

38. Chieppa, M., Rescigno, M., Huang, A. Y. C. & Germain, R. N. Dynamic imaging of dendritic cell extension into the small bowel lumen in response to epithelial cell TLR engagement. *J Exp Med* **203,** 2841–2852 (2006).

39. Morton, A. M., Sefik, E., Upadhyay, R., Weissleder, R., Benoist, C. & Mathis, D. Endoscopic photoconversion reveals unexpectedly broad leukocyte trafficking to and from the gut. *Proceedings of the National Academy of Sciences* **111,** 6696–6701 (2014).

40. Springer, T. A., Dustin, M. L. & Kishimoto, T. K. The lymphocyte function associated LFA-1, CD2, and LFA-3 molecules: cell adhesion receptors of the immune system. *Annual Review of ...* (1987).

41. Landsman, L., Bar-On, L., Zernecke, A., Kim, K.-W., Krauthgamer, R., Shagdarsuren, E., Lira, S. A., Weissman, I. L., Weber, C. & Jung, S. CX3CR1 is required for monocyte homeostasis and atherogenesis by promoting cell survival. *Blood* **113,** 963–972 (2009).

42. Böttcher, J. P., Beyer, M., Meissner, F., Abdullah, Z., Sander, J., Höchst, B., Eickhoff, S., Rieckmann, J. C., Russo, C., Bauer, T., Flecken, T., Giesen, D., Engel, D., Jung, S., Busch, D. H., Protzer, U., Thimme, R., Mann, M., Kurts, C., Schultze, J. L., Kastenmuller, W. & Knolle, P. A. Functional classification of memory CD8(+) T cells by CX3CR1 expression. *Nat Commun* **6,** 8306 (2015).

43. Springer, T. A. Traffic signals for lymphocyte recirculation and leukocyte emigration: the multistep paradigm. *Cell* **76,** 301–314 (1994).

44. de Fougerolles, A. R., Stacker, S. A., Schwarting, R. & Springer, T. A. Characterization of ICAM-2 and evidence for a third counter-receptor for LFA-1. *J Exp Med* **174,** 253–267 (1991).

45. Yona, S., Kim, K.-W., Wolf, Y., Mildner, A., Varol, D., Breker, M., Strauss-Ayali, D., Viukov, S., Guilliams, M., Misharin, A., Hume, D. A., Perlman, H., Malissen, B., Zelzer, E. & Jung, S. Fate mapping reveals origins and dynamics of monocytes and tissue macrophages under homeostasis. *Immunity* **38,** 79–91 (2013).

46. Voehringer, D., Liang, H.-E. & Locksley, R. M. Homeostasis and effector function of lymphopenia-induced 'memory-like' T cells in constitutively T cell-depleted mice. *The Journal of Immunology* **180,** 4742–4753 (2008).

47. Jung, S., Aliberti, J., Graemmel, P., Sunshine, M. J., Kreutzberg, G. W., Sher, A. & Littman, D. R. Analysis of fractalkine receptor CX(3)CR1 function by targeted

deletion and green fluorescent protein reporter gene insertion. *Mol Cell Biol* **20,** 4106–4114 (2000).

48. Cañedo-Solares, I., Calzada-Ruiz, M., Ortiz-Alegría, L. B., Ortiz-Muñiz, A. R. & Correa, D. Endothelial cell invasion by Toxoplasma gondii: differences between cell types and parasite strains. *Parasitol. Res.* **112,** 3029–3033 (2013).

49. Hickey, M. J. & Kubes, P. Intravascular immunity: the host-pathogen encounter in blood vessels. *Nat Rev Immunol* **9,** 364–375 (2009).

50. Jones, S. M., Feldmann, H., Ströher, U., Geisbert, J. B., Fernando, L., Grolla, A., Klenk, H.-D., Sullivan, N. J., Volchkov, V. E., Fritz, E. A., Daddario, K. M., Hensley, L. E., Jahrling, P. B. & Geisbert, T. W. Live attenuated recombinant vaccine protects nonhuman primates against Ebola and Marburg viruses. *Nat Med* **11,** 786–790 (2005).

51. Müller, U., Steinhoff, U., Reis, L. F., Hemmi, S., Pavlovic, J., Zinkernagel, R. M. & Aguet, M. Functional role of type I and type II interferons in antiviral defense. *Science* **264,** 1918–1921 (1994).

52. Lachenmaier, S. M., Deli, M. A., Meissner, M. & Liesenfeld, O. Intracellular transport of Toxoplasma gondii through the blood–brain barrier. *Journal of Neuroimmunology* **232,** 119–130 (2011).

53. Feustel, S. M., Meissner, M. & Liesenfeld, O. Toxoplasma gondiiand the blood-brain barrier. *Virulence* **3,** 182–192 (2014).

54. Kim, K. S. Mechanisms of microbial traversal of the blood–brain barrier. *Nat Rev Microbiol* **6,** 625–634 (2008).

55. Farrar, M. A. & Schreiber, R. D. The molecular cell biology of interferon-gamma

and its receptor. *Annu. Rev. Immunol.* **11,** 571–611 (1993).

56. Stetson, D. B., Mohrs, M., Reinhardt, R. L., Baron, J. L., Wang, Z.-E., Gapin, L., Kronenberg, M. & Locksley, R. M. Constitutive cytokine mRNAs mark natural killer (NK) and NK T cells poised for rapid effector function. *J Exp Med* **198,** 1069–1076 (2003).

57. Groom, J. R., Richmond, J., Murooka, T. T., Sorensen, E. W., Sung, J. H., Bankert, K., Andrian, von, U. H., Moon, J. J., Mempel, T. R. & Luster, A. D. CXCR3 chemokine receptor-ligand interactions in the lymph node optimize CD4+ T helper 1 cell differentiation. *Immunity* **37,** 1091–1103 (2012).

58. Luster, A. D., Unkeless, J. C. & Ravetch, J. V. Gamma-interferon transcriptionally regulates an early-response gene containing homology to platelet proteins. *Nature* **315,** 672–676 (1985).

59. Farber, J. M. A macrophage mRNA selectively induced by gamma-interferon encodes a member of the platelet factor 4 family of cytokines. *Proc Natl Acad Sci USA* **87,** 5238–5242 (1990).

60. Betts, M. R., Brenchley, J. M., Price, D. A., De Rosa, S. C., Douek, D. C., Roederer, M. & Koup, R. A. Sensitive and viable identification of antigen-specific CD8+ T cells by a flow cytometric assay for degranulation. *J Immunol Methods* **281,** 65–78 (2003).

61. Yuzefpolskiy, Y., Baumann, F. M., Kalia, V. & Sarkar, S. Early CD8 T-cell memory precursors and terminal effectors exhibit equipotent in vivo degranulation. *Cell Mol Immunol* **12,** 400–408 (2015).